STUDY OF THE ELECTRONIC SURFACE STATE OF III - V COMPOUNDS

(2)

SEMI-ANNUAL TECHNICAL PROGRESS REPORT

W. E. Spicer, Principal Investigator
Telephone: (415) 497-4643

15 September, 1975

NIGHT VISION LABORATORY
U. S. Army Electronics Command
Fort Belvoir, Virginia 22060

Sponsored by

DEFENSE ADVANCED RESEARCH PROJECTS AGENCY
DARPA ORDER NO. 2182
PROGRAM CODE NO. 4D10

CONTRACT NO. DAAK02-74-C-0069

Effective: 1973 September 01 Expiration: 1976 September 30 ($391,349)

SOLID-STATE ELECTRONICS LABORATORY

STANFORD ELECTRONICS LABORATORIES

STANFORD UNIVERSITY • STANFORD, CALIFORNIA

(6) STUDY OF THE ELECTRONIC SURFACE STATE OF III - V COMPOUNDS.

(9) SEMI-ANNUAL TECHNICAL PROGRESS REPORT.

(10) W. E. Spicer, Principal Investigator
Telephone: (415) 497-4643

(11) 15 September 1975

(12) 178 p.

NIGHT VISION LABORATORY
U. S. Army Electronics Command
Fort Belvoir, Virginia 22060

Sponsored by

DEFENSE ADVANCED RESEARCH PROJECTS AGENCY
DARPA ORDER NO. 2182
PROGRAM CODE NO. 4D10

CONTRACT NO. DAAK02-74-C-0069

Effective: 1973 September 01 Expiration: 1976 September 30 ($391,349)

STANFORD ELECTRONICS LABORATORIES
STANFORD UNIVERSITY
STANFORD, CALIFORNIA 94305

(15) DAAK02-74-C-0069
DARPA Order-2182

332400 LB

TABLE OF CONTENTS

	Page
Abstract	v
Chapter I Overview	1
I. Introduction	1
II. Clean 3-5's Surface States	2
III. Significance of the GSCH Model and its Relationship to Interface States	12
IV. Oxygen and Other Gases on Clean 3-5 (110) Surfaces	13
V. Formation of Schottky Barriers by Alkali Metal Adsorption	21
VI. Summary and Conclusion	30
References	33
Chapter II Photoemission Study of the Adsorption of O_2, CO and H_2 on GaAs	36
I. Introduction	36
II. Experimental Technique	36
III. Results and Discussion - O_2	41
A. EDCs	41
B. Fermi Level Movement	53
C. Comparison with Other Work	56
D. Site of Oxygen Adsorption	59
E. Oxidation of "Bad Cleave"	64
IV. Results and Discussion - CO	68
V. Results and Discussion - H_2	75
VI. Concluding Remarks	86
References	88
Chapter III Photoemission Studies of the GaAs-Cs Interface	90
I. Introduction	90
II. Experimental Details	91

		Page
III.	Results	95
IV.	Discussion	110
V.	Conclusions	121
	Appendix	123
	References	125
Chapter IV	Ultraviolet Photoemission Study of Cesium Oxide Films on GaAs	127
I.	Introduction	127
II.	Experimental Procedure	131
III.	Results and Discussion	135
IV.	Conclusions	152
	References	154
Chapter V	Surface States and Schottky Barrier Pinning on InP and GaAs	156
	References	164
Chapter VI	GaSb Surface States and Schottky Barrier Pinning	165
	References	168
Chapter VII	Future Work	169
	References	169
List of Figures and Tables		170

ABSTRACT

A model for the surface state distribution on the clean (110) face of GaAs, InP, and GaSb has been established. Any filled surface states lie well below the valence band maximum (VBM) for all three materials. There is an empty surface state band with a lower edge 0.7 eV below the conduction band minimum (CBM) in GaAs, and 0.25 eV below the CBM for InP. There are no empty (or filled) surface states within the bandgap for GaSb. As will be seen later, this profoundly affects the behavior of GaSb when Cs is added to the surface. For all three materials the empty states are associated with the column III surface atoms, and the filled surface states are associated with the column V surface atoms. This model can probably be generalized to other III-V semiconductors and to faces other than the (110) face.

Ultraviolet photoemission spectroscopy (UPS) with $h\nu < 12$ eV was used to study O_2, CO and H_2 adsorption on the cleaved GaAs (110) face. It was found that O_2 exposures above 10^5L (1L = 10^{-6} Torr second) were required to produce changes in the energy distribution curves. At O_2 exposures of 10^6L on p-type and 10^8L on n-type an oxide peak is observed in the EDCs located 4 eV below the valence band maximum. On p-type GaAs, O_2 exposures cause the Fermi level at the surface to move up to a point 0.5 eV above the valence band maximum, while on n-type GaAs O_2 exposures do not remove the Fermi level pinning caused by empty surface states on the clean GaAs. CO was found to stick to GaAs, but to desorb over a period of hours, and not to change the surface Fermi level position. H_2 did not affect the EDCs, but atomic H lowered the electron affinity and raised the surface position of the Fermi level on p-type GaAs. A correlation is found in which gases which stick to the GaAs cause an upward movement of the Fermi level at the surface on p-type GaAs, while gases which stick only temporarily do not change the surface position of the Fermi level.

Photoemission was used to study changes in the electronic structure of the surface of GaAs, InP and GaSb as sub-monolayer quantities of Cs where added to the surface. The observed behavior has implications for the theory of the formation of Schottky barriers. As Cs is applied to GaAs and InP, strong changes occur near the VBM, indicating a strong interaction between the Cs and the GaAs or InP. The Fermi level pinning position changes as a function of Cs coverage, but at saturation coverage the pinning position is well correlated with the edge of the empty surface state band. The behavior of Cs on GaSb is different: a fraction of a monolayer moves the Fermi level pinning position by almost the full bandgap, and there are no strong changes near the VBM. This behavior correlates with the fact that the Cs layer which produces a minimum threshold for photoemission is stable for GaAs and InP, but evaporates from GaSb.

Ultraviolet photoemission energy distribution curves (EDCs) were measured from a GaAs (110) surface covered with Cs-oxide layers of varying thickness. There is no evidence of emission from Cs-oxide in the EDCs from GaAs with a surface treatment that produces optimum yield, but structure characteristic of the GaAs is present in the EDCs. However, EDCs characteristic of bulk Cs-oxide were measured from GaAs with a thick (at least several molecular layers) Cs-oxide surface layer, but no structure characteristic of the GaAs was present in the EDCs. Compared to the GaAs with the optimum surface treatment, this thick Cs-oxide film produced yield throughout the photon energy range studied ($1.4\ eV \leq h\nu \leq 11.6\ eV$). These measurements indicate that the Cs-oxide layer required for activation of GaAs to negative electron affinity is so thin that the Cs-oxide layer does not have bulk properties which can be detected by photoemission. Measurements similar to those reported here on narrower bandgap III-V alloys should determine if the thickness of the Cs-oxide layer required for activation increases with decreasing bandgap or is independent of bandgap.

CHAPTER 1 - OVERVIEW

I. INTRODUCTION

Since our last semiannual report our studies of the surface of GaAs and GaSb have continued, and have been extended to InP. All studies so far have been confined to the (110) cleavage face of these materials. To date, four differently doped GaAs samples, for a total of 12 cleavage faces, have been studied. In addition to studies of the clean surface, the adsorption of oxygen, carbon monoxide, hydrogen, cesium, sodium, and cesium oxide on the cleaved GaAs surface has been studied. Future GaAs work will be performed on faces other than the cleavage face, and at photon energies > 11.8 eV, by using the Stanford Synchrotron Radiation Project.

Photoemission studies of the cleavage face of GaSb and InP are in progress. To date, n-type samples have been studied extensively (7 cleaves on GaSb and 5 cleaves on InP). One cleavage of p-type GaSb has been studied, and further work on the p-type sample will begin soon. Experiments on p-type InP are also planned.

The body of this report is taken from papers prepared for publication in the open literature. This first chapter contains an overview of the III-V studies accomplished under this contract. Chapter 2 presents the gas adsorption studies on GaAs in greater detail. Chapter 3 presents the Cs and Na adsorption on GaAs, and the relation of that work to Schottky barriers. Chapter 4 discusses the results of building up a cesium oxide layer on GaAs, and relates the results to the bulk cesium oxide work reported in our last semiannual report. Chapters 5 and 6 discuss some aspects of the InP and GaSb work, respectively, and Chapter 7 briefly discusses our plans for future work.

Most of the results in this report were obtained by more conventional photoemission spectroscopy[1,2,3] in the range $h\nu < 12$ eV; however, to investigate a key question concerning the oxidation of GaAs, Pianetta et al.[4] have used the Stanford Synchrotron Radiation Project (SSRP) for experiments with photons up to 300 eV. This facility will play an increasingly important role in our future work.

The overall strategy we have adopted was first to attempt to obtain some understanding of the electronic structure of surfaces of Si and then to use that knowledge as background in moving on to the 3-5 semiconductors. The results of this strategy will be apparent in this report.

Once some knowledge of the clean surface was obtained, an effort was made to understand the interface produced by oxidizing the surface or by adding metal to it. A strong motivation here was to move toward real surfaces, represented either by surfaces passivated with native oxides, Schottky barriers, or the complicated Cs layers which make negative electron affinity photocathodes possible.[5] In all cases, it is recognized that most of the critical phenomena occur within a few atomic layers of the interface.

All of the Stanford work reported here was done on crystals cleaved (110 face) in ultrahigh vacuum (order 10^{-10} Torr). Except where specifically mentioned, the measurements were for $h\nu < 12$ eV with techniques well described in the literature. Surface Fermi level positions were determined using a Cu reference.[1,3]

II. CLEAN 3-5's SURFACE STATES

The first material we studied was GaAs. Prior to our work there had been three rather recent studies of surface states on GaAs. The most recent by Eastman and Grobman[6] reported filled surface states in the gap

similar to Si and Ge. Although we made many cleaves (including bad cleaves) on four different crystals, we were never able to reproduce those results. Rather, we found agreement with the earlier results of Dinan, Galbraith and Fischer[7] and for the filled surface with Van Laar and Scheer.[8] Eastman and Freeouf have recently reported GaAs[9] results also in agreement with these results. A very important difference was found between the surface states on (110) GaAs and those on (111) Si. This is illustrated by Fig. 1.[10]

The most striking difference between the Si and GaAs surface states is the large gap which opens up between the empty and filled surface states for GaAs. Our first reaction on seeing this was to try to understand the reason for this striking difference. Here collaboration with Walter Harrison and Salim Ciraci proved most fruitful. Making use of the Bond Orbital Model, a first order calculation was made of the energy levels associated with surface as compared to bulk orbitals. The results were striking. They showed[2] that, because of the difference between the Ga and As potentials, there would be an "electronic" reconstruction of the "dangling" bond electrons in which each As surface atom obtains two surface electrons, forming a filled surface band, and each surface Ga is depleted of "dangling bond" electrons so that the empty surface states are localized on the Ga atoms. This result is shown symbolically in Fig. 2. Surface reconstruction has not been taken into account in that Figure.

More recent work reviewed by Spicer and Gregory[14] gives strong experimental verification of this model (termed the GSCH - Gregory, Spicer, Ciraci, Harrison model) and also suggests that its general features - the localization of the filled and empty surface bands on the column 5 and 3 atoms respectively and the band gap separating them - can be generalized to all faces of all 3-5 semiconductors.

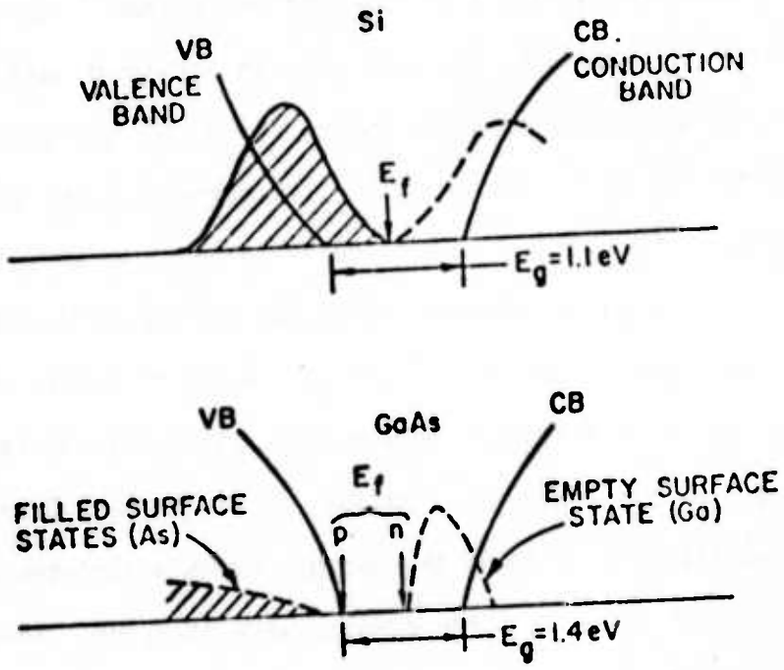

FIG. 1--Models for surface states on the cleavage faces of Si and GaAs. For Si, there are surface states through most of the bandgap. For GaAs, there are empty surface states in the upper half of the bandgap, but no surface states in the lower half of the bandgap. Any filled surface states (which have not been detected) lie below the valence band maximum. From Refs. 1 and 2.

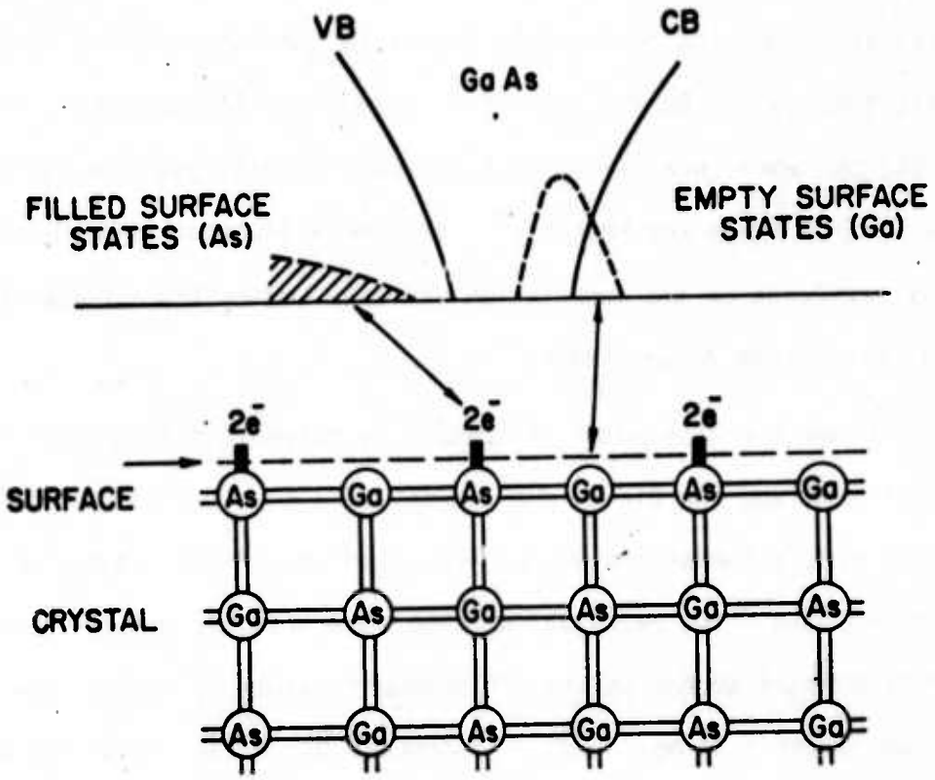

FIG. 2--Surface state density of states and spatial location of surface states for GaAs. The filled surface states have not been detected, and are shown to indicate that they lie below the valence band maximum and are lacking in sharp structure.

One very important tool which has confirmed the GSCH model and suggested its extension to other faces, has been excitation of electrons from core 3d states of either the column 3 or 5 atom to the empty surface states. This was first done by Ludeke and Esake[15] in energy loss measurements on GaAs (111) and (100) and more recently in photoemission partial yield measurements from (110) GaSb by Eastman and Freeouf.[9] These very important experiments give definitive evidence of the association of empty and filled surface states with column 3 and 5 atoms respectively.

In generalizing the GSCH model, it should be noted that Bond Oribtal calculations of Harrison and Ciraci are not specific to any crystal face, but rather just give a comparison of the energy of electronic states on surface and bulk atoms. The calculations also show that the principal features of the GSCH model depend on the difference in atomic potential between the column 3 and 5 atoms. Such differences, of course, occur for all the 3-5 compounds. The GSCH model is closely related to the suggestions made byLevine et al.[16] based on ionic considerations.

Based on the generalization of the GSCH model and making use of the results of Ludeke and Esaki,[15] a model for the surface states on the (111) and ($\bar{1}\bar{1}\bar{1}$) faces of GaAs is shown in Fig. 3. A similar model was proposed by Gatos and Lavine,[17] based on the different etching characteristics of the (111) A and B faces.

After, but independent of, the work reported in Ref. 2, two groups have made more detailed calculations specific to the (110) face of GaAs. Joannopoulous and Cohen[12] and Calandra and Santoro[13] have performed a tight binding calculation for the GaAs (110) surface, and Chelikowski and Cohen[12] have made a self consistent pseudopotential calculation for this surface.

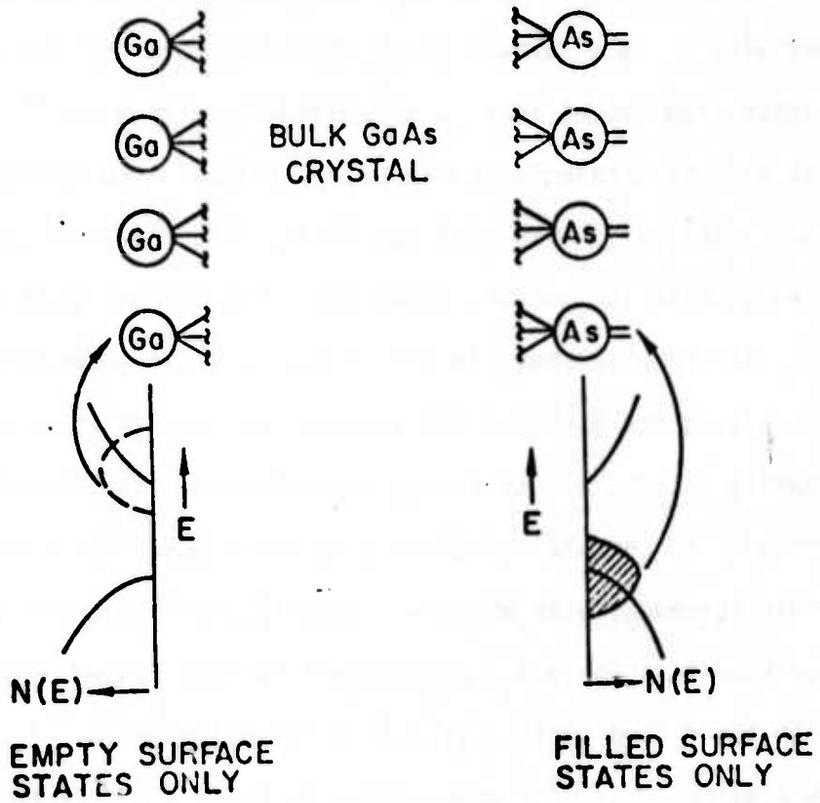

FIG. 3--Model for surface state density of states and spatial location for (111) faces of GaAs.

In Fig. 4 we show a sample of the theoretical work. Part (a), taken from the work of Chelikowsky and Cohen,[12] shows a total density of states for GaAs, with surface states for the (110) surface shaded. They find that the surface state in the upper part of the band gap is primarily Ga derived, while the surface state at the valence band maximum is As derived.

Figure 4(b) shows a surface state band structure for the GaAs (110) surface, taken from recent results of Calandra and Santoro.[13] Their calculation is a tight binding calculation including second nearest neighbor interactions They also find that the surface state in the upper band gap is Ga derived, while the surface state below the valence band maximum is As derived. The results shown in Fig. 4 are in basic agreement with the GSCH model, giving the band gap and associating the filled band and empty bonds primarily with As and Ga atoms, respectively. The position of the empty band is in reasonable agreement with experiment, the width is also in reasonable agreement with what we presently know about the empty bands; however, we need less ambiguous experiments in this regard. There is a problem with the filled surface states in the calculations of Fig. 4. These give a narrow band near the valence band maximum. If this existed, it should have been seen unambiguously by photoemission experiments, but it has not been seen despite many careful attempts. It is most likely that the filled bands are lowered by surface reconstruction. A surface reconstruction suggested by Harrison[18] is shown in Fig. 5. Our lack of detailed knowledge of the surface reconstruction is one of the greatest areas of uncertainty in surface work on the 3-5's. It is hoped that LEED and other techniques will help provide this type of vital information in the future.

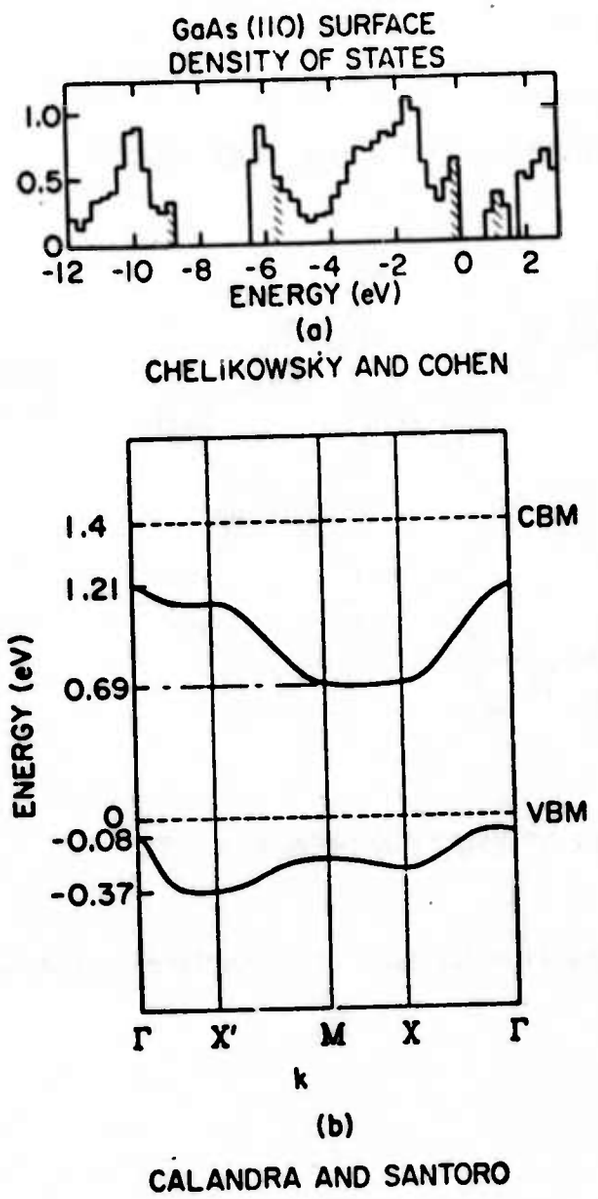

FIG. 4--Surface state calculations for GaAs (110). a) Density of states for (110) surface, with surface states cross-hatched. From Chelikowski and Cohen, Ref. 12. b) Surface state band calculation, from Calandra and Santoro, Ref. 13. Note that in both a) and b) there is a surface state in the upper part of the band gap, no surface states in the lower part of the band gap, but there is a surface state just below the valence band maximum.

RECONSTRUCTION FOR GaAs (110) FACE

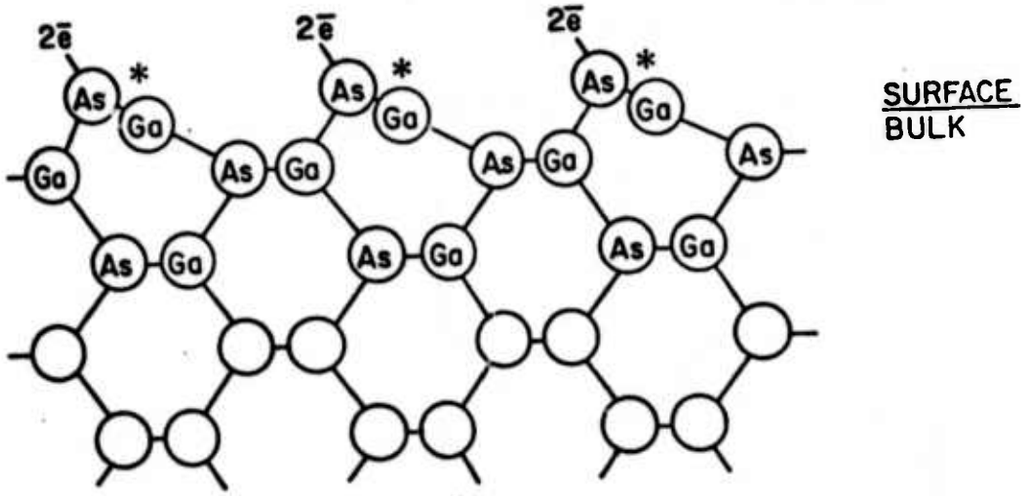

*LOCATION OF EMPTY SURFACE STATE

FIG. 5--Suggested reconstruction for GaAs (110) surface. From Harrison, Ref. 18.

It should also be recognized that if the surface state bands are lowered well into the middle of the valence band, the width of the surface state bands may be increased due to interaction with the bulk states, i.e., their resonant character may become much more important.

Chye et al. have made extensive studies of the (110) cleavage faces of n-type InP[19] (5 cleaves on one crystal) and GaSb[20] (5 cleaves on two n-type crystals and 1 cleave on one p-type crystal). In no case did we find evidence for filled states in the gap. For InP the lower edge of the empty surface states is located 0.25 eV below the CBM. For GaSb, it appears that the bottom of the empty state band lies at or above the bottom of the conduction band. The accuracy with which we can locate the states is ± 0.1 eV.

Eastman and Freeouf[9] have recently published a compilation of their 3-5 surface state results. These include GaAs and GaSb but not InP. Their results are now in agreement with the GaAs results of Dinan et al.[7] and Gregory et al.[2] However, there is disagreement on GaSb where Chye et al.[20] locate the bottom of the empty states at or above the CBM and Eastman and Freeouf[9] locate it near the VBM (i.e., about 0.4 eV below our lower limit). One might suggest (following suggestions of Lapeyre[21]) that excitonic effects are important in excitation from the Ga 3d states into the empty surface states, and these effects lower the excitation energy below that of the one electron states. However, this would not account for Eastman and Freeouf's location of the surface Fermi level position on their n-type sample so much lower than the limit set by Chye et al.[20] Insufficient experimental details are given in the paper by Eastman and Freeouf to allow for detailed evaluation of the methods they used to locate the surface Fermi level. As will be seen in detail in Section VI, the situation with GaSb is important since

Eastman and Freeouf[9] have used the correlation between the empty surface state position on the clean surfaces and the Fermi level pinning position for Schottky barriers to draw strong generalizations.

III. SIGNIFICANCE OF THE GSCH MODEL AND ITS RELATIONSHIP TO INTERFACE STATES

A very important aspect of the GSCH model (see Fig. 2) is that it emphasizes the atomic or chemical nature of the surface states on the GaAs. Surface states might be expected simply due to the termination of a solid at a surface, from the exponential attenuation of the traveling waves at the surface. However, the states on the 3-5 compounds are much more chemical in nature than this, and can only be understood in terms of the local potential associated with the column 3 and 5 atoms at the surface. It is these potentials that force the "dangling" electrons onto the column 5 atoms and leave the column 3 atoms devoid of "dangling" electrons so that they form the empty surface states. Again, the band gaps separating these filled and empty surface states are a reflection of the local atomic potentials which characterize each column 3 and column 5 atom.

The local and chemical nature of the surface states is emphasized here because we feel it is critical to understanding the interfacial states which develop when foreign atoms are placed in contact with the surface of the semiconductor. For example, the chemistry of oxygen at the (110) surface of GaAs (Fig. 2 or 5) will be quite different from the chemistry of oxygen with bulk arsenic or gallium. An important question here is whether the oxygen can bond to the surface without breaking the covalent bonds which bind the surface atoms to each other and the rest of the crystal. If the oxidation does break other bonds, leaving some of them unsatisfied, this will produce interfacial states which will adversely affect the device behavior of the material. Even if a thick oxide is grown on the 3-5, it is the detailed nature of the atomic layers where the oxide bonds to the GaAs which will determine the all important interfacial properties of the material.

To understand this, the interaction of oxygen with the atoms at the interface must be understood.

Even though the chemistry is quite different, the same set of arguments apply to the interface between the semiconductor and a metal in, for example, a Schottky diode. In this case, the most important question concerns the pinning of the Fermi level at the interface since this determines the characteristic of any Schottky barrier formed.

In the next two sections, we will detail our studies of the adsorption of oxygen on clean 3-5 surfaces, and our studies of the effect of Cs on the interface. In all cases, the work involves starting from the clean surface and studying the results of slowly building toward and (in some cases) beyond a monolayer.

IV. OXYGEN AND OTHER GASES ON CLEAN 3-5 (110) SURFACES

The procedure followed in this work was to provide an atomically clean (110) surface by cleaving a single crystal in vacuum (order of 10^{-10} Torr) and, after determining the electronic structure of the clean surface, to expose it to gradually increasing amounts of oxygen.[2,22] Two important things were measured: 1) the photoemission energy distribution curves (EDC's) which gave us a measure of the filled electronic states, and 2) the surface Fermi level position, which gave us a measure of the pinning of the Fermi level at the surface or interface. For GaAs both n and p type samples were studied. A typical set of curves is shown in Fig. 6. As can be seen, up to 10^5 Langmuir (1 Langmuir = 10^{-6} Torr-sec. exposure), the most apparent change is a sharpening of the structure due to bulk transitions associated with the GaAs band structure. This sharpening is often seen and is tentatively associated with removal of strain caused by the cleaving process. Correlating our work with that of Dorn et al.,[23] we believe that an exposure of 10^6-10^7L

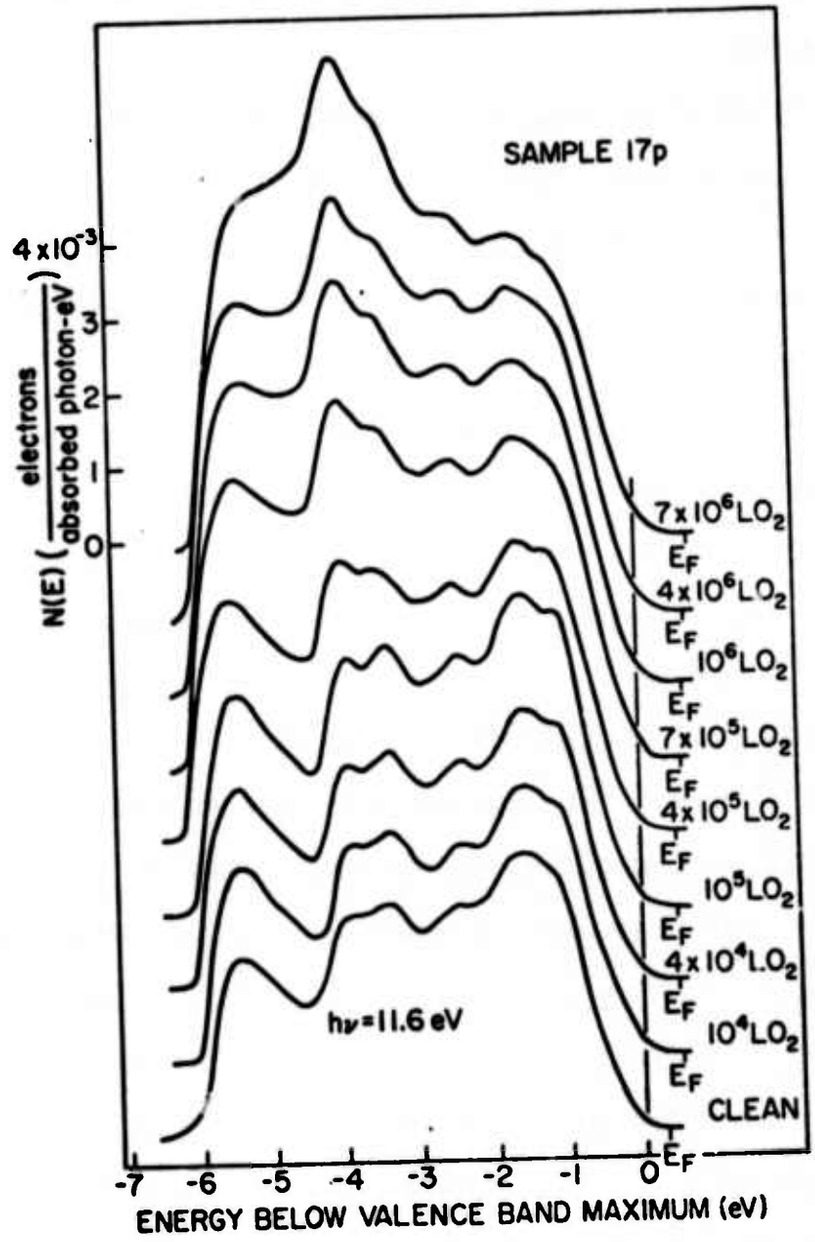

FIG. 6--EDCs for 1.5 X 10^{17} cm^{-3} p-type GaAs, with oxygen exposure increasing upwards. Photon energy is 11.6 eV.

produces approximately a half monolayer of adsorbed oxygen. The escape depth for the final state energies of Fig. 16 are probably in the range of 10 to 40 Å. The work of Pianetta[4] et al. shows that at higher photon energies, the effect of oxygen can be seen at much lower exposures. For example, for hν in the range of 26 eV, where escape depths are much shorter, the effects of oxygen can be seen at exposures as low as 10^3L. This shows the importance of varying hν in order to enhance surface sensitivity.

For exposures above 10^5L, a peak grows near -4 eV. This peak is associated with oxygen bonded to the As surface atoms as shown symbolically by Fig. 7. As can be seen in Fig. 6, the electron affinity does not change significantly with oxygen exposure (if the electron affinity changes, the width of the EDCs would change). This indicates that adsorbed oxygen, which we expect to have a net negative charge, does not extend out from the surface but is "nestled" into the surface as is shown symbolically in Fig. 7.

In Fig. 8 we indicate how the surface Fermi level for n and p type GaAs and Si changed with oxygen exposure. The behavior is strikingly different for the two semiconductors. In Si all changes which take place in the pinning have been completed by the time a monolayer (approximately 10^3L exposure) of oxygen has been adsorbed. In contrast, for GaAs, changes only start to take place after about a half a monolayer of oxygen has been adsorbed.[23] Some insight into this can be obtained from Fig. 1 where the Si surface states extend across the band gap; whereas, the bottom half of the GaAs bandgap is free of surface states. Further, as Fig. 2 indicates, the filled As surface states lie <u>below</u> the top of the valence band. If one assumes that it is these As states to which the oxygen bonds (the basis of this assumption is the desire of oxygen to acquire added electrons and the availability of electrons on the As sites), then the energy of the filled

MODEL FOR GaAs (110) OXYGEN ADSORPTION

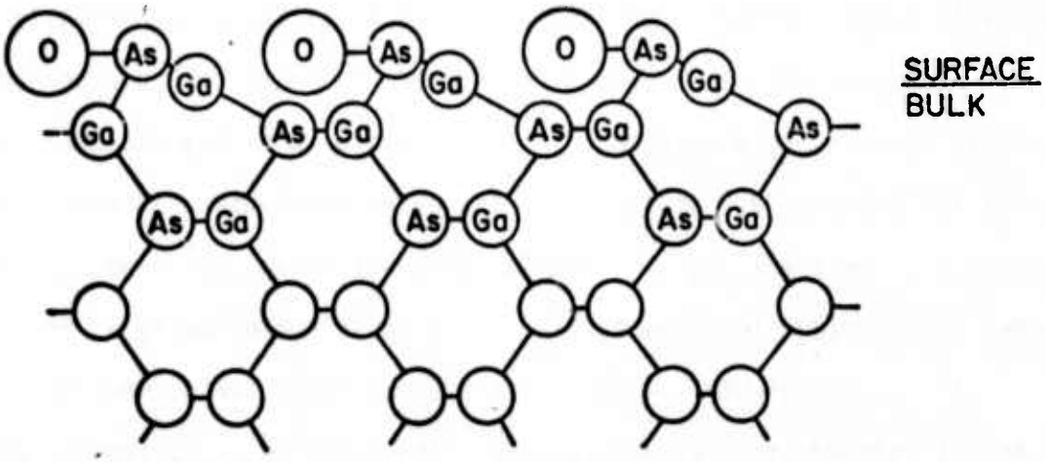

FIG. 7--Model for oxygen adsorption on GaAs (110) surface. The model is suggested by the lack of change in electron affinity caused by oxygen adsorption, and by the evidence that oxygen is adsorbed on the As site (see Fig. 10).

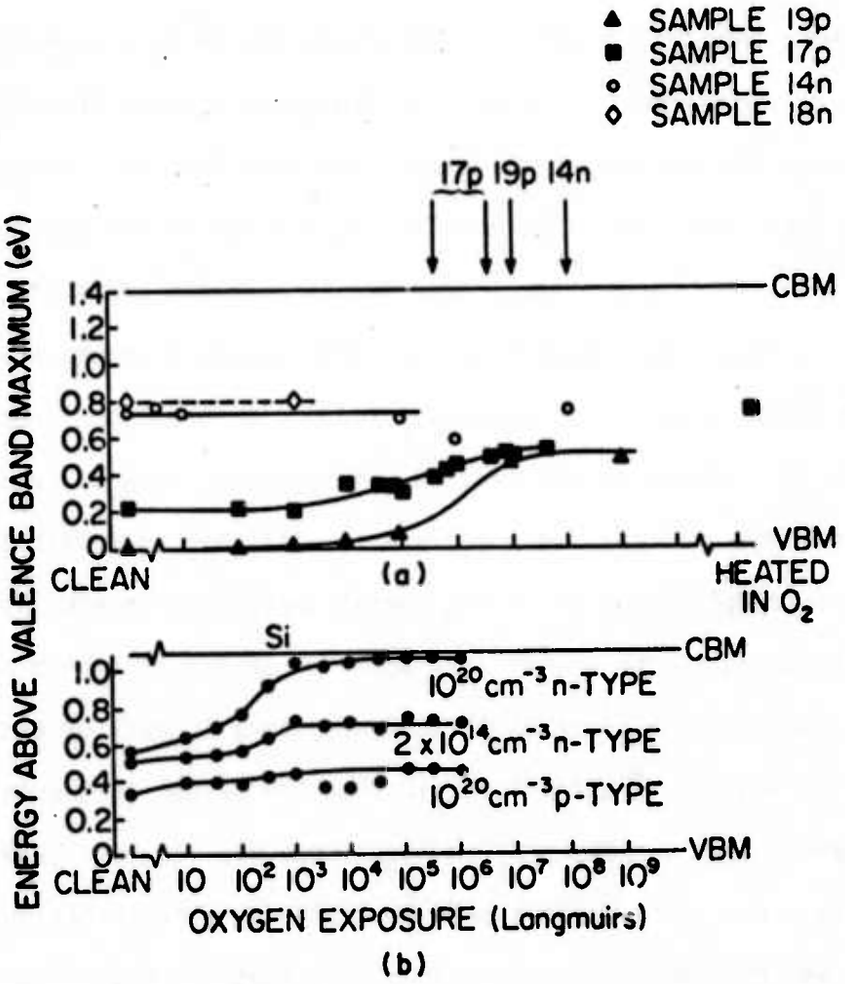

FIG. 8--a) the position of the Fermi level relative to the bands at the surface for four GaAs samples. Sample 19p is 3 X 10^{19} cm^{-3} p-type, 17p is 1.5 X 10^{17} cm^{-3} p-type, 14n is 6 X 10^{14} cm^{-3} n-type and 18n is 1.7 X 10^{18} cm^{-3} n-type. Point marked "Heated in O_2" was for sample 17p which was heated to 350° C in 1 X 10^{-5} Torr for 15 minutes, following 4 X 10^7 L O_2 exposure at room temperature. b) The position of the Fermi level relative to the bands at the surface for three differently doped Si samples (Part b taken from Ref. 1).

As states will be lowered. However, since they always lie below the VBM there will be no change in the pinning conditions due to this movement.[2]

After all of the surface As atoms are tied up by oxygen, the oxidation could only proceed via the surface Ga atoms, but according to a literal extension of the GSCH model (Fig. 2), this can only occur if the electrons necessary for the oxidation are taken from the Ga covalent bonds since Ga has only empty surface states (see Fig. 9). This explanation which was originally put forth in Ref. 2 is obviously subject to question. For example, when one puts oxygen on the surface, is it appropriate to retain the charge distribution of the clean surface or will this be redistributed because of the large perturbation of the overall potential created by the oxygen? Further doubt to the use of this model of oxidation (which at best should be considered a crude first approximation) is cast by the results of Ludeke and Koma[24] which indicate that the oxygen goes onto the Ga first. However, it must also be recognized that the electron beam in their energy loss experiment could itself be acting as a perturbation by breaking bonds and thus enhancing the probability that the oxygen goes to the Ga rather than the As. If one had elemental Ga and As, the oxidation of Ga would be energetically strongly favored.

In order to gain further information on this question, a series of experiments have been performed by Pianetta et al.[4] using synchrotron radiation up to 300 eV from the Stanford Synchrotron Radiation Project (SSRP). One object of this work was to investigate the early stages of the oxidation process by looking for a shift in the core 3d levels of As and Ga as the sample is exposed to oxygen. The key result is shown in Fig. 10.

As can be seen from Fig. 10 after exposures of 10^7L of oxygen, a very strong shift is observed in some of the core As d's but no shift, just a

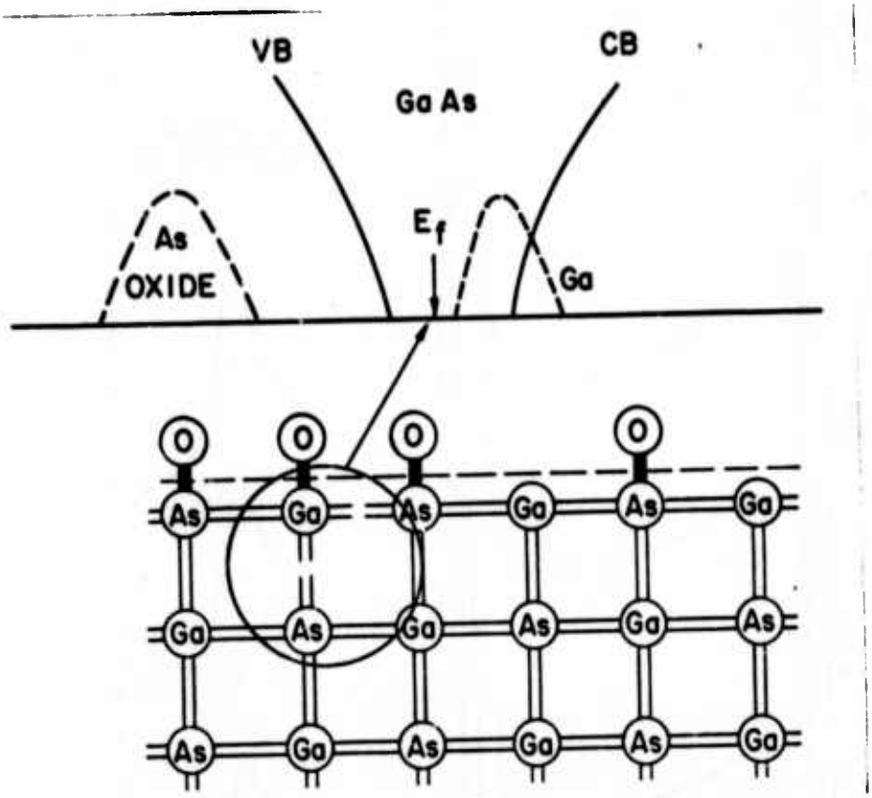

FIG. 9--A model for the oxidation of GaAs for O_2 exposures which cause the downward band bending on p-type GaAs. Broken bonds are assumed to cause the downward band bending.

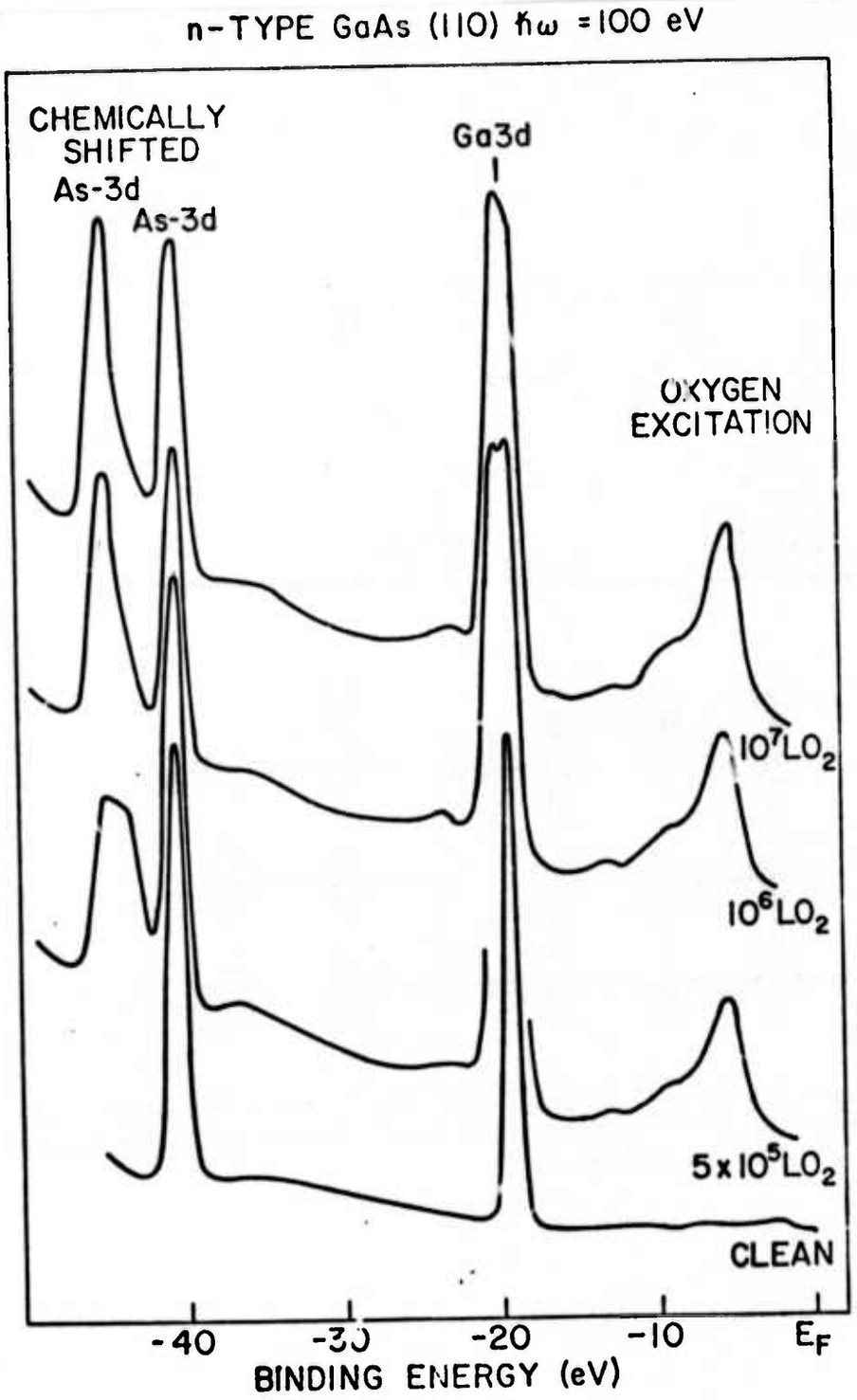

FIG. 10--EDCs showing As 3-d and Ga 3-d band of GaAs as a function of O_2 exposure, with O_2 exposure increasing towards the top. Compare the large chemical shift in the As 3-d band caused by the O_2 to the very small changes in the Ga 3-d band.

slight broadening is seen in the Ga d-states. Only some of the As d-levels are shifted because the experiment probably samples several atomic layers and only the surface As's are shifted. We believe these results give direct evidence that the oxygen first is bonded to the As and not the Ga. When one considers factors such as the possible reconstruction of the surface and the lack of change in electron affinity it is clear that the detailed situation is complicated and much more work is necessary in order to get a detailed description of the oxidation of GaAs and other 3-5's including not only the (110) but other faces.

V. FORMATION OF SCHOTTKY BARRIERS BY ALKALI METAL ADSORPTION

Alkali metals (mostly Cs) were placed on the surface of GaAs, InP and GaSb after cleaving in ultrahigh vacuum. The data so produced can be related to the general Schottky diode literature since Uebbing and Bell[25,26] have shown that a thick dot of Cs on (110) GaAs provides Schottky barrier pinning which correlates well with the pinning position found in the Schottky barrier work of Mead and his coworkers.[27]

Gregory and Spicer[3] have shown that the Fermi level pinning at the largest coverages reported here is the same as that found by Uebbing and Bell. (The largest coverage used here was approximately a monolayer of Cs, while Uebbing and Bell used several hundred Å thick Cs films.) It is in this way that we make contact between the Schottky barrier literature and our own work.

Another motivation for the use of Cs is its importance in the surface coatings used to produce negative affinity photocathodes.[26,28] In the present work we are striving to provide a better understanding of those surface coatings.

From an experimental point of view, the use of alkali metals in general and Cs in particular is very advantageous because it is well established that one can put down even sub-monatomic layers of the alkalis without having clumping or island formation; whereas, with many materials such as Au, Cu, In and other metals there is a very strong tendency for islands to form for thicknesses under about 100 Å. It is very important to know that one can form thin layers without forming islands since one can only use external photoemission as an accurate tool to examine the interface if one can be sure the added metal is going on uniformly even in very thin layers without leaving areas uncovered due to island formation.[26,27,29] (The metal layer must be very thin so that electrons can be emitted from the interface region without overwhelming inelastic scattering from the metal.)

Another advantage of Cs is that detailed studies have been made of change in the surface potential barrier versus coverage in the submonolayer range.[29,30] This has given us the method of determining the coverage used in this work. We have increased the Cs coverage up to the point where we obtain the pinning position characteristic of thick Cs-GaAs Schottky barriers. In Fig. 11 we present a set of EDCs which show the effect of increasing Cs on the EDCs and Fermi level position. The EDCs have been normalized at the strong bulk transition at -1.2 eV. The data of Fig. 11 is from a moderately ($10^{17}/cm^3$) doped p-type sample. Similar EDC changes were observed[3] in all samples studied (2 p-type and 2 n-type crystals) independent of doping and photon energy. The Fermi level changes were, of course, different for n and p type doping.

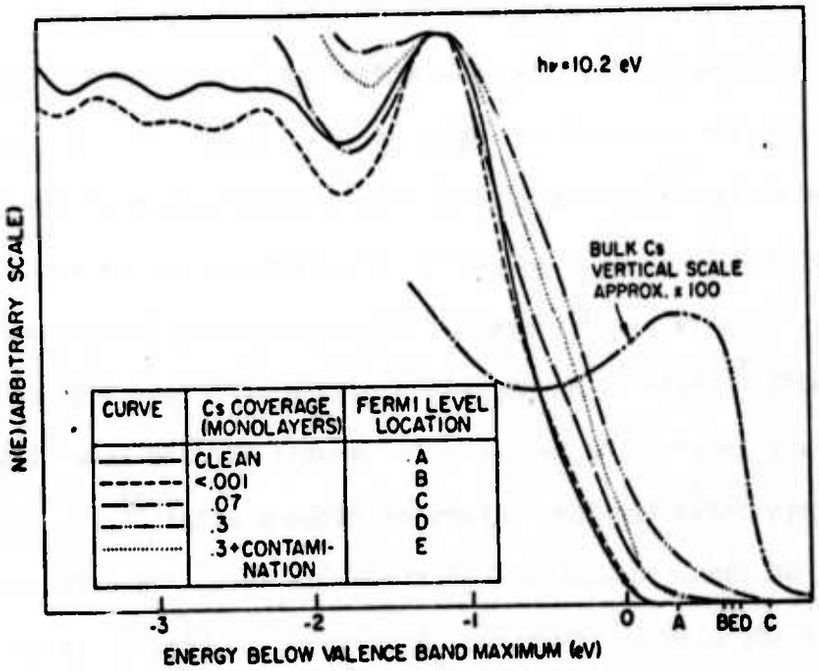

FIG. 11--The high energy portion of GaAs EDCs showing the upward movement of states into the energy gap as Cs coverage is increased. Note that the emission from the states which have moved into the energy gap is not the same as the EDC from a bulk Cs sample.

The most striking thing about Fig. 11 is the movement of the upper edge of the EDCs to higher energy with increasing Cs coverage. The emission from a bulk sample of Cs is also included in Fig. 11 to establish that the changes cannot be explained in terms of an addition of metallic Cs to the GaAs emission. We suggest that the movement of the emission edge shown in Fig. 11 is due to strong interaction between the Cs and GaAs. It seems to us most likely that it is explained by "dielectric interactions" of the type suggested by Inkson[31] although we believe that his model does not properly explain the Fermi level pinning for Schottky barriers on (110) GaAs. Further, we suggest (in conformity with the experimental data) that the movement of the upper edge of the EDCs seen in Fig. 11 is due to interactions at the interface involving, at most, several atomic layers. If one examines Eastman and Freeouf's data for Pd on GaAs,[9] there is a suggestion of the same band edge movement we report here, and there is no evidence for a well defined Fermi level such as the one that was found for thin layers of Pd on a metal.[32]

In Fig. 12, we show the movement of the Fermi level and extrapolated upper edge of the EDC with Cs coverage. Also shown in Fig. 12 is the lower edge of the empty surface state band for the clean surface (0.7 eV above the valence band maximum). As can be seen, the general tendency is for the pinning with the heaviest coverage to assume a position just below the bottom of the empty surface state band. The "monolayers" here are defined in terms of surface Ga and As atoms. Thus, at "one monolayer" coverage there would be one Cs atom for each Ga or As surface atom. Because of the large size of the Cs atom, the actual maximum coverage usually taken to correspond to a saturated Cs layer is 0.3 monolayers as defined here. Any additional Cs is

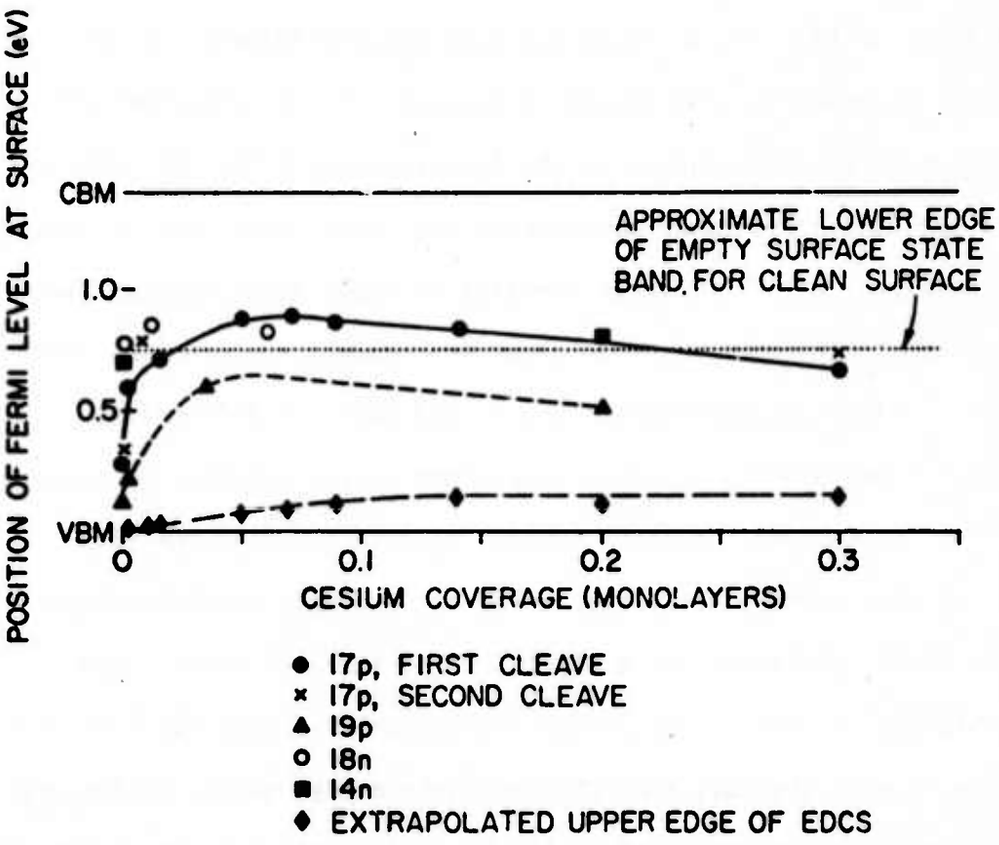

FIG. 12--Position of the Fermi level at the surface relative to the valence band maximum (VBM) and conduction band minimum (CBM) as a function of cesium coverage. The movement of states upward into the energy gap is indicated by extrapolated upper edge of the EDCs.

much more loosely bound to the surface and is assumed to form a second layer. The lowest threshold for photoemission is also obtained with the first saturated Cs layer.

As is shown in Fig. 13, we found the same general behavior in InP, where the bottom of the empty surface states is located 0.25 eV below the CBM, i.e., we observed 1) the upward movement of the leading edge of the EDC with increasing Cs and 2) a complicated movement of the Fermi level with Cs coverage, with the Fermi level after the first complete Cs layer being located just below the bottom of the empty intrinsic surface states. We conclude that there are strong interactions between the Cs and GaAs and InP surfaces (so that the Fermi level pinning cannot be explained simply in terms of placing electrons from the Cs into the empty surface states) but that the final pinning position is closely correlated with, and probably determined by, the position of the bottom of the empty intrinsic surface states. The fact that this occurs despite the strong interactions between the GaAs and Cs is associated with the fact that the intrinsic empty surface states are basically "atomic" states localized on the Ga or In surface atoms as described by the GSCH model (Fig. 2). We believe that it is this strong local atomic and chemical nature of these states that allows them to dominate the surface state pinning. Thus, in the overall picture for GaAs and InP we agree with Eastman and Freeouf[9] concerning the strong relationship between the empty intrinsic surface state position and the Schottky barrier pinning position. However, we have more evidence of strong interactions than they report in their work.

The situation found by Chye et al.[20] for GaSb is quite different from that for GaAs and InP. As mentioned in Section II, the experiments of Chye et al. indicated that the band gap of GaSb is free of surface states,

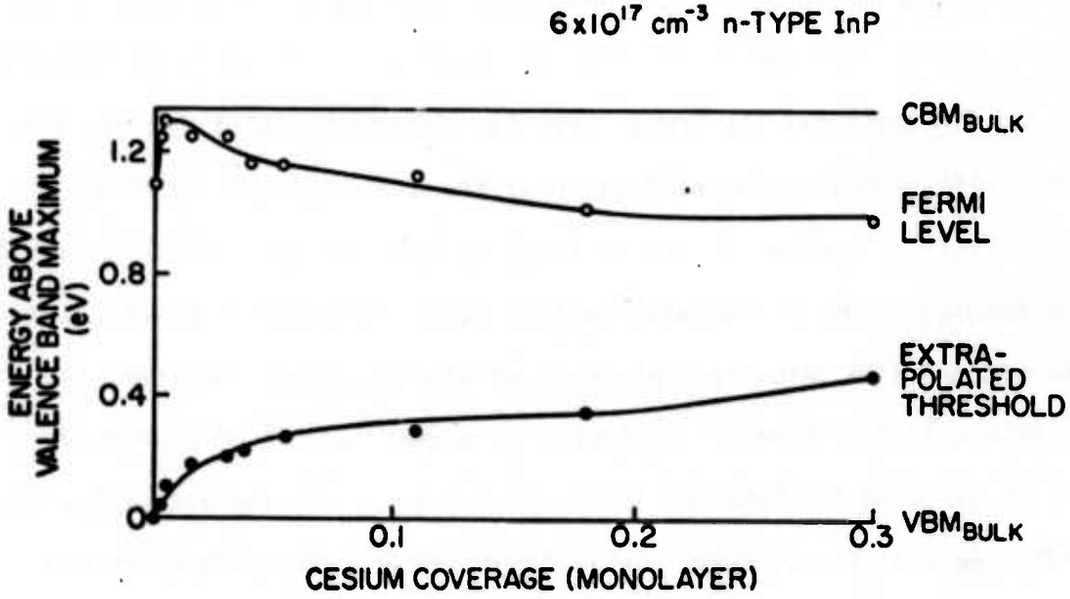

FIG. 13--Fermi level pinning position and extrapolated upper edge of EDC for n-type InP as a function of cesium coverage.

i.e., the filled surface states must lie below the VBM and the empty surface states above the CBM. This, of course, is quite different from the situation we found for GaAs and InP; interestingly, we found the Fermi level movement with Cs application to be quite different from that on GaAs and InP.

Experimental curves and Fermi level positions for GaSb are shown in Fig. 14. In Fig. 14, we also show the effect of Cs on the n-type sample. As can be seen, the Fermi level drops very strongly with Cs addition. At 0.1 monolayer coverage (again defining a monolayer coverage to correspond to one Cs for each surface atom and estimating the coverage by the shift in threshold of emission with coverage) the Fermi level has dropped by about 0.5 eV, and lies in the bottom half of the band gap near the pinning point found for Schottky barriers. As Figs. 12 and 13 show, on GaAs and InP, the Fermi level on n-type samples tends to rise with initial Cs addition and it never drops more than about 0.1 eV below the intrinsic pinning position. Further, the movement of the leading edge of the EDCs with a small amount of Cs addition which was so striking for GaAs and InP is much less or missing altogether for GaSb. Thus, one must conclude that the behavior of GaSb is quite different from GaAs and InP. There is a third way in which GaSb differs from GaAs and InP. For the latter two materials the coverage which corresponds to about 0.3 monolayers (i.e., about 1 Cs atom for every 3 Ga or As surface atoms) is very stable; the Cs has no tendency to evaporate. This Cs coverage also provides the minimum energy threshold for photoemission and the minimum work function. However, for GaSb, coverages above about 0.1 monolayer are unstable, i.e., Cs evaporates from the surface. In particular, if a Cs coverage is provided which gives the minimum photon energy threshold of response (and minimum work function), Cs will evaporate at room temperature.

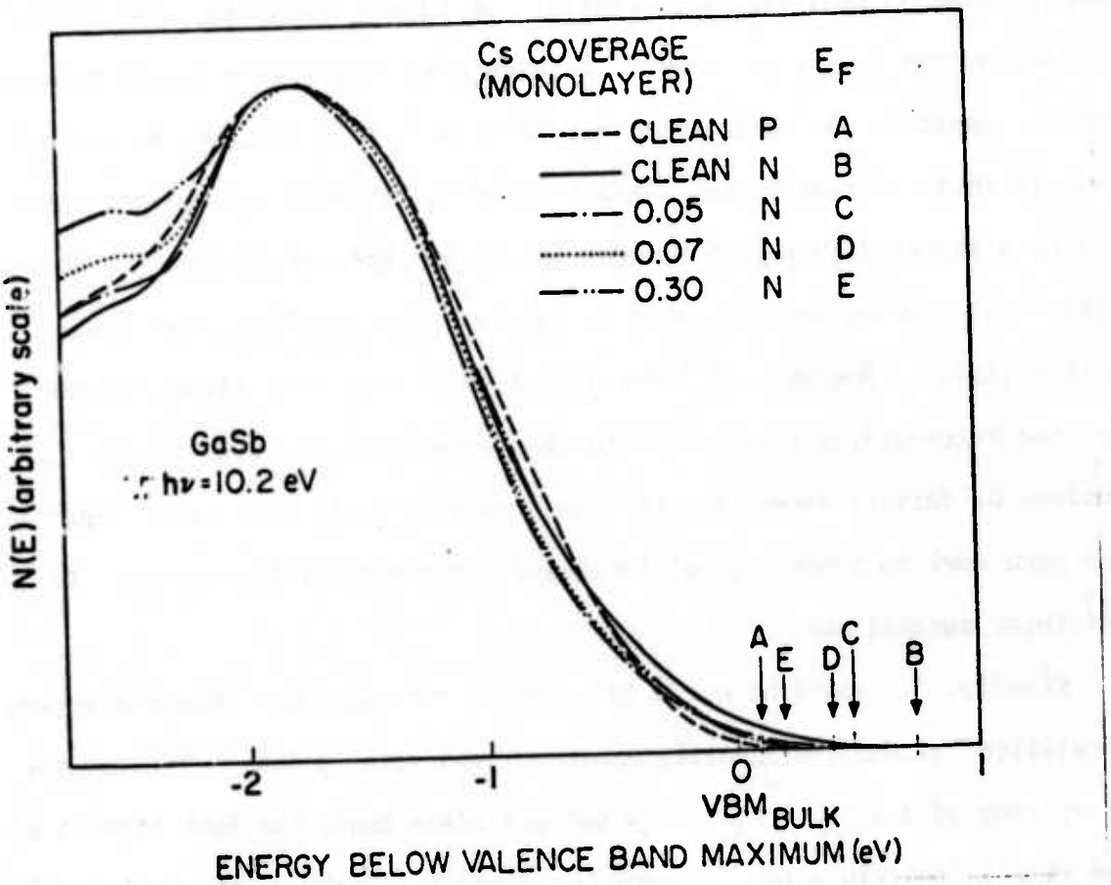

FIG. 14--The high energy portions of clean and cesiated GaSb EDCs. The Fermi level (E_F) of the n-type sample shows a large movement with cesiation and the Fermi levels of the clean p- and n-type samples differ in energy by 0.65 eV. This shows that the Fermi level of the n-type sample lies near the CBM and indicates the absence of empty intrinsic surface states in the bandgap.

Thus, one concludes that Cs is less tightly bound to GaSb than to GaAs and InP. Further, we suggest that this weaker bonding is also reflected in the lack of motion in GaSb of the upper edge of the EDC with light Cs coverage. This we believe indicates a smaller interaction between GaSb and the Cs than is found in GaAs and InP. Finally, we relate the strength of bonding and interaction to the presence of intrinsic surface states in the band gap region. Based on the three materials studied in this program, we suggest that, if empty intrinsic states are present in the band gap region, there will be a strong interaction between the Cs and the semiconductor, and the Fermi level pinning position will be determined primarily by the empty surface states. However, if there are no empty intrinsic states in the gap, the interactions are weaker and the Fermi level position can be determined by factors other than the empty surface state position. Clearly, much more work on other crystal faces and 3-5 compounds is necessary to test these suggestions.

Finally, it should be noted that, while previous work showed a strong correlation between the Schottky barrier Fermi level pinning position and the minimum of the intrinsic empty surface state band, the GaSb studies of Chye et al. indicate a lack of such correlation. Further, the data available suggests that this lack of correlation is associated with the fact that the intrinsic empty surface states in GaSb lie above the CBM.

VI. SUMMARY AND CONCLUSION

In Fig. 15, we summarize the information we have gained on the intrinsic surface state of GaAs, GaSb, and InP. In all cases, the filled surface states are associated with the column V surface atoms and the empty surface states with the column III surface atoms, in agreement with the GSCH model. For GaAs we have shown that the initial step in oxidation is the bonding of an

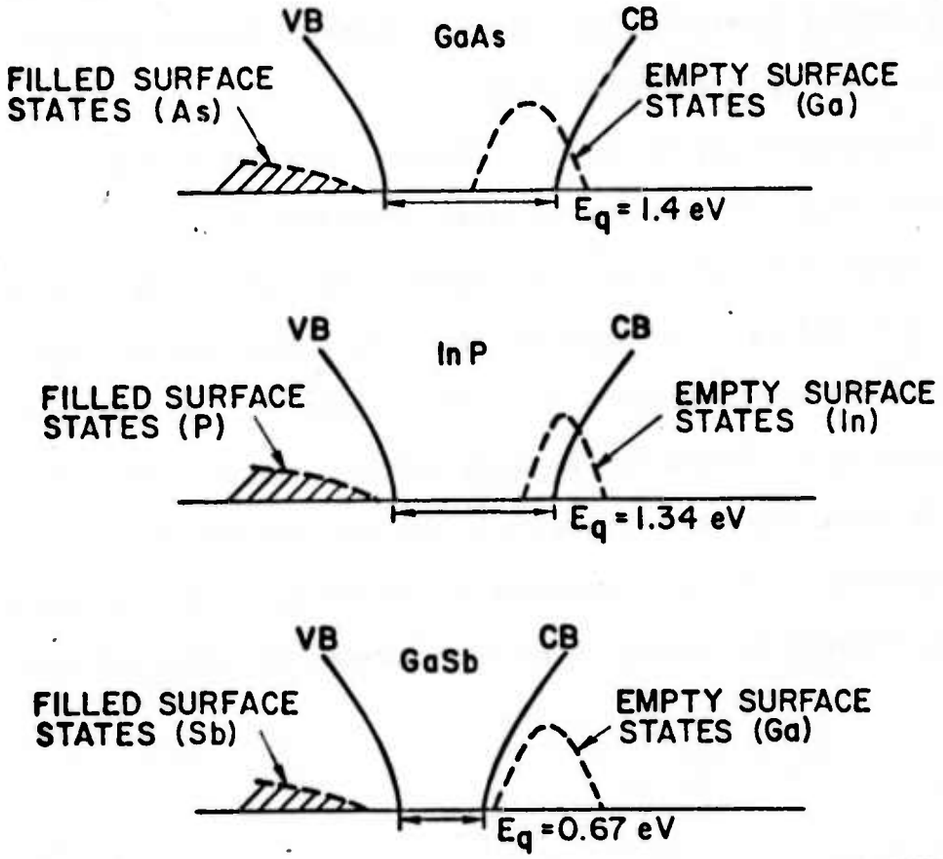

FIG. 15--Surface state model for the (110) face of GaAs, InP, and GaSb. Note that there are no surface states in the lower bandgap for all three materials, and that the position of the empty surface state band is different for the different materials.

oxygen atom to the surface As atom. Further, we have evidence that oxygen bonding to the surface Ga may produce interface states. Similar behavior is expected for other faces and other 3-5's

We have investigated the formation of Schottky barriers on GaAs, GaSb, and InP and found strong differences dependent on whether or not intrinsic empty surface states fall in the band gap region. For GaAs and InP, where empty states lie in the bulk forbidden gap there are strong interactions between the metal and semiconductor and the final Fermi level pinning position is determined by the bottom of the empty intrinsic surface state band. However, in GaSb where there are no states in the gap (see Fig. 15) the Fermi level pinning position is independent of the intrinsic surface states and there is no evidence for strong interaction between the metal and semiconductor.

REFERENCES

1. L. F. Wagner and W. E. Spicer, Phys. Rev. Lett. 28, 1381 (1972; Phys. Re· B 9, 1512 (1974).
2. P. E. Gregory, W. E. Spicer, S. Ciraci, and W. A. Harrison, Appl. Phys. Lett. 25, 511 (1974).
3. P. E. Gregory and W. E. Spicer, Phys. Rev. (in press).
4. P. Pianetta, I. Lindau, C. Garner and W. E. Spicer, in preparation.

   [This portion of the work was partially supported by NSF (DMR 73-07692-A02) in cooperation with SLAC and ERDA, ONR Contract N00014-75-C00289.]
5. P. E. Gregory and W. E. Spicer, in preparation
6. D. E. Eastman and W. D. Grobman, Phys, Rev. Lett. 28, 1378 (1972).
7. J. H. Dinan, L. K. Galbraith, T. E. Fischer, Surf. Sci. 26, 587 (1971).
8. J. Van Laar and J. J. Scheer, Surf. Sci. 8, 324, (1967).
9. D. E. Eastman and J. L. Freeouf, Phys. Rev. Lett. 34, 1624 (1975).
10. The estimate of the filled Si surface states is obtained directly from Wagner and Spicer (Ref. 1). The empty Si surface states are an estimate. Van Laar and Scheer (Ref. 8), Dinan et al., (Ref. 7), Gregory et al. (Refs. 1 and 11) have shown that the filled GaAs surface states lie below the valence band maximum. Careful studies by Gregory and Spicer (Ref. 11) find that there is no strong sharp surface state structure within 4 eV of the valence band maximum. Particularly careful attention has beer paid to the first 0.5 eV below the valence band maximum and no evidence for surface states is found there. The filled GaAs surface states are dashed in to indicate that their position and detailed shape are not known. The bottom of the empty bands were obtained from the Fermi level pinning of n-type samples. The shapes of

these empty bands were estimated using the experimental results of Eastman and Freeouf (Ref. 9) and the theoretical results of Chelikowski and Cohen and Joannopoulos and Cohen[12] and Calandra and Santoro.[13] The details of the empty states in Fig. 2, except for their lower edge, should not be taken seriously.

11. P. E. Gregory and W. E. Spicer, in preparation.
12. J. D. Joannopoulos and M. L. Cohen, Phys. Rev. B 10, 5075 (1974); J. R. Chelikowski and M. L. Cohen, to be published.
13. C. Calandra and G. Santoro, J. Phys. C: Solid State Phys. 8, L86 (1975), and private communication.
14. W. E. Spicer and P. E. Gregory, in press, CRC Critical Reviews of Solid State Physics.
15. R Ludeke and L. Esaki, Phys. Rev. Lett. 33, 653 (1974).
16. J. D. Levine and S. Freeman, Phys. Rev. B 2, 3252 (1970).
17. H. C. Gatos and M. C. Lavine, J. Phys. Chem. Solids 14, 169 (1960); J. Electrochem. Soc. 107, 427 (1960).
18. W. A. Harrison, private communication.
19. P. W. Chye, I. A. Babalola, T. Sukegawa and W. E. Spicer, in preparation.
20. P. W. Chye, P. E. Gregory, H. Sunami, T. Sukegawa, I. A. Babalola, and W. E. Spicer, in preparation.
21. G. J. Lapeyre and J. Anderson, Phys. Rev. Lett. 35, 117 (1975).
22. P. E. Gregory and W. E. Spicer, in preparation.
23. R. Dorn, H. Luth and G. J. Russel, Phys. Rev. B 10, 5049 (1974).
24. R. Ludeke and A. Koma, CRC Critical Review of Solid State Physics, in press.
25. J. J. Uebbing and R. L. Bell, Appl. Phys. Lett. 11, 357 (1967).

26. R. L. Bell, Negative Electrons Affinity Devices, Oxford (1973).

27. C. A. Mead, Solid State Electronics 9, 1023 (1966); T. C. McGill, J. Vac. Sci. Technol. 11, 935 (1974).

28. R. L. Bell and W. E. Spicer, Proc. IEEE 58, 1788 (1970).

29. T. E. Madey and J. T. Yates, Jr., J. Vac. Sci. Tech. 8, 39 (1971).

30. H. Clemens and W. Monch, to be published.

31. J. C. Inkson, J. Phys. C. 6, 1350 (1973).

32. D. E. Eastman and W. D. Grobman, Phys. Rev. Lett. 30, 177 (1973).

CHAPTER 2

PHOTOEMISSION STUDY OF THE ADSORPTION OF O_2, CO AND H_2 ON GaAs (110)

I. INTRODUCTION

In the last few years increasing attention has been given to the study of the adsorption of gases on clean, well defined semiconductor surfaces. One objective of these studies is to learn about the surface states of the clean semiconductor surface, using the adsorbed gas to perturb the surface. Another objective is to learn something about the binding of the gas to the semiconductor surface. This latter objective has potential practical applications regarding the growth of passivating layers on the semiconductor surface. Studies of gas adsorption can provide information about interface states at the overlayer-semiconductor interface.

In this paper we report ultraviolet photoemission spectroscopy (UPS) studies of the adsorption of O_2, CO, and H_2 on the cleaved (110) GaAs surface. Primary emphasis is given to the study of O_2 adsorption. The studies of CO and H_2 adsorption are interesting in their own right and also help to illuminate the results of the O_2 adsorption study.

The cleavage (110) face was chosen because it is easily prepared and is probably the most completely characterized GaAs surface. UPS provides a good technique for studying gas adsorption because it perturbs the surface only slightly. Techniques depending on irradiating the surface with electrons can cause much greater perturbations, including sample heating and electronic effects such as electron stimulated desorption.

II. EXPERIMENTAL TECHNIQUE

Four single crystal samples of GaAs were studied and are described in Table 1. Sample 18n was only given a small exposure to oxygen, but the other three samples were given very high oxygen exposures. A separate cleave

TABLE I

SAMPLES STUDIED

Doping (cm^{-3})	Type	Dopant	Sample Name	Property Studied
6×10^{14}	n	O	14n, cleave # 2	O_2 adsorption
			14n, cleave # 3	"Bad Cleave" O_2 adsorption $< 10^4$L
1.7×10^{18}	n	Si	18n, cleave # 2	O_2 adsorption $< 10^3$L
1.5×10^{17}	p	Zn	17p, cleave # 1	O_2 adsorption
			17p, cleave # 4	CO, H adsorption
3×10^{19}	p	Zn	19p, cleave # 2	O_2 adsorption

of sample 17p was exposed to CO and H_2. The samples were cleaved in ultra high vacuum by squeezing the samples between a tungster carbide blade and an annealed OFHC copper anvil. The cleaved face was usually mirror like with a small number of tear marks visible on the surface. The samples were 1 cm × 1 cm in cross section, and a slab from about 1.3 to 3 mm thick was removed in each cleave.

The experiment was performed in an ion-pumped stainless steel vacuum chamber with a base pressure of better than 1×10^{-10} Torr. High purity O_2, CO, and H_2 were leaked into the system from one liter glass flasks through a Varian ultra-high vacuum leak valve. (Manufacturers analysis of gases is less than 10 ppm impurities for O_2, less than 2 ppm for H_2 and less than 50 ppm for CO. For the hydrogen exposures below 6×10^4 L, tank H_2 of 99.99% purity was used.) Gas exposures were made at room temperature, except for one O_2 exposure and one H_2 exposure, as discussed below.

Gas exposures were monitored by measuring the pressure versus time of exposure. For larger exposures both the pressure of the admitted gas and the time of exposure were raised to keep the pressures and time of exposures within reasonable limits. The exposure times used ranged from 100 seconds to over 24 hours, and pressures used were from 10^{-8} Torr to 10 Torr, in one case. For pressures above 10^{-5} Torr the ion pump was turned off. In all cases in this experiment, the gases were pumped out and the ion pump was restarted before any data measurements were made.

For all of the experiments, pressures up to 10^{-5} Torr were monitored by a Redhead gauge. This gauge is a cold-cathode gauge capable of measuring pressures from below 10^{-12} Torr up to 10^{-5} Torr, and was used here because it does not have a hot filament. The system also has a conventional nude-ion

gauge, but it was not turned on, except as noted below, to prevent contamination from its hot filament. Typically, a hot tungsten filament evolves CO, especially when it is exposed to oxygen. As will be seen below, however, GaAs (110) is only weakly affected by CO.

For the higher gas exposures, two different methods of monitoring the pressure were used. For the experiments on sample 14n, pressures from 10^{-5} to 10^{-4} were monitored with the nude-ion gauge. Pressures above that were monitored crudely with a thermocouple gauge. For the experiments on samples 19p and 17p, a Varian Militorr gauge was used to monitor pressures above 10^{-5} Torr. The Militorr gauge was located in a short side port, out of line of sight of the sample in an effort to reduce contamination of the sample.

For measuring the exposures it was assumed that the Redhead gauge reads low by a factor of 2.[1] However, the exposure measurements probably have an uncertainty of at least a factor of 2 caused by the difficulty of maintaining a constant pressure and by the difficulty of measuring the higher pressures accurately. In this paper, gas exposures are quoted in Langmuirs(L), where $1L = 10^{-6}$ Torr-second.

For the hydrogen exposures, the molecular hydrogen was dissociated into atomic hydrogen by a tungsten filament heated to approximately 1000^{o} C[2] in line of sight with the crystal. The dissociation efficiency of the filament is not known, and neither is the geometrical distribution of the atomic hydrogen produced. Thus, the amount of exposure of the sample to atomic hydrogen is not known. The values of the exposure based on the pressure of molecular hydrogen in the system during the exposure to atomic hydrogen will be given as a crude indication of relative exposures.

Two types of measurements were made on the samples: spectral distribution of photoemitted yield, and photoemitted electron energy distribution curves (EDCs). The yield was measured relative to a Cs_3Sb photodiode with known response.[3] The yield is corrected for the GaAs reflectivity data of Phillip and Eherenreich as tabulated by Eden.[4,5] The EDCs were measured by the standard A.C. modulated retarding potential technique.[6] A hemispherical collector was used. EDCs presented in this paper are normalized so that the area under an EDC is proportional to the yield at the photon energy used to measure the EDC.

The light source for the experiment was a McPhearson model 225 monochromator having a hydrogen discharge lamp modified to include a hot filament.[7] Light entered the sample chamber through a LiF window. Thus the measurements for this experiment were limited to photon energies between the GaAs threshold of about 5.4 eV and the 11.8 eV cutoff of the LiF window.

A copper emitter formed by <u>in situ</u> evaporation could be substituted for the GaAs sample. EDCs measured from this emitter were used to locate the position of the Fermi level on the GaAs EDCs. Since copper is a metal, EDCs of Cu have a well defined Fermi edge. The position of an EDC with respect to the retarding voltage is determined by the collector work function. Thus for EDCs measured with the same collector can, at the same photon energy, the Fermi level will appear at the same retarding voltage for both a Cu EDC and a GaAs EDC.

When the collector work function changes, the position of the EDC shifts with respect to the retarding voltage. To compensate for such shifts, it was necessary to measure copper EDCs frequently, particularly after a gas exposure. The Fermi level was easily detectable on the Cu EDCs up to oxygen

exposures of about 10^7L, although there are changes in the Cu EDCs caused by the oxygen exposures.[8] Beyond 10^7L oxygen exposures, the Cu becomes a semiconductor and there is no emission at the Fermi energy. For oxygen exposures beyond 10^7L, it was necessary to evaporate a fresh Cu film on the Cu emitter in order to determine the Fermi level. At the same time, fresh Cu was evaporated on the inner surface of the collector. Since the Cu EDCs change reproducably with O_2 exposure, the shape of the Cu EDCs can serve as a secondary measurement of oxygen exposure for exposures $\leq 10^7$L.

The escape depth for electrons in the energy range of 8-12 eV has not been measured for GaAs, but measurements for similar materials[9] suggest that it is 25-10 Å. Except for sample 19p, typical band bending lengths for several tenths of an electron volt of band bending exceed 100 Å for the samples studied. Thus, the position of the Fermi level measured here is the position at the surface of the GaAs.

III. RESULTS AND DISCUSSION - O_2

A. EDCs

Figure 1(a) shows EDCs for sample 17p as a function of oxygen exposure for $h\nu$ = 10.2 eV, while Fig. 1(b) shows the same data for $h\nu$ = 11.6 eV. Figures 2 and 3 show data for sample 19p and 14n at $h\nu$ = 11.6 eV. All oxygen exposures in Figs. 1-3 were made at room temperature. Since the escape depth for the higher $h\nu$ should be shorter than that for $h\nu$ = 10.2 eV, it is reasonable that the $h\nu$ = 11.6 eV EDCs show the strongest effect of O_2.

Perhaps the most striking feature of the oxidation data is the insensitivity of GaAs to oxygen exposure. From Fig. 1 it can be seen that up to about 10^5L O_2 exposure, there is no effect of the shape of the EDCs. Beyond about 10^5L O_2 exposure the low energy end of the EDC increases in magnitude,

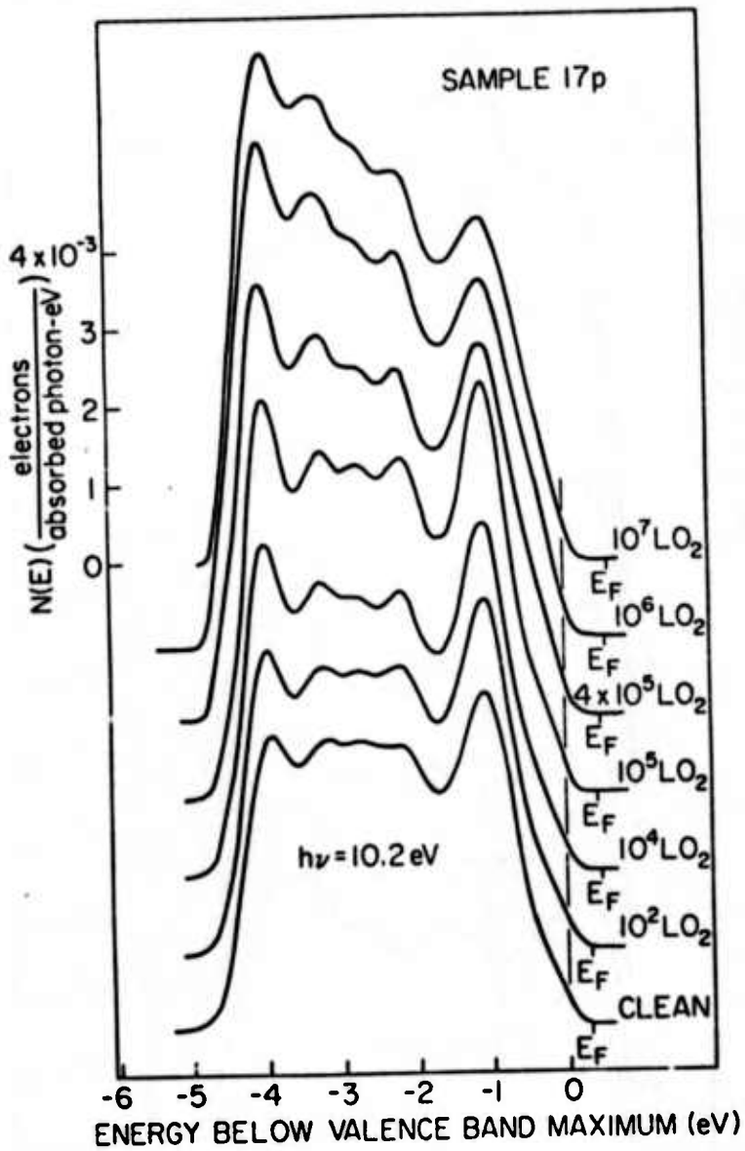

1a

FIG. 1--EDCs for sample 17p with oxygen exposure increasing upwards.
a) photon energy of 10.2 eV.

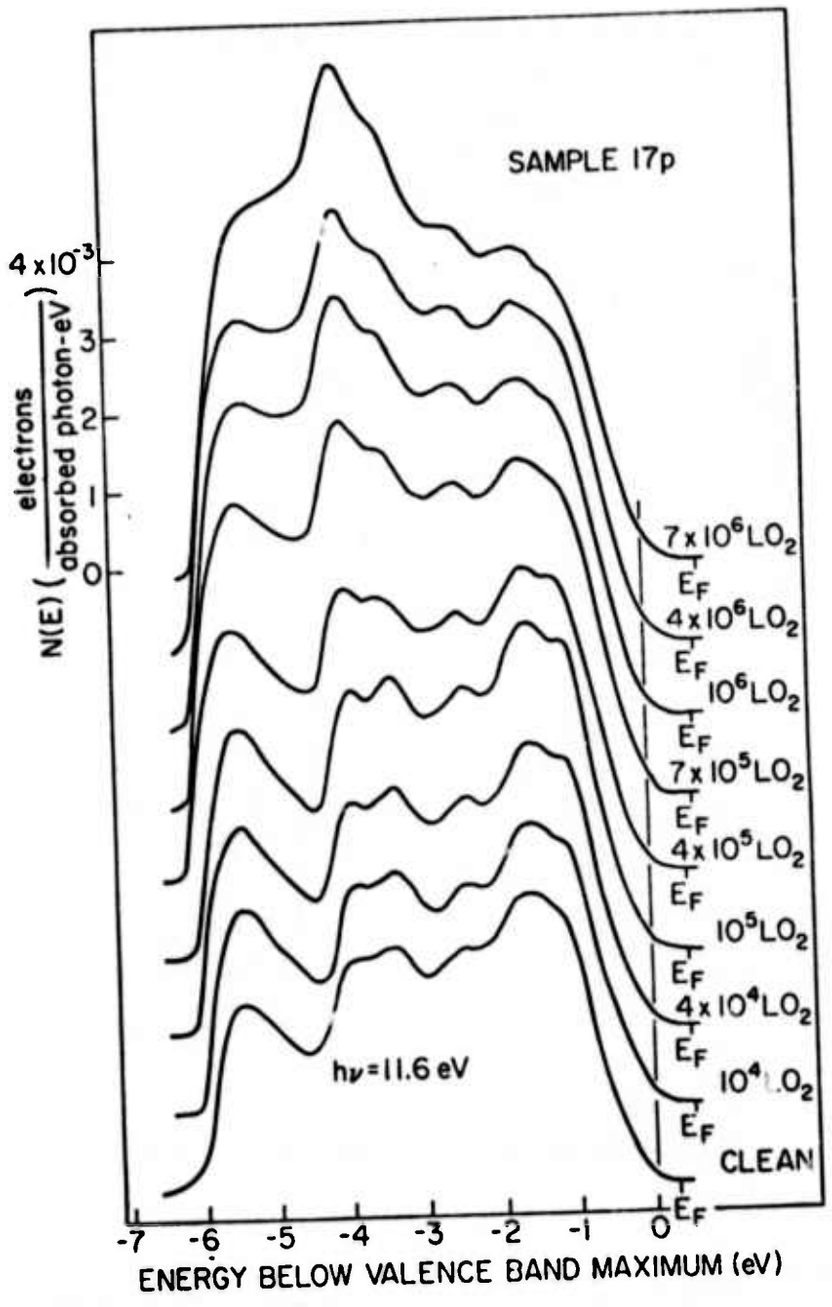

1b

FIG. 1b--photon energy of 11.6 eV.

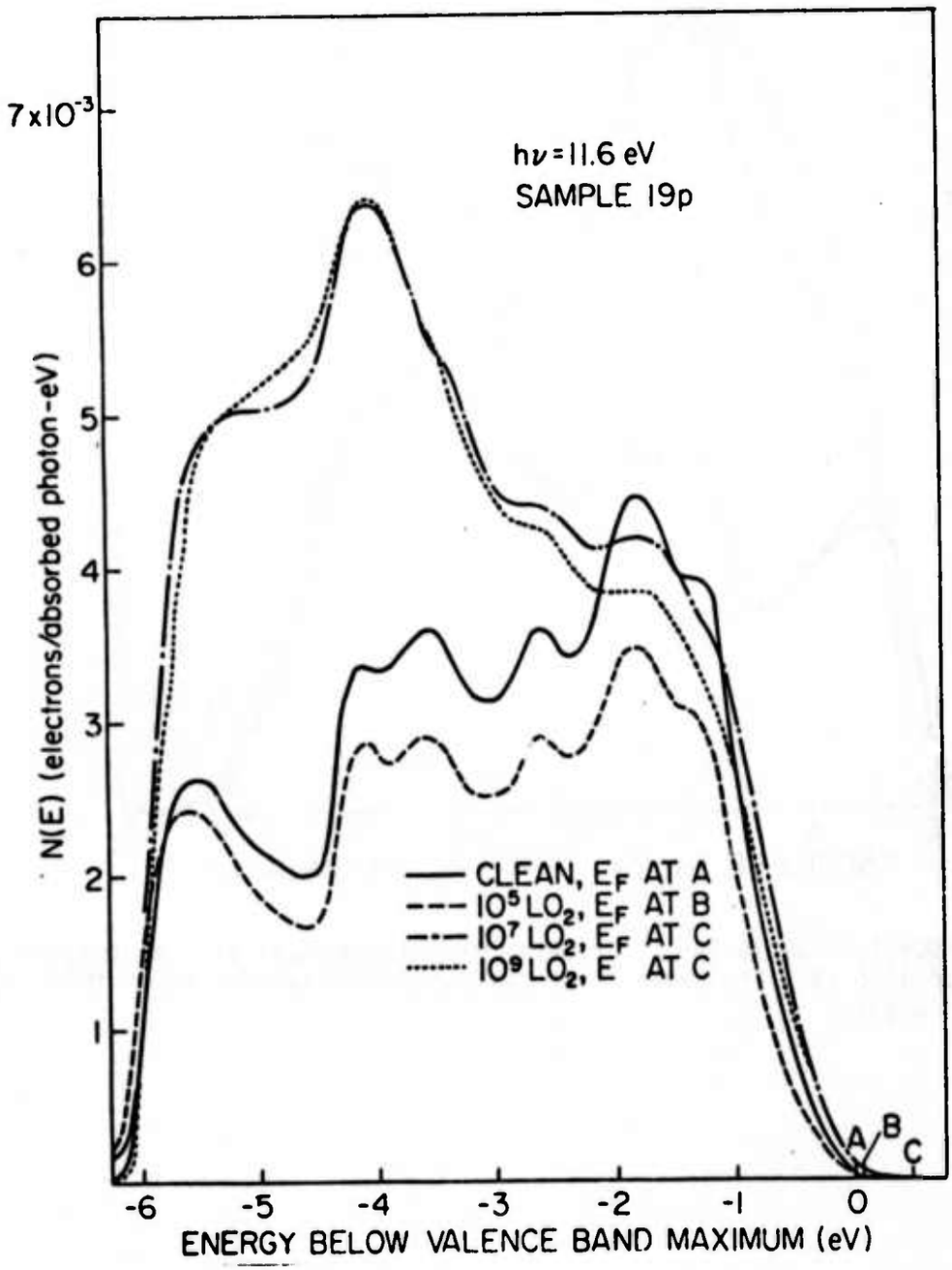

FIG. 2--EDCs for sample 19p for several oxygen exposures at a photon energy of 11.6 eV.

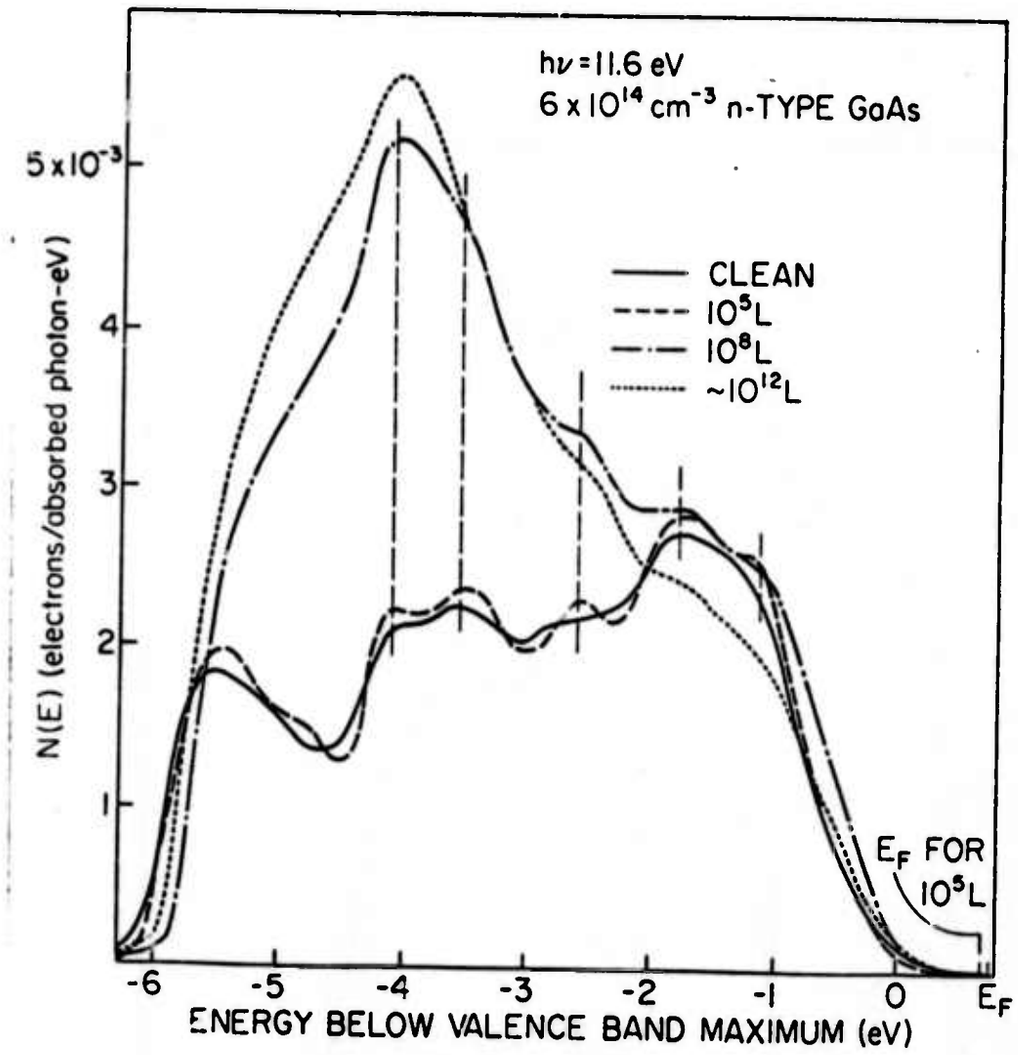

FIG. 3--EDCs for sample 14n for several oxygen exposures at a photon energy of 11.6 eV. The Fermi level was not determined for the $\sim 10^{12}$L O_2 exposure.

and an oxide peak evolves at approximately 4.1 eV below the valence band maximum. This insensitivity of GaAs to oxidation is in qualitative agreement with the sticking coefficient for oxygen on GaAs which has been reported to be 1×10^{-6} to 3×10^{-5}.[10,11]

It is helpful in understanding the behavior of GaAs upon oxidation to contrast it to the behavior of silicon. EDCs for the oxidation of n-type silicon are shown in Fig. 4, taken from the work of Wagner and Spicer.[12] It is important to note that the silicon EDCs show oxygen exposures up to 10^3L, while the GaAs EDCs show oxygen exposures to 10^7L and beyond. In the case of Si, there are large changes even with 100L exposure. The most important change in the silicon data is the disappearance of the surface state peak located approximately 0.5 eV below the valence band maximum after 10^3L O_2 exposure. Note also that the yield (represented by the area under the EDC) increases with oxygen exposure. Exposures beyond 10^3L (not shown here, see Reference 12) increase the yield further and lead to the growth of the oxide peak located at the extreme lower energy edge of the EDC. Evidence for this peak begins to appear for 10^3L exposure.

In contrast to Si, the GaAs EDCs show almost no change up to about 10^5L oxygen exposure, after which an oxide peak develops. It is very important to notice that there is no selective removal of structure in the GaAs EDCs as oxidation progesses, in contrast to the removal of the surface state peak in the Si EDCs. This fact is important evidence for the lack of filled surface states in the band gap of GaAs, and for the lack of strong structure in any filled surface states located below the valence band maximum.

It is also important to note that there is no significant increase in the GaAs yield with oxygen exposure until the oxide peak grows, and then

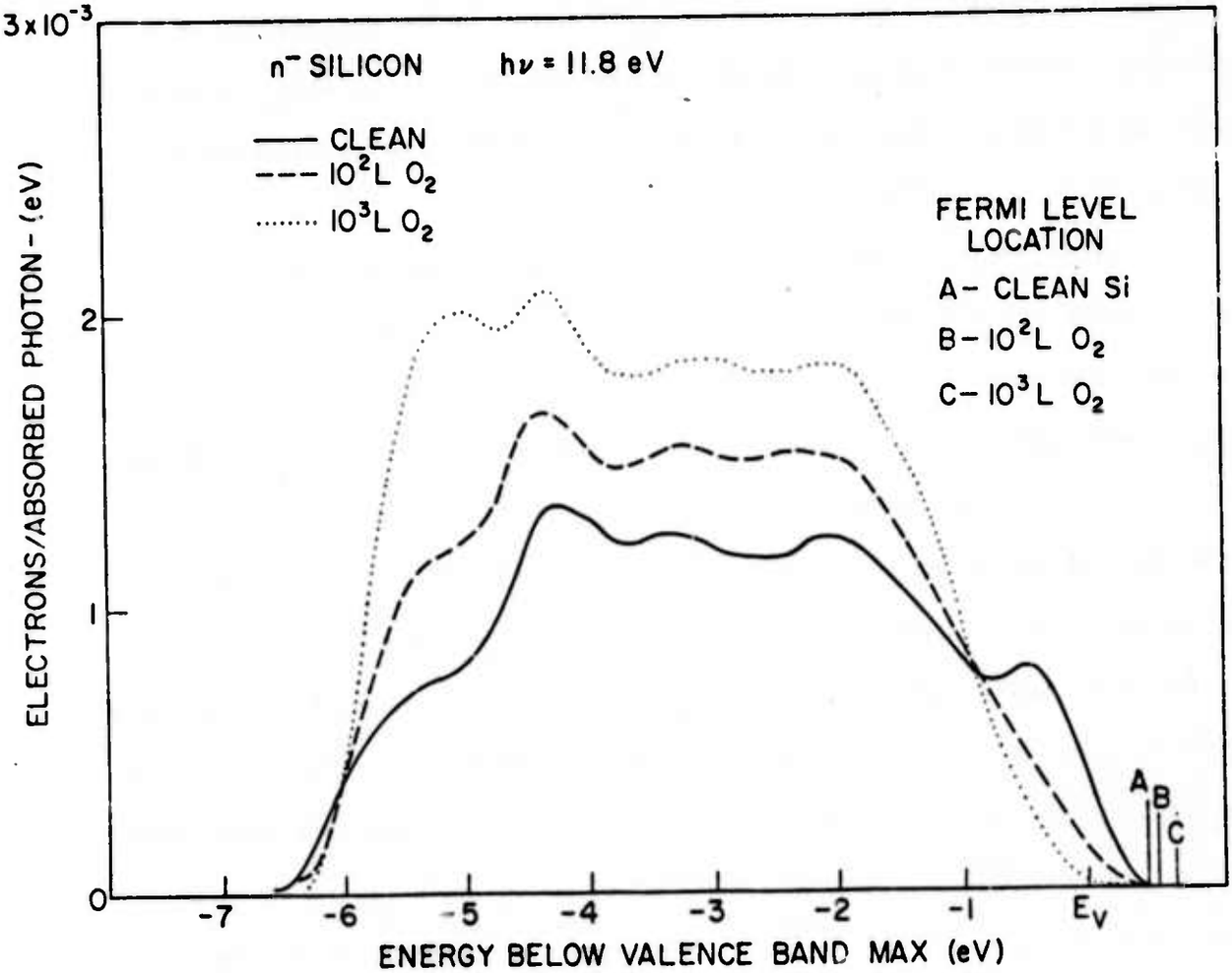

FIG. 4--EDCs for n-type silicon as a function of oxygen exposure. Taken from Wagner and Spicer, Ref. 12.

the increase in yield is approximately enough to account for the oxide peak, leaving the magnitude of the other peaks largely unchanged.

The development of the oxide peak at 4 eV below the valence band maximum can be seen in Fig. 1(b) for sample 17p. The growth of the peak begins at an exposure of 4×10^5 L. By 7×10^5 L it is well developed, and the peak shows only small changes after 7×10^6 L. The growth of the peak was not followed in detail for the other two samples because the oxygen exposures were made at intervals too wide to see the development of the peak. For sample 19p, Fig. 2 shows that the oxide peak is not present at the 10^5 L exposure, but it is fully developed by the 10^7 L exposure. For sample 14n, Fig. 3 shows that the oxide peak is not present at the 10^6 L exposure, but is fully developed at approximately 10^8 L. The fact that a larger O_2 exposure was required to produce measurable changes on n-type GaAs than on p-type GaAs is in contrast to the results of Dorn, Lüth and Russell,[10] and will be discussed below.

For all three samples the oxide peak is located 4 eV below the valence band maximum. A peak on the clean GaAs is also located at 4 eV below the valence band maximum. Since the peaks present on the clean GaAs EDCs are still present on the oxidized GaAs EDCs, it is difficult to decide how much the apparent location of the oxide peak is influenced by the presence of the peaks from the clean GaAs. EDCs from GaAs are dominated by "direct" transitions,[5,13] that is, k-conservation causes peaks to move in both initial and final state energy, and to suddenly appear and disappear as the photon energy is changed. However, in the photon energy range over which we can follow the oxide peak here, 10.2 to 11.8 eV, the peak position below

the valence band maximum is constant to within 0.1 eV for both the clean and oxidized GaAs. Between 11.4 and 11.8 eV, the magnitude of the peak at -4 eV on the clean GaAs decreases relative to the nearby peaks. At a photon energy above 11.8 eV, it may disappear completely, allowing the location of the oxide peak to be measured with more confidence. One would expect that the oxide layer would not be crystalline enough to be subject to k-conservation so that the location of the oxide peak in the EDCs should remain at a constant energy below the valence band maximum as the photon energy is increased. Thus, it would appear to be useful to make additional photoemission measurements at intervals of several tenths of an electron volt in photon energy in the photon energy range of 11.6 to 20 eV.

The oxide peak at 4 eV below the valence band maximum in the GaAs EDCs falls at a higher energy than the oxide peak in the Si EDCs. The oxide peak in the Si EDCs is located approximately 6 eV below the valence band maximum, and is only partially visible in the EDCs measured at a photon energy of 11.8 eV.[12]

The oxide peak appears to be quite broad--at least 4 eV wide. The fact that structure characteristic of the clean GaAs is also visible in the EDCs indicates that the oxide layer is thin enough so that there is appreciable electron emission from the GaAs below the oxide layer.

In Fig. 3 we show an EDC for an O_2 exposure of approximately 10^{11} to 10^{12}L (oxygen pressure up to 10 Torr for about 17 hours). For this exposure the oxide peak has increased in magnitude slightly, and the peaks associated with the clean GaAs have decreased somewhat. These facts indicate that the oxide thickness has increased by a small amount. However, the differences between the EDCs for 10^{8}L and for 10^{11}-10^{12}L are quite small considering the 3 to 4

orders of magnitude increase in O_2 exposure. This very slow oxidation of GaAs at these large exposures is in qualitative agreement with the slow uptake of O_2 by GaAs reported by Rosenberg.[14]

The width of an EDC, at a given photon energy, is a measure of the vacuum energy relative to the valence band maximum. The electron affinity is given by

$$\chi = h\nu - w - E_g \quad ,$$

where χ is the electron affinity, w the width of the EDC, E_g the band gap, and $h\nu$ the photon energy used to measure the EDC. Gas adsorption on many materials can cause changes in the electron affinity of several tenths of an electron volt. For example, an exposure of 10^3L of oxygen in Si causes the electron affinity to increase by just over 0.2 eV.

Careful measurement of the widths of the EDCs shown in Figs. 1-3 shows only a very small change in the electron affinity of GaAs with oxygen exposure. For samples 19p and 17p there is a drop in electron affinity, or increase in the width of the EDCs of up to 0.1 eV at about 10^5L O_2 exposure, but for larger exposures the electron affinity returns to its original value. The measurements of the width of the EDCs are made by extrapolating the edges of the EDC to the baseline and measuring the distance between the extrapolated edges. Since there is some arbitrariness in making the extrapolation, especially when the shape of the EDC changes with oxidation, the measurements of the change in electron affinity are difficult to make accurately. The observed drop in electron affinity of up to 0.1 eV is about equal to the expected error. However, the measured changes in electron affinity do show a trend to a slight drop at about 10^5L for both samples, and measurements from EDCs at several photon energies fit the same trend.

Measurements from EDCs for sample 14n do not show a drop in electron affinity at 10^5L. For the 10^8L exposure, some of the EDCs show an apparent rise in electron affinity of 0.1-0.2 eV, that is, the EDCs become narrower. The EDCs showing this change in width were taken with a collector can having an oxidized Cu collection surface. These EDCs showed sharper structure than EDCs for the 10^8L exposure made with a clean Cu collection surface. The 10^8L EDCs made with the clean Cu collector did not show the apparent rise in electron affinity. The narrowness of the EDCs taken with the oxidized collector was evident independent of photon energy throughout the energy range measured, 7.7 eV - 11.8 eV. Therefore, it appears that the apparent rise in electron affinity was caused by the oxidized collector can having a more uniform work function than the clean Cu collector, and there was no real change in electron affinity. Thus the p-type material showed a small decrease in electron affinity for intermediate oxygen exposures, while the n-type GaAs showed no measurable change in electron affinity.

As Figs. 1-3 show, the shape of the EDC does not change much beyond 10^8L O_2 exposure. In an effort to produce more oxide, and because experiments to study practical oxides are often performed on oxides formed by high temperature oxidation,[15] sample 17p was heated in oxygen after the 4×10^7L exposure had been made. The sample was heated to 350° C, as measured by an infrared pyrometer, and was then exposed to O_2 at a pressure of 1×10^5 Torr for 15 minutes. The tungsten sample heater was then turned off and the sample allowed to cool in O_2 for 10 minutes before the O_2 was pumped out and EDCs were measured. The resulting EDCs are shown in Fig. 5. The solid line EDC shows the 4×10^7L O_2 exposure before heating, the dotted EDC was measured immediately after heating, and the dash-dotted EDC was measured about 20 hours after heating. The dotted EDC represents a transient

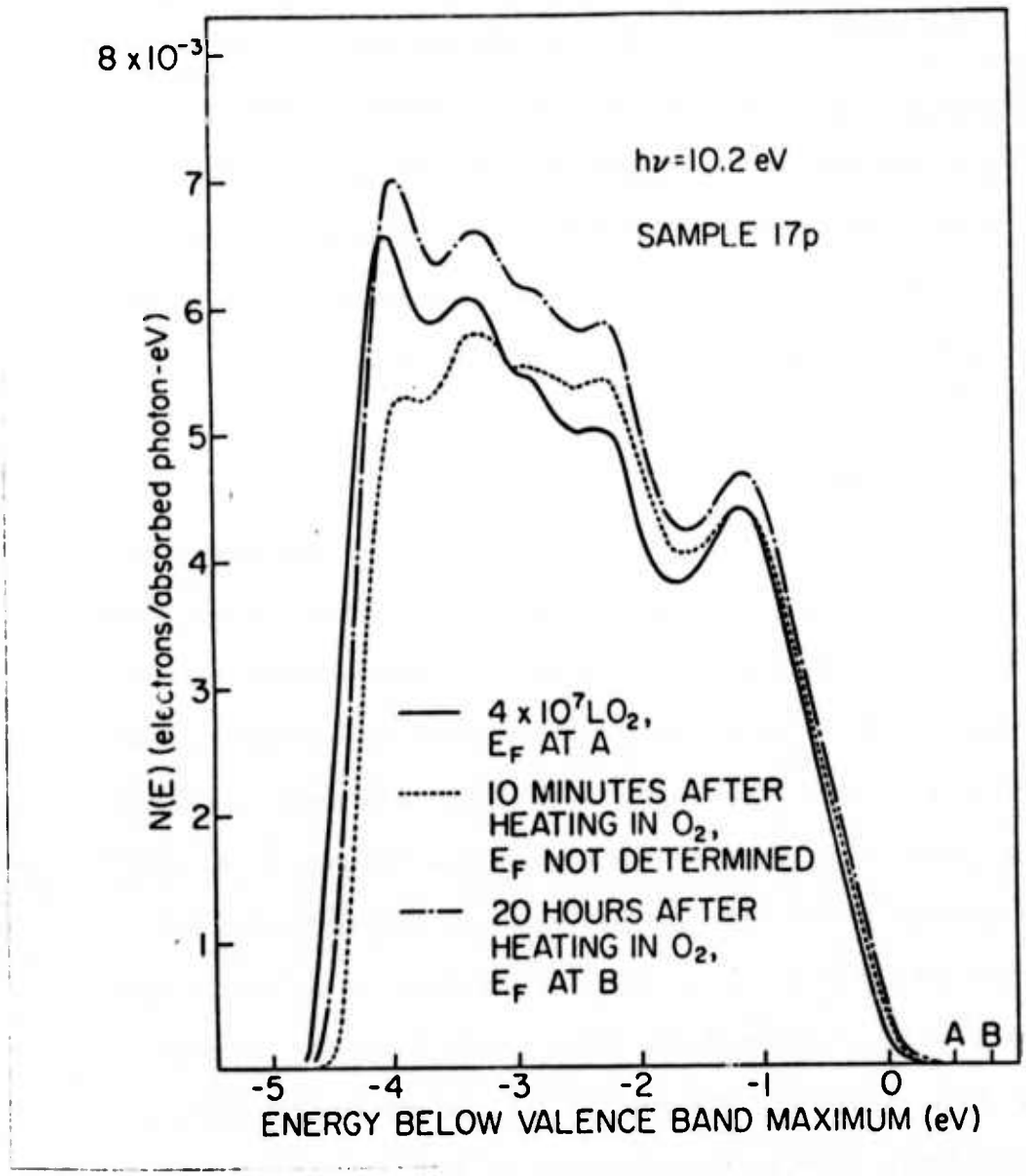

FIG. 5--EDCs for sample 17p at a photon energy of 10.2 eV showing the effect of heating the sample in oxygen. The dotted line shows a transient condition which changed rapidly. The Fermi level was not determined for the dotted EDC.

condition; 30 minutes after heating the sample the EDCs were the same as those taken 20 hours later. For the transient EDC the electron affinity is about 0.2 eV higher than it was for the 4×10^7L exposure; then the electron affinity stabilized at 0.1 eV greater than the value for the 4×10^7L O_2 exposure. The Fermi level position was not determined for the transient EDC, but for the top EDC it moved to 0.25 eV above the position for the 4×10^7L EDCs or 0.6 eV above the Fermi level position for the clean EDCs.

B. Fermi Level Movement

The movement of the position of the Fermi level on the EDCs has been mentioned for the sample heated in oxygen. Figure 6(a) summarizes the Fermi level movement for all the O_2 exposures studied. The figure shows that the Fermi level movement is quite different for the n and p-type samples. For the n-type samples, the Fermi level is pinned at about mid-gap by a band of empty, Ga-derived surface states extending upward from mid gap.[16] As Fig. 6(a) shows, the pinning of the Fermi level for the n-type samples is not affected by the oxygen exposure, up to the 10^6L exposure. The drop in pinning position at 10^6L is not understood, particularly since the pinning position for the 10^8L exposure is the same as for the exposures $\leq 10^5$L. Unfortunately, the Fermi level position for the 10^{11}-10^{12}L exposure could not be determined because the Cu evaporator had been exhausted of Cu previous to that exposure. Only one O_2 exposure was made for sample 18n, and it did not affect the Fermi level pinning position.

The p-type samples behave differently from the n-type samples. The band of empty surface states does not affect the position of the Fermi level for the clean p-type samples, and there are no filled surface states in the lower half of the band gap.[16] Thus, the Fermi level is not pinned

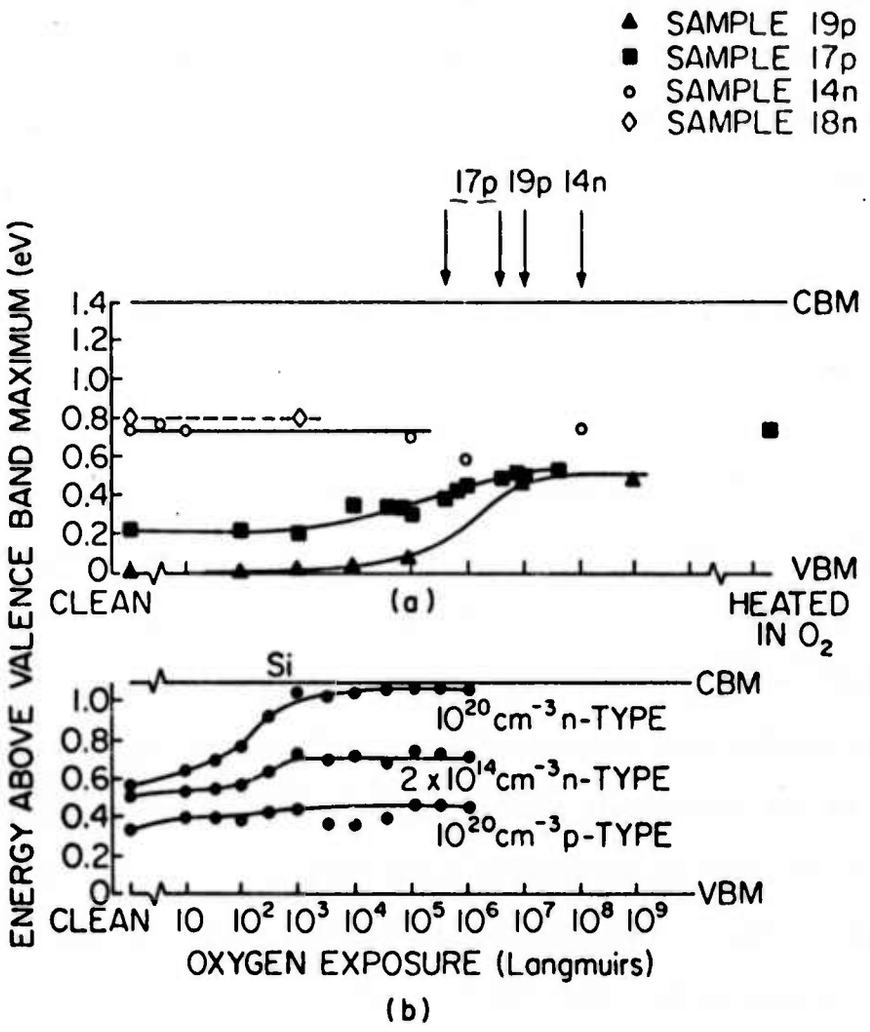

FIG. 6--a) The surface position of the Fermi level in the band gap as a function of O_2 exposure for four differently doped GaAs samples. b) The surface position of the Fermi level in the band gap as a function of O_2 exposure for three differently doped Si samples. (Part b taken from Wagner and Spicer, Ref. 12).

on the clean p-type GaAs samples and the bands are flat. However, as Fig. 6(a) shows, the Fermi level position begins to move up, that is the bands begin to bend down, after an O_2 exposure of 10^4 L. For both p-type samples the pinning position saturates about 0.5 eV above the valence band maximum, or 0.2 eV below the pinning position for the n-type GaAs. Also shown is the Fermi level position for the sample which was heated in O_2. As can be seen, the pinning position for the p-type sample heated in O_2 is the same as the pinning position for the n-type samples.

Figure 6(b) shows similar data for the oxidation of Si, taken from Wagner and Spicer.[12] This figure is included to emphasize the difference in oxidation behavior of Si and GaAs. For Si, the Fermi level is pinned by surface states on both n and p-type samples. Oxidation removes the Si surface states and destroys the Fermi level pinning on the n-type samples. On the p-type Si the Fermi level pinning is not destroyed by the oxidation, although the oxygen removes the surface state peak from the EDCs. A small density of surface states remains as interface states after the oxidation, and causes the pinning on the p-type Si.[12]

The Fermi level pinning on the GaAs is quite different from that of the Si. Oxidation does not destroy the pinning on the n-type samples, so we conclude that oxygen leaves enough of the empty surface states unaffected to provide pinning. However, oxygen causes pinning on the p-type samples. The pinning on the p-type samples is probably caused by the creation of a small number of interface states. No emission from the interface states can be seen in the GaAs EDCs. Apparently the density of interface states is too low to be detected by photoemission.

In Fig. 6(a), the vertical arrows labeled 19p and 14n mark the O_2 exposure for which the EDCs characteristic of the oxidized GaAs appear. For sample 17p, two arrows are shown, indicating the range over which the oxide peak was seen to grow. For the p-type samples, the formation of the oxide peak and the movement of the Fermi level pinning position takes place over the same range of oxygen exposure.

Figure 6(a) shows that the Fermi level pinning behavior is different for the n and p-type GaAs samples. Another difference in oxidation behavior is the fact that it takes a somewhat higher oxygen exposure for the n-type material to produce the oxide peak in the EDCs. For sample 14n, EDCs after the 10^6 L exposure had the same shape as the EDCs from the clean sample. In contrast, EDCs from sample 17p with a 10^6 L exposure showed the oxide peak almost completely developed.

Figure 7 illustrates another difference between the oxidation of n- and p-type GaAs. EDCs showing the fully-developed oxide peak are shown, replotted from Figures 1-3. The p-type samples have very similar EDCs. The EDC from sample 14n also has a similar shape, but the low energy shoulder which is strong for sample 19p and somewhat weaker for sample 17p is almost missing for sample 14n. (The EDC for sample 14n is narrower than those for samples 17p and 19p because the EDC for sample 14n was made with the oxidized collector. As discussed above, the narrowness is an artifact, and does not represent a real difference in electron affinity.) The fact that the 14n EDC has a lower magnitude than the p-type EDCs may be caused by small errors in measuring the yield.

C. Comparison with Other Work

The small differences in behavior between the n and p-type GaAs upon oxidation seen here are interesting in view of the differences reported by

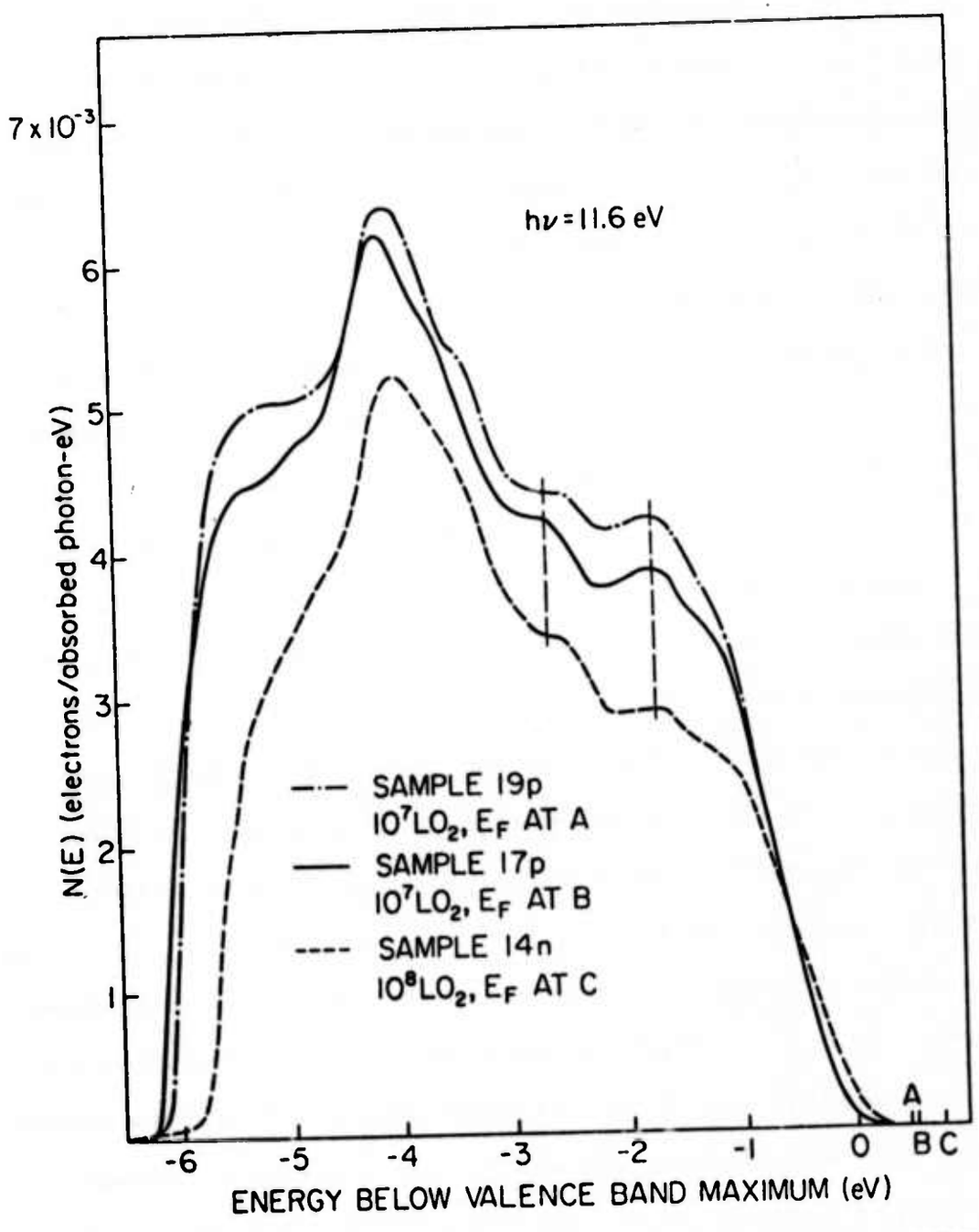

FIG. 7--EDCs at a photon energy of 11.6 eV for three different dopings of GaAs given large O_2 exposures.

Dorn, Luth and Russell.[10,11] They report that for a dose of 7×10^6 L of O_2 the LEED pattern on n-type GaAs was very weak, while the same O_2 exposure affected the LEED pattern of p-type GaAs only slightly. Electron loss spectra are slightly different for the n- and p-type samples, and Auger spectra show that the As peak height decreases with O_2 exposure for p-type GaAs, but not for n-type material. Based on Auger measurements they find a higher sticking coefficient and faster oxygen uptake on n-type GaAs than on p-type GaAs. Energy loss spectra also show changes at lower oxygen coverage for n-type than for p-type GaAs. This result is opposite to that seen here, where larger exposures are required to produce a change on the n-type samples. This discrepancy could be caused by differences in properties to which the techniques of photoemission, Auger, and electron energy loss are sensitive. The differences in oxygen uptake could also be caused by differences in the quality of the cleaves used in the experiments, rather than differences caused by conductivity type. For example, Ibach, Horn, Dorn and Lüth have recently reported that the sticking coefficient for O_2 on Si is strongly influenced by the step density on the Si surface.[17]

Dorn, Lüth and Russell[10] found that for n-type GaAs, the first detectable oxygen Auger signal appeared at 100L O_2 exposure, while for p-type GaAs a 5000L O_2 exposure was required to produce a measurable oxygen Auger signal. As Figs. 1-3 and 6 show, for the n-type sample studied here, there was no detectable effect of the oxygen exposures below 10^6 L. However, for the p-type samples, Fermi level movement was detectable starting at about 10^4 L exposure, and for sample 17p the changes in the shape of the EDCs began at about 10^5 L. Thus the Fermi level movement for the p-type samples is

the feature of the photoemission data which is most sensitive to oxygen coverage, and is approximately as sensitive as Auger measurements. For the n-type sample, however, the photoemission measurements appear to be much less sensitive to oxygen coverage than Auger spectroscopy.

Lüth and Russell[11] report that the exposure required to produce saturated oxygen coverage of about a half-monolayer (where a monolayer is defined as one O atom for each surface Ga or As atom) is 10^7L for p-type GaAs and 5×10^6L for n-type GaAs. Figure 6 shows that the value of 10^7L for p-type GaAs agrees quite well with the exposure at which the Fermi level movement saturates and the growth of the oxide peak in the EDCs is completed. Our EDCs for sample 14n do not show the oxide peak at 10^6L exposure, and show it fully developed at 10^8L exposure. Therefore, the value of 5×10^6L for saturation coverage[11] falls within the limits between which the oxide peak develops in the EDCs.

D. Site of Oxygen Adsorption

Figure 8 shows the model for the clean GaAs (110) surface derived from photoemission measurements and from the bond orbital model of Harrison and Ciraci.[16] The empty surface state band in the upper part of the band gap is primarily Ga-derived, while the filled surface state band, which is masked by the valence band, is primarily As-derived. Our measurements detect the position of lower edge of the band of empty surface states, but we cannot directly measure the empty surface state distribution. The peak for the empty surface state band in Fig. 8 is drawn to schematically indicate the data of Eastman and Freeouf.[18] We can detect no evidence for filled surface states in the bandgap region, and we find no evidence for structure due to filled surface states below the valence band maximum.[16,19] Thus,

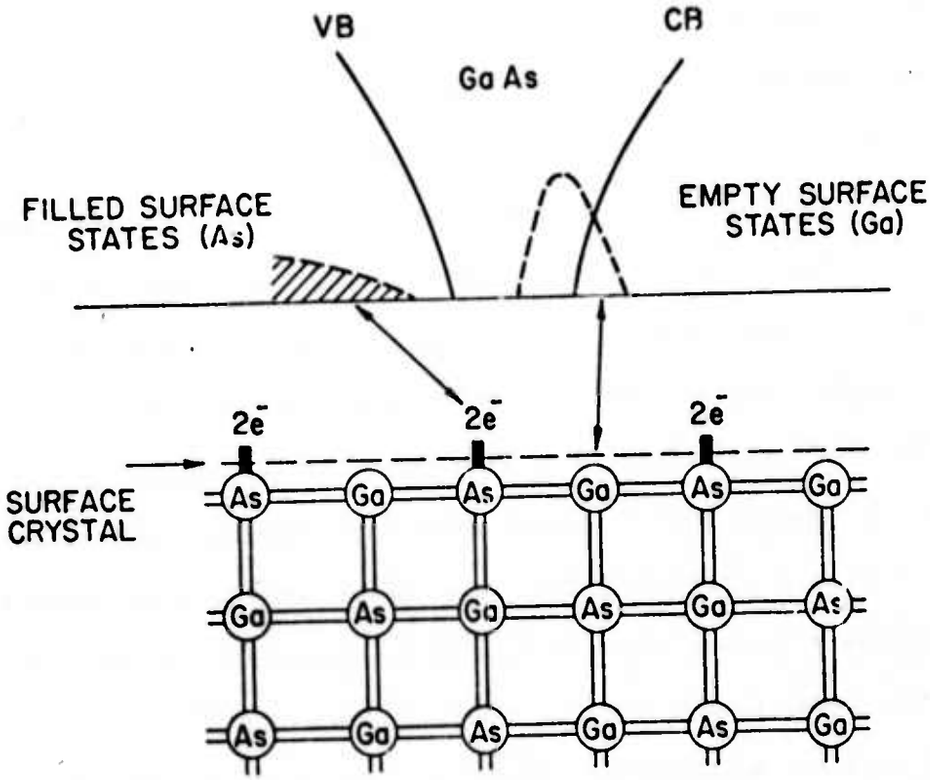

FIG. 8--Model for the surface state distribution on the clean (110) GaAs surface. Our measurements accurately locate the lower edge of the empty surface state band; the distribution of empty surface states as drawn is suggested by the work of Eastman and Freeouf.[18] No emission from filled surface states is detected; the indicated distribution is intended only to suggest that any filled surface states lie somewhere below the valence band maximum and are lacking in strong structure. The association of the filled surface states with surface As atoms and empty surface states with surface Ga atoms is based on calculations from the bond orbital model.[16]

the filled surface state distribution indicated in Fig. 8 has not been directly measured, and is intended to show that any filled surface states lie somewhere below the valence band maximum, and lack any strong structure. If one assigns one electron from each atom to the covalent bands (an oversimplified model), surface As atoms have their normal 5 valence electrons, leaving two electrons in a dangling bond, and the surface Ga atoms have 3 valence electrons, leaving an unoccupied dangling bond. Our evidence for the band of empty surface states is the Fermi level pinning on n-type GaAs;[16] Ludeke and Esaki subsequentally have also detected the empty surface state using low energy electron loss spectroscopy,[20] while Eastman and Freeouf[18] have detected it with photoemission partial yield spectroscopy. Ludeke and Esaki[20] identify the empty surface state as being Ga-derived. Eastman and Freeouf[21] have also identified the empty surface state on the closely related material GaSb as being Ga-derived. We have generalized this model to all faces of all III-V compounds.[22]

The fact that the adsorption of oxygen on GaAs (110) does not change the Fermi level pinning on n-type GaAs indicates that the oxygen adsorption does not completely remove the empty surface states, as oxygen adsorption does on n-type Si.[12] However, the oxygen could reduce the density of empty surface states, leaving a high enough density of empty surface states to maintain the Fermi level pinning. The fact that the Fermi level pinning caused by the Ga-derived empty surface states is not changed by oxidation has led us to speculate that the oxygen bonds preferentially to the surface As atoms.[16] If the oxygen is bonded as atomic oxygen to the surface As atoms, the oxygen would have its normal chemical valence of -2, both

dangling As electrons would be involved in bonds to the O atoms, and the surface Ga atoms would be undisturbed.

Available experimental evidence does not all support the surface As atom as the site for initial oxygen adsorption, however. Ludeke and Koma[23] have measured the second derivative of the low energy electron loss spectrum for the (100) GaAs surface as a function of oxidation. They find that the spectral feature at about 20 eV, which represents excitations from the Ga 3d core level into the Ga empty surface state, is greatly reduced in size by oxygen coverage as little as 0.2 of the saturation coverage. One difficulty with comparing their work to the work reported here is that the electron energy loss experiment involves irradiating the sample surface with electrons. Electron irradiation can cause adsorbates to desorb or change their bonding state.[24] In fact, Ranke and Jacobi have studied the effect of electron irradiation on oxygen adsorbed on the GaAs (111) faces.[25] They find that oxygen adsorbs as an O_2 molecule. Subsequent irradiation with electrons dissociates the O_2 molecule, and the atomic oxygen diffuses into the lattice and reacts with the Ga and As. As is depleted in this oxide layer, a fact which they interpret as being caused by sublimation of As_4O_6. On the other hand, Dorn, Lüth and Russell[10] looked for, but did not find, such effects on GaAs (110). Thus it is not clear if such effects are present on the (100) surface studied by Ludeke and Koma.[23] Effects such as those caused by electron beam--adsorbate interactions are not expected in photoemission experiments because the photon flux is typically much lower than the electron flux, and the majority of the photons are absorbed far below the surface of the GaAs.

Luth and Russell[11] have used low energy electron loss spectroscopy to study oxygen adsorption on GaAs (110). Their technique involves a retarding potential analyzer and no derivitives of the loss spectrum, rather than a cylindrical mirror analyzer and the second derivative of the loss spectrum used by Ludeke and Koma.[23] They report a surface transition at 18.5 eV, which is the nearest transition to the 20 eV feature reported by Ludeke and Koma.[23] This feature at 18.5 eV may represent the same Ga-3d core to empty surface state transition as the 20 eV transition reported by Ludeke and Koma. Since Lüth and Russell[11] use the loss spectrum directly rather than the second derivative, it is easier to follow the effect of oxygen on their data. As oxygen coverage increases, the peak appears to broaden and move to lower energy until it merges with the plasma loss peak. This broadening would show up as a loss in strength of the second derivative. The movement of the peak could be caused by a shifting of the empty surface state band, or by a chemical shift of the Ga 3d level.

Another fact which suggests that oxygen is preferentially adosrbed at surface Ga atoms is that flash desorption of oxidized GaAs (111) surfaces has shown that Ga_2O is the species evolved.[26] The flash desorption data does not unambiguously identify the surface adsorption site, however. It is possible that any oxygen adsorbed on an As site will combine with a Ga atom as the temperature is raised during the flash desorption experiment. Evidence that this type of surface chemical reaction does occur is given in recent flash desorption studies of Cs and O adsorbed on GaAs (100).[27] Although it is commonly believed that the Cs and O are present on the GaAs surface in the form of a Cs oxide, the flash desorption experiment observed mostly Ga_2O and Cs desorbing from the surface. No Cs oxides were seen in

the experiment, implying that the Cs oxides dissociate and the oxygen reacts with the Ga as the temperature is raised.

One final uncertainty about the site for oxygen adsorption on GaAs is that the bond orbital calculations on which the prediction of bonding to the As side was based[16] involved only the clean GaAs surface. If the calculations were made including an oxygen layer, it is possible that electronic rearrangement would occur which would favor adsorption on the Ga site. Harrison has recently modified the surface model to include vertical displacement of the outer layer of atoms.[28] In this revised model the As atoms move out and the Ga atoms move in by a large fraction of a lattice constant. Oxygen adsorption would likely modify this vertical movement and lead to electronic rearrangement.

As the above discussion indicates, more experimental data is needed to produce an unambiguous model for the adsorption of oxygen on GaAs. It is planned in the near future to use radiation in the 20-200 eV range from the Stanford Synchrotron Radiation Project to look for core level chemical shifts from the surface Ga and As atoms upon oxygen adsorption. Hopefully, this data will give insights into the adsorption site or sites.

E. Oxidation of "Bad Cleave"

The EDCs of Figs. 1-3 show no changes for oxygen exposures below 10^5L. In one case, however, an exposure of 100L O_2 caused large effects in the EDCs. We deliberately attempted to produce a "bad cleave" to see if we could reproduce the filled surface states reported[29] from a GaAs face which has since been characterized as containing many cleavage steps.[16,18] Our bad cleave was made on GaAs sample 14n, and is a different cleave from the one discussed above, in connection with the large O_2 exposures. We did not see emission from filled surface states, but the results, shown in Fig. 9, are nevertheless quite interesting.

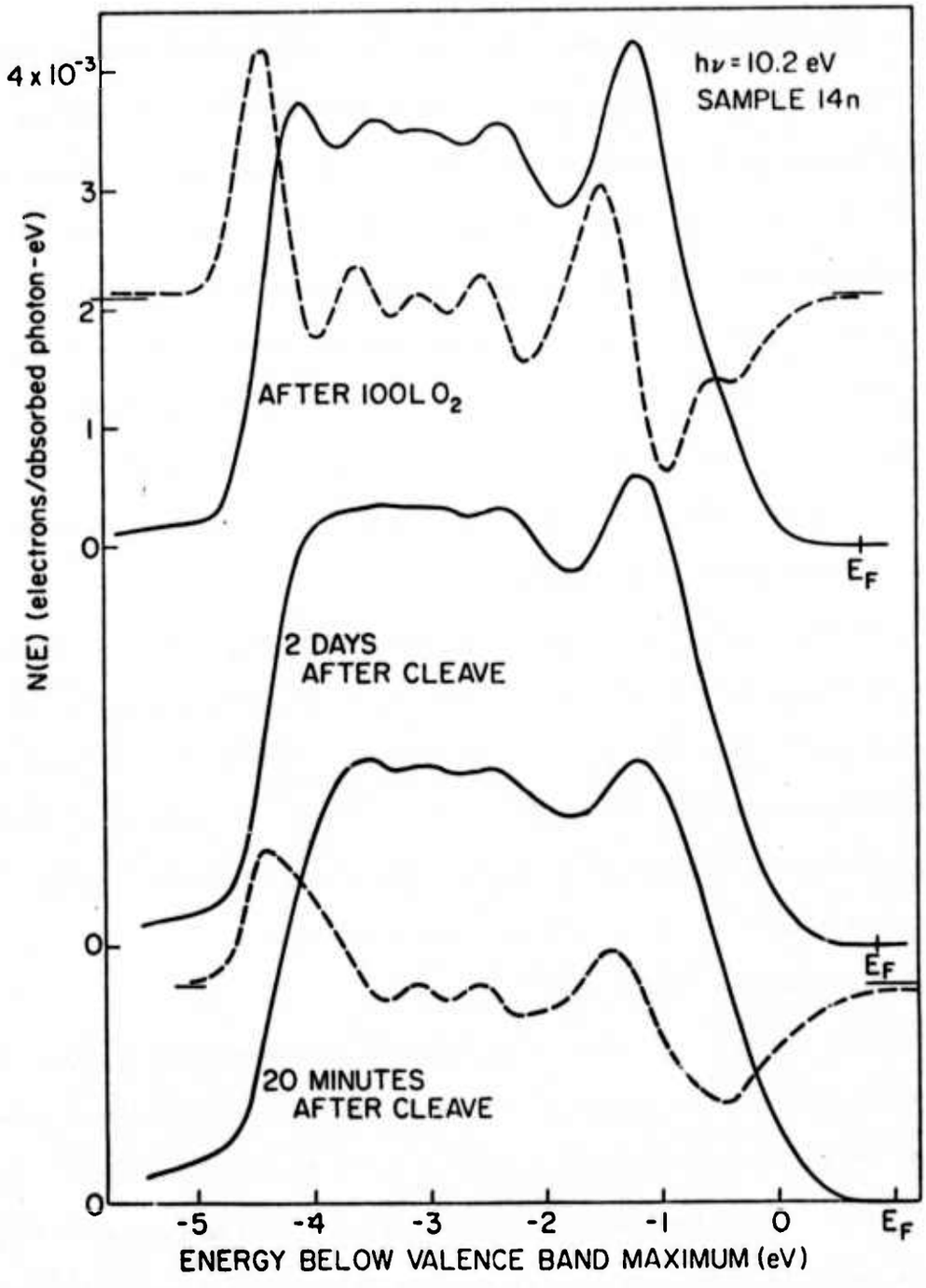

FIG. 9--EDCs at a photon energy of 10.2 eV for a "bad cleave" of sample 14n. Dashed lines are the derivative of the EDCs.

The bad cleave was produced by attempting to force the crystal to cleave at a slight angle to the (110) face. This was done by notching two opposing sides of the crystal about 0.5 mm deep by 0.5 mm wide. The notches were slightly offset, so that if the crystal cleaved along a line connecting the notches, the resulting cleave should be at a slight angle to the (110) face. The cleavage blade was inserted into one notch, and a hard ceramic rod of diameter greater than 0.5 mm was inserted into the other notch. The Cu cleaving anvil pressed on this rod, forcing it into the notch. The resulting cleave did not follow a straight line between the two notches; it cleaved close to a normal (110) plane, except for the last 2 mm where a roughend area formed which connected with the offset notches. To the eye, the cleave did not appear noticeably different from cleaves which produced EDCs of the shape which usually characterizes GaAs.

As Fig. 9 shows, the EDCs produced by this cleave were considerably different from the usual GaAs EDCs. The structure is very broadened, and there are only 4 peaks instead of the usual 5 peaks and a shoulder. The spacing between the peaks is also different from the usual values. After sitting for two days in a vacuum with pressure below 2×10^{-11} Torr (measured on a Redhead gauge), the EDCs became somewhat sharper, although the usual structure is still not clearly present. An EDC representative of this condition is shown in the middle of Fig. 9.

When the cleave was exposed to 100L of O_2 the structure associated with normal, or "good" cleaves became apparent, and the EDCs became indistinguisable from EDCs characteristic of normal, or "good" cleaves. An EDC made subsequent to the 100L O_2 exposure is shown at the top of Fig. 9. To emphasize the changes from the initial bad cleave to the cleave after the 100L

exposure was made, first derivatives of these EDCs are also shown in Fig. 9. The first derivatives were made by detecting the second harmonic of the AC modulation voltage used to produce the EDCs. After the 100L O_2 exposure, the sample was exposed to 10^3L and 10^4L of O_2, but no further changes were detected.

One may ask if the effect seen above could have been caused by a change in the resolution of the energy analyzer. The energy resolution can be determined by measuring the broadening of the Fermi edge on the Cu emitter used to determine the position of the Fermi level on the EDCs. Measurement of the broadening from 10% to 90% of the Fermi edge height shows no difference before and after the 100L O_2 exposure. Furthermore, the Fermi edge broadening of 0.23 ± 0.03 eV for this experiment is typical of the value found in other experiments with this system, for which normal EDCs were produced. Therefore, we conclude that the effect shown in Fig. 9 is a real effect, not caused by a change in the resolution of the energy analyzer.

The origin of the effect shown in Fig. 9 is not known. The effect may have been caused by surface strains caused by attempting to force the cleave to propagate in a direction other than the usual direction. These surface strains could have caused distortion of the energy bands at the surface, leading to the distorted EDC. After two days, the distortion of the EDCs was less, suggesting that the strain was disappearing. The oxygen would then have acted to further relieve the strain.

The appearance of the cleavage face in terms of visible steps or roughness, does not seem to be correlated with the occurance of normal or distorted EDCs. The "bad cleave" discussed above does not appear to be noticeably

different from cleaves which produce normal EDCs. Therefore, the variations in the cleave which produce the different EDCs must be on a microscopic scale. Henzler[30] has pointed out that the number of visible steps in a cleaved surface is not a good measure of the quality of the surface. Whatever the origin of the effect, it demonstrates that photoemission can be very sensitive to subtle differences in surface structure.

In several cases with "good" cleaves producing normal EDCs we have noticed a slight improvement in the sharpness of structure in the EDCs upon O_2 or even Cs adsorption. However, in those cases the effect was small enough that an improvement in the energy resolution of the analyzer cannot be ruled out.

IV. RESULTS AND DISCUSSION - CO

Since the sticking coefficient for O_2 on GaAs is so low, there is some question in making the large O_2 exposures reported above as to whether the observed results could be caused by a residual gas in the system. The residual gas partial pressure usually increases in a vacuum chamber when a gas is leaked into the system, so the question of the effect of residual gases is important. In order to directly check on the effects of residual gases, we deliberately exposed sample 17p to two common residual gases: CO and H_2. The CO results are reported in this section, while the H_2 results are given in the next section. Happily, the results show that CO and H_2 contamination could not have been important in our O_2 results.

The CO and H_2 exposures were made on a fresh cleave of sample 17p which had not been used for the O_2 exposures. Figure 10 shows the results of CO adsorption on sample 17p. As can be seen from the figure, the clean EDCs appear to be very similar to the "bad cleave" discussed above. However,

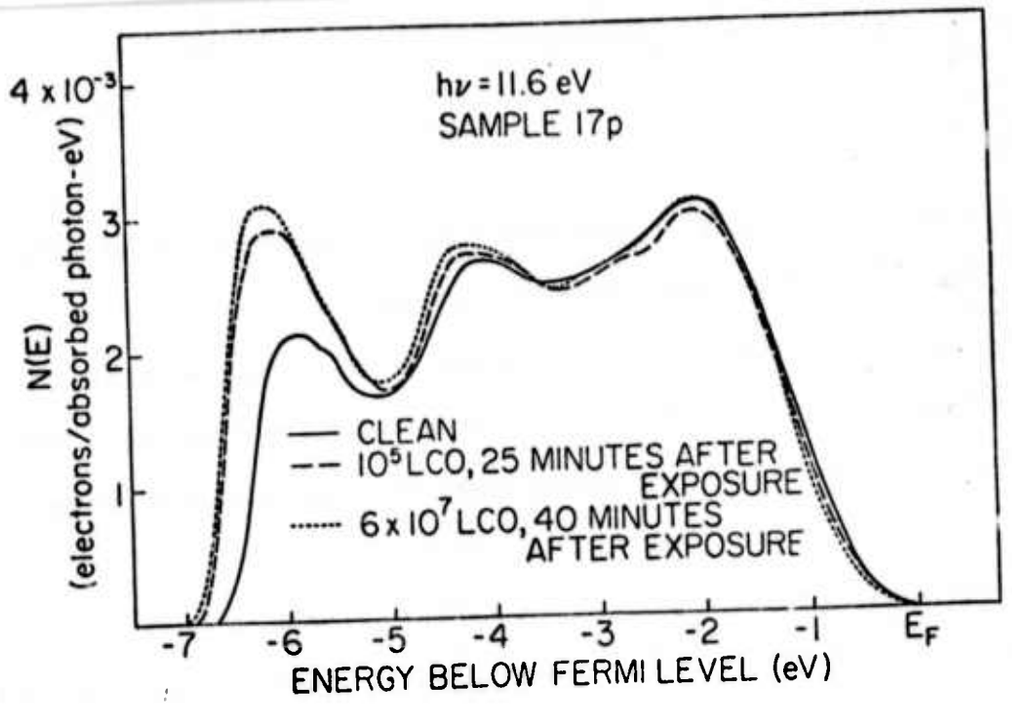

10a

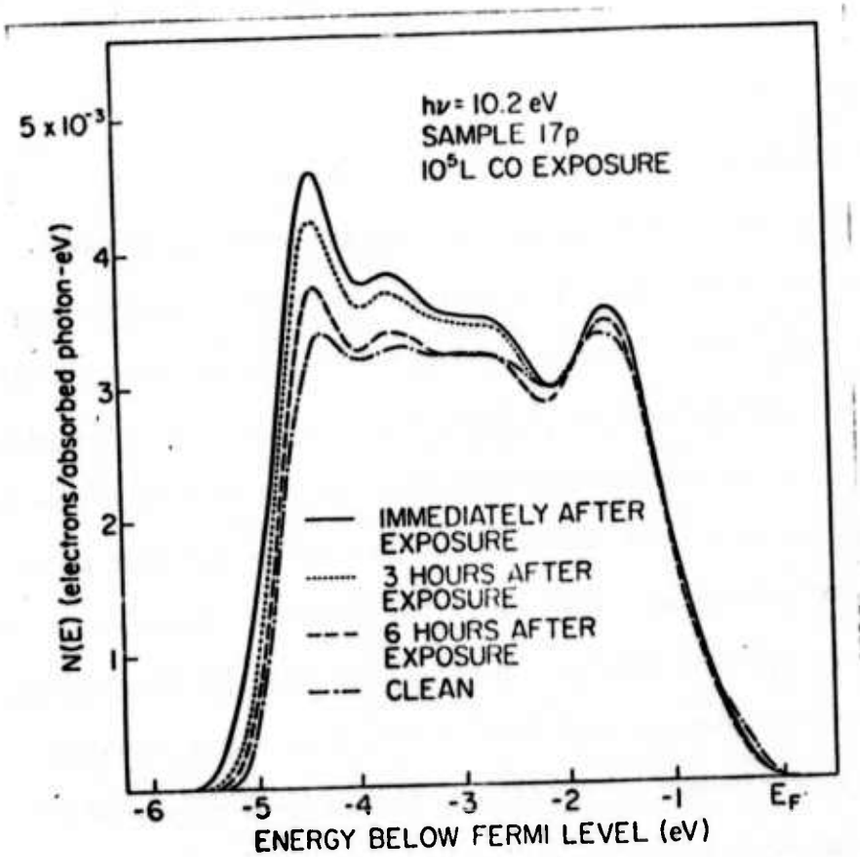

10b

FIG. 10--Results of CO exposure on GaAs. a) EDCs for two CO exposures at $h\nu$ = 11.6 eV, b) EDCs showing change with time of 10^5L CO exposure, for $h\nu$ = 10.2 eV.

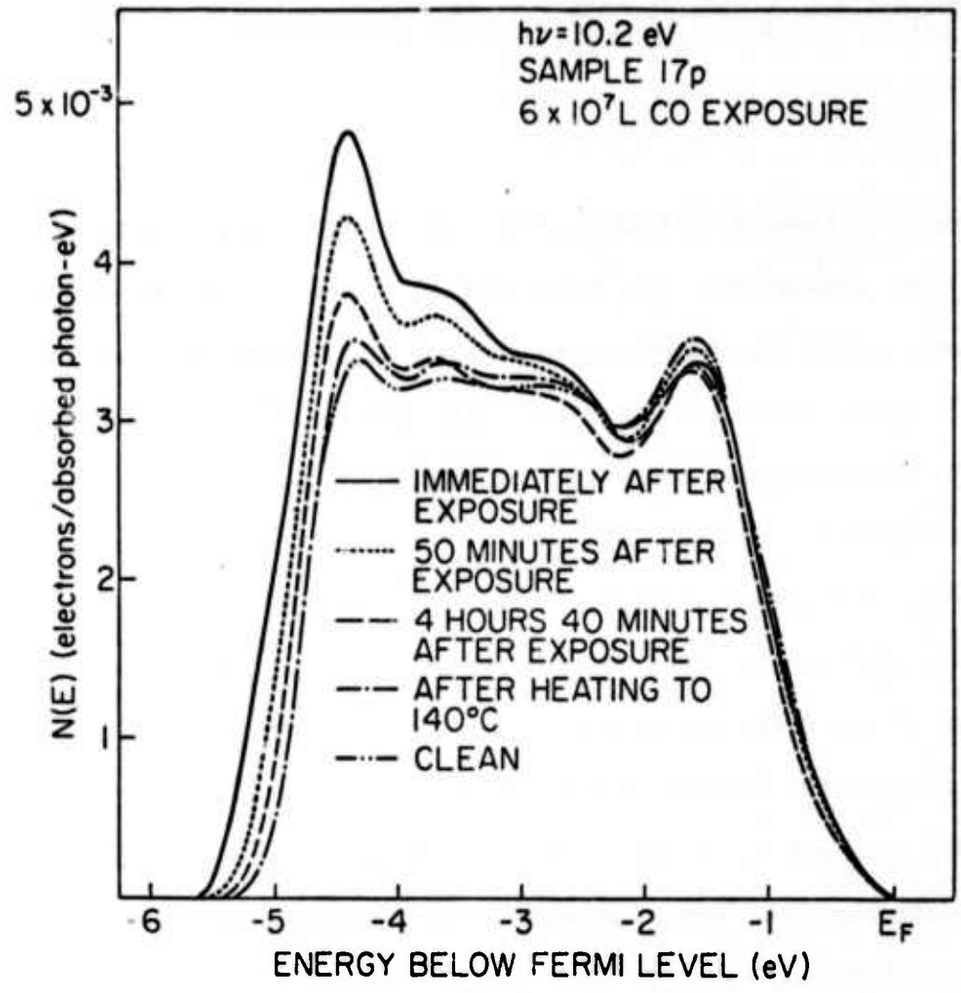

10c

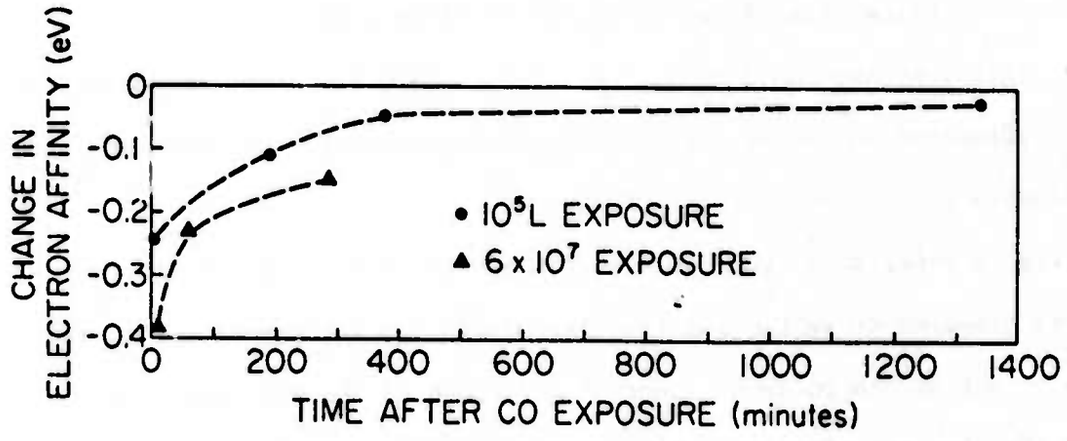

10d

FIG. 10--c)EDCs showing change with time and heat cleaning of 6 X 10^7L CO exposure, for hν = 10.2 eV, d) change in electron affinity with time after CO exposure, for 10^5L and 6 X 10^7L exposures.

in this case it appears that this effect is at least partially caused by poor analyzer resolution. The inner surface of the energy analyzer had become contaminated in the course of several experiments performed on sample 17p prior to the CO adsorption. The 10% to 90% Fermi edge broadening for the Cu emitter during the course of the CO and H_2 experiments was 0.42 ± 0.03 eV compared to the value of 0.23 ± 0.03 eV for the "bad cleave". The value for the bad cleave is typical of the "collection" Fermi level broadening for the work on the other samples reported above. Since the natural broadening of the Fermi function is 0.114 eV at 300° K for 10% to 90% of the edge height, the broadening for the CO and H_2 experiment is two to three times worse than usual. Since we are interested in changes in the EDCs caused by the gas adsorption, the relatively poor resolution in this section is not a great handicap.

CO exposures of 10^2L, 10^3L, 10^4L, 10^5L, 10^6L and 6×10^7L were made. No effect was seen in the EDCs for exposures less than 10^5L. However, as will be seen below, the effect of the CO disappears with time. Thus, it is possible that any small effect on the EDCs from the lower exposures may have disappeared in the several minutes that elapsed between the end of the CO exposure and the measurement of the EDC.

Figure 10(a) shows EDCs at a photon energy of 11.6 eV for two CO exposures compared to an EDC for the clean GaAs. As the figure shows, the major effect of the CO is to increase the width of the EDC, that is, to lower the electron affinity. The lowest energy peak height is increased by the CO exposure. The increase in height of the low energy structure was seen in EDCs for photon energies from 8.9 to 11.6 eV. (No EDCs were measured for photon energies below 8.9 eV for the CO adsorption experiment.)

The increase in height of the low energy structure is probably caused by a change in the escape function for excited electrons due to the lowering of the electron affinity by the CO. Thus, the increase in low energy structure is caused by an increase in the escape probability for low energy electrons, and not by a CO resonance peak. The fact that no CO peak is seen in the EDCs means that any CO peak must lie at a greater binding energy than we can measure with a photon energy of 11.6 eV, that is, lower than 6.5 eV below the valence band maximum.

A striking feature of the CO adsorption results is shown in Fig. 10(b) and 10(c), where EDCs are shown for several time intervals after the 6×10^{7} L and 10^{5} L CO exposures. As is shown, the effect of the CO is greatly diminished after a few hours. Figure 10(b) shows EDCs taken after the 10^{5} L CO exposure. An EDC measured 22 hours after the 10^{5} L CO exposure shows small changes from the EDC for six hours after the exposure, but the changes are too small to be distinguishable in the figure. The EDC measured after 22 hours is still not exactly the same as the EDC for clean GaAs; the electron affinity is slightly lower and the low energy peak is slightly higher relative to the front peak than for clean GaAs. It is possible that with additional time the remaining effects of the CO would have disappeared.

Figure 10(c) shows similar EDCs for the 6×10^{7} L CO exposure. The EDC measured immediately after the CO exposure has a lower electron affinity than the initial EDC for the 10^{5} L CO exposure. After several hours, when it became clear that the effect of the CO was again disappearing, the sample was heated to 140° C for approximately five minutes. An EDC measured after the heating, shown in Fig. 10(c), had the same width as for the GaAs before any CO exposures were made, and is almost identical to the EDC for clean GaAs

Spectral yield curves for the clean GaAs and for the 6×10^{7}L CO after heating are identical within experimental error.

Figure 10(d) shows the change in electron affinity with time after the CO exposures. The electron affinity is computed from the width of the EDCs measured at a photon energy of 10.2 eV. The error in measuring the electron affinity from the EDCs is approximately 0.05 eV. The electron affinity change is referenced to the value for the clean GaAs.

We believe that the fact that the EDCs, with time, change back almost to the shape for clean GaAs indicates that at room temperature the CO desorbs from the GaAs. The CO initially sticks to the surface, but has a residence time of only a few hours before desorbing. Another possible explanation for the change in the EDCs with time is that the CO diffuses into the GaAs lattice; however, this explanation seems unlikely. The fact that the effect of the CO disappears almost completely in 22 hours would require that either the CO dissolved in the GaAs have no effect on the EDCs, or that almost all the CO must diffuse deeper than the electron escape depth of 10-25 Å.

Since desorption of the CO occurs at room temperature, measurement of exposures in units of pressure times time is not necessarily meaningful; the amount of CO adsorbed could depend on the peak pressure reached in the exposure. In this experiment the pressures used were 1×10^{-6} Torr for the 100L exposure, 1×10^{-5} Torr for 10^{3}L and 10^{4}L, 7×10^{-5} Torr to 1.3×10^{-4} Torr for 10^{5}L, 2 to 3×10^{-3} Torr for 10^{6}L, and 1 to 2×10^{-2} Torr for 6×10^{7}L. The fact that the EDCs are very similar for the three highest exposures, although the peak pressures used vary by two orders of magnitude, indicates that the pressures used have little effect on the amount of CO adsorbed.

Another important feature of the CO adsorption, illustrated in Fig. 10(a-c) is the lack of Fermi level movement with CO exposure. The position of the Fermi level during the CO exposures remained constant to within ± 0.04 eV, i.e., experimental accuracy. In contrast, for sample 17p oxygen exposure caused the position of the Fermi level at the surface to raise by 0.3 eV.

To summarize the differences between CO and O_2 adsorption on p-type GaAs, we find that

1) CO desorbs from GaAs at room temperature, while temperatures of 600° C are required to desorb oxygen.[26]
2) CO causes the electron affinity to drop by as much as 0.4 eV, but O_2 causes only negligible changes in electron affinity.
3) O_2 causes a peak to form in the EDCs at 4 eV below the valence band maximum, but any CO peak must fall at least 6 eV below the valence band maximum.
4) O_2 causes the Fermi level position at the surface to rise on p-type GaAs, while CO leaves the Fermi level position unaffected.

Pretzer and Hagstrum[31] studied the adsorption of several gases, including CO, on GaAs (110) and (111) surfaces using ion neutralization spectroscopy. They found no effect from the CO up to 3×10^{5} L exposures. This is in contrast to our results where we see effects for exposures of 1×10^{5} L. There are several possible explanations for the fact that they saw no effect from the CO. One possibility is that the CO desorbed before the ion neutralization measurements were made. This possibility would be

especially likely if their sample was somewhat warmer than ours, the warmer temperature causing faster desorption. Another possibility is that the helium ion bombardment used in ion neutralization spectroscopy caused the weakly bound CO to desorb. A third possibility is that the sticking coefficient for CO could have been different for the sample used by Pretzer and Hagstrum, since the sample had a different doping than our sample, and their sample was cleaned by sputtering and annealing rather than by cleaving. Ion neutralization spectroscopy should be sensitive to any CO which adsorbed because Pretzer and Hagstrum detected significant changes in the ion neutralization spectrum for oxygen adsorption with an exposure of 2.4×10^4 L for the (110) face, a somewhat smaller exposure than produced noticable changes in the photoemission results reported here.

Joyce and Neave[32] report that CO is only weakly bound to Si, and desorbs at only a few degrees above room temperature. Using gas uptake measurements on vacuum crushed GaP, van Velzen and Morgan[33] report that the adsorption of CO on GaP is negligible. Both of these results are consistent with the weak binding we find for CO on GaAs.

V. RESULTS AND DISCUSSION - H_2

The same cleaved surface was used for the hydrogen adsorption experiments as had been used for the CO adsorption experiments. Since the CO desorbed at room temperature, it is believed that the surface used in this experiment was clean. To insure cleanliness, the sample was heated to 140° C after the last CO exposure. The EDCs measured after the heat cleaning were essentially identical to EDCs measured before the CO exposures were made.

EDCs for several exposures of atomic hydrogen are shown in Fig. 11. The effects of the hydrogen can be summarized as 1) a growth of the low

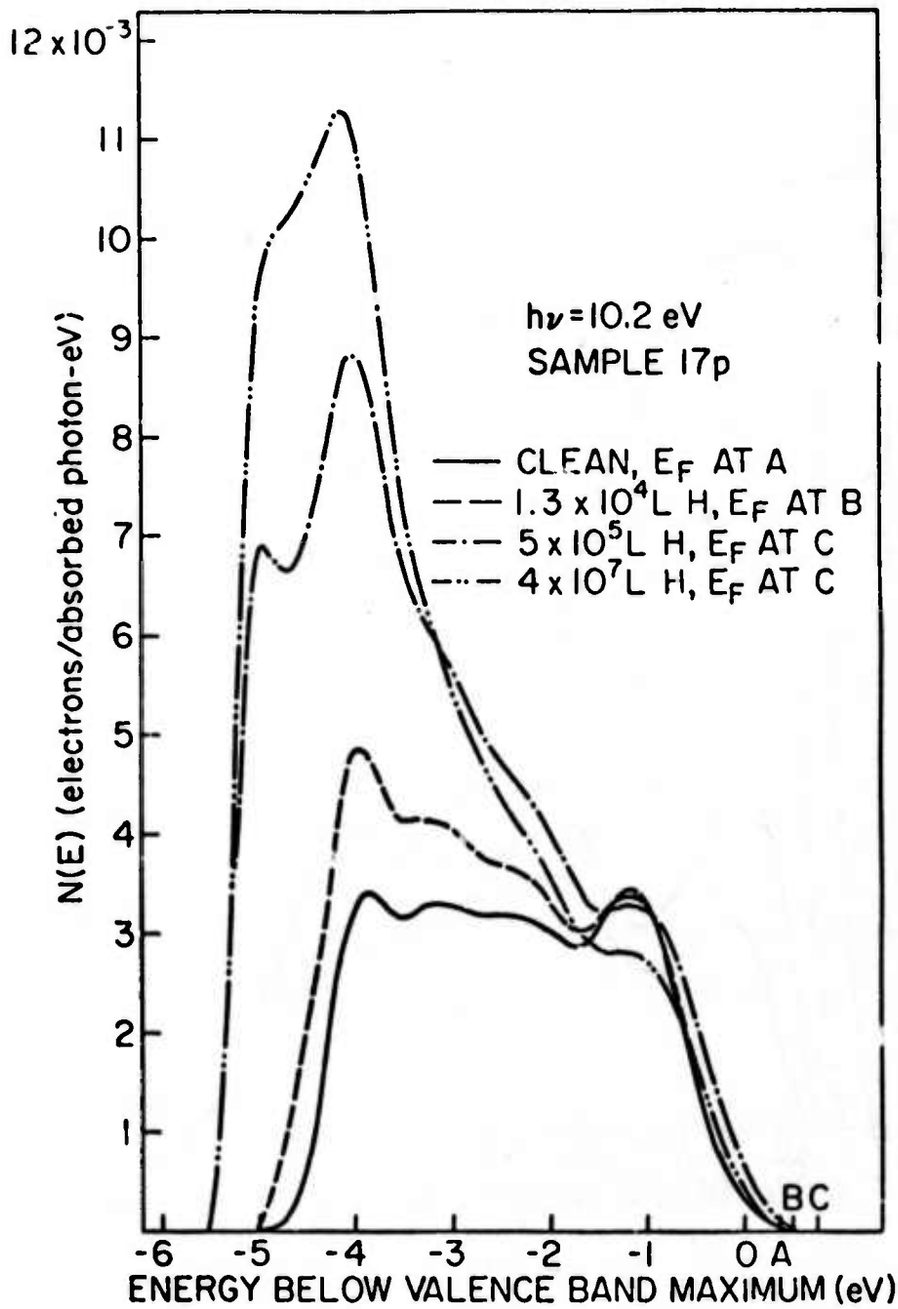

Figure 11a

FIG. 11--a) EDCs for three atomic hydrogen exposures for hν = 10.2 eV,

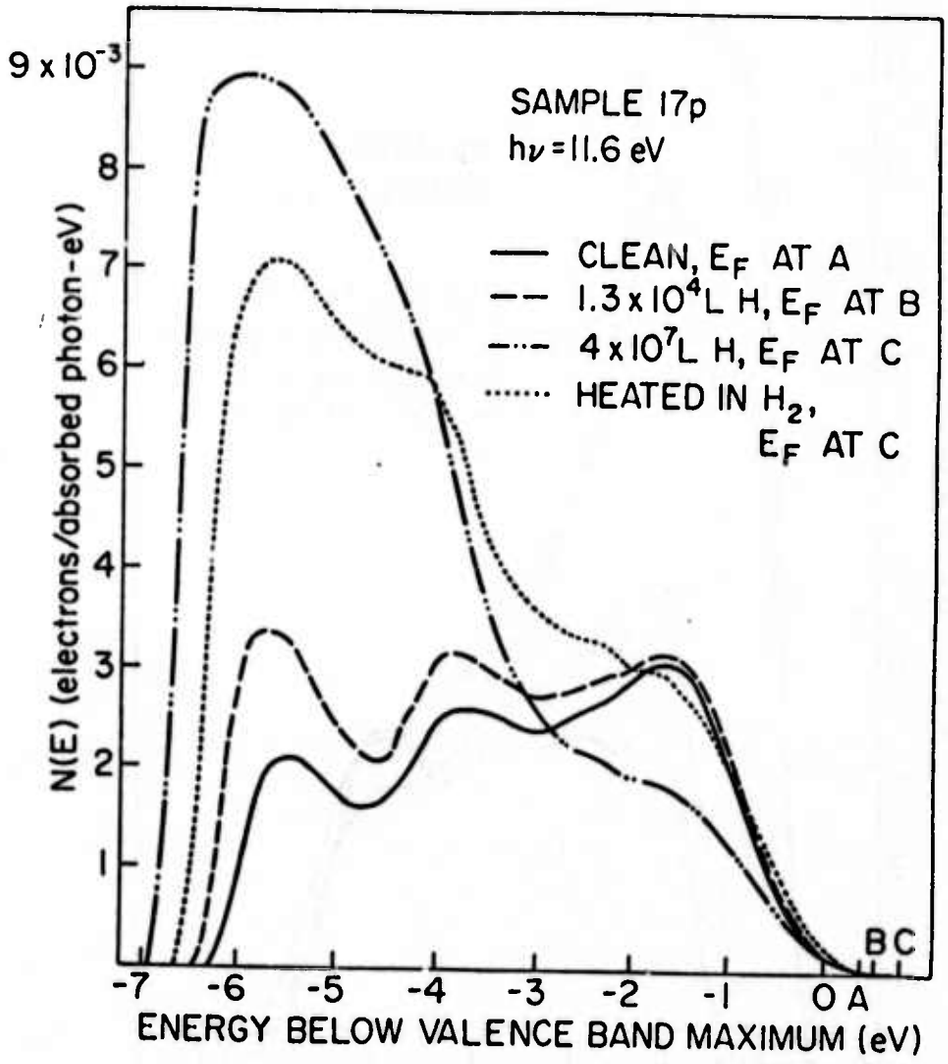

Figure 11b

FIG. 11--b) EDCs for two atomic hydrogen exposures and for sample heated in molecular hydrogen, for hν = 11.6 eV.

energy end of the EDC with respect to the high energy edge of the EDC, 2) a lowering of the threshold (i.e., E_a) for photoemission by up to 0.8 to 0.9 eV, 3) a raising of the surface position of the Fermi level by up to 0.4 to 0.5 eV, and 4) an increase in the yield. In all of these respects the effect of the atomic hydrogen on the GaAs EDCs is similar to that of Cs at low Cs coverages. In Fig. 12, EDCs for low Cs coverage on GaAs, taken from a previous experiment on sample 17p,[34] are compared to the lower H exposures. As can be seen, the overall shape of the EDCs is quite similar. (Remember that the resolution of the energy analyzer was much worse for the H adsorption experiments. The analyzer resolution was normal during the Cs adosrption experiments.) However, for H covered GaAs, the low energy peak is higher relative to the highest energy peak and the Fermi level is lower than for Cs covered GaAs at a Cs coverage such that the thresholds are about the same for the Cs and H covered GaAs. For larger H exposures the differences between Cs and H on GaAs become more apparent. With increasing H exposures the threshold lowering saturates at about 0.8 to 0.9 eV, while monolayer Cs coverages lower the threshold by 4 eV. At the highest H exposures investigated here, the EDCs for a photon energy of 10.2 eV show a continued increase in magnitude of structure around 5 eV below the Fermi level. However, as Cs coverage is increased, the greatest increase in structure occurs at energies from 5 to 9 eV below the Fermi level. Furthermore, the increase in yield is much greater with Cs than with H. For example, at a photon energy of 10.2 eV, a monolayer of Cs can cause an increase in yield by a factor of 20, while the greatest increase at 10.2 eV seen with H was a factor of about 2 over the yield of the clean GaAs. Nevertheless H behaves

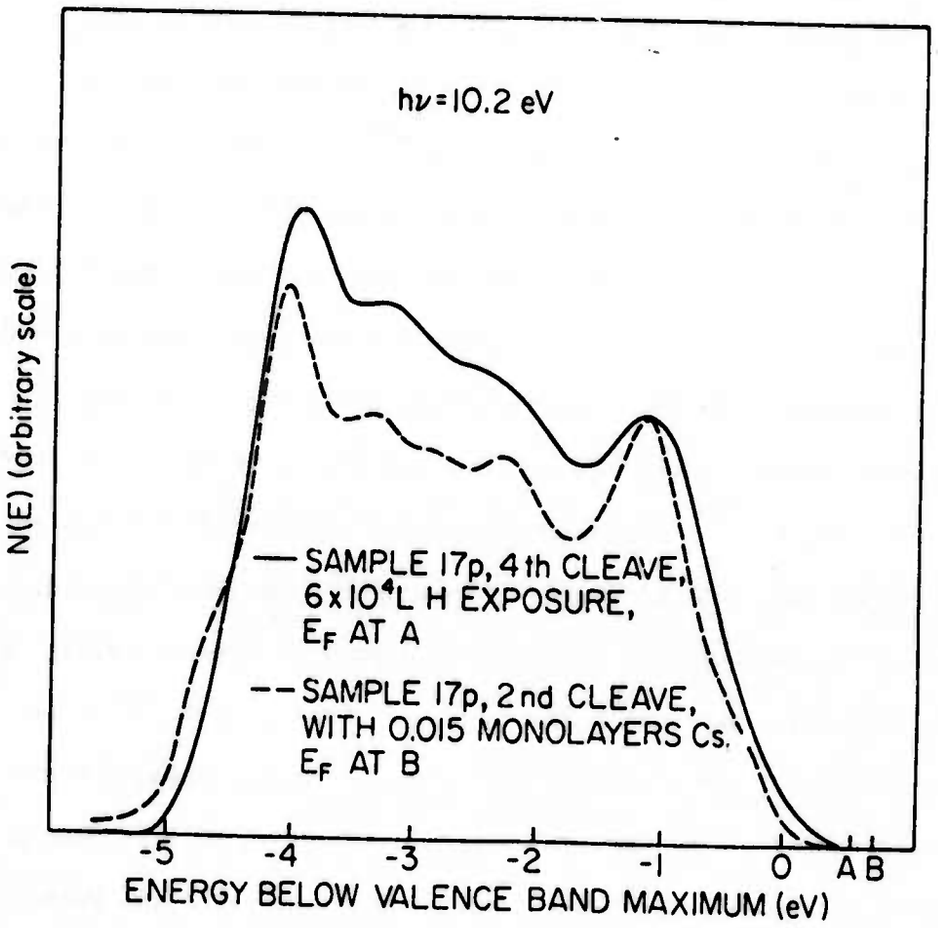

FIG. 12--EDCs at hν = 10.2 eV comparing GaAs exposed to atomic hydrogen to GaAs covered with Cs. The vertical scale is arbitrary. a) 6 X 10^4L H exposure, 0.015 monolayers Cs coverage.

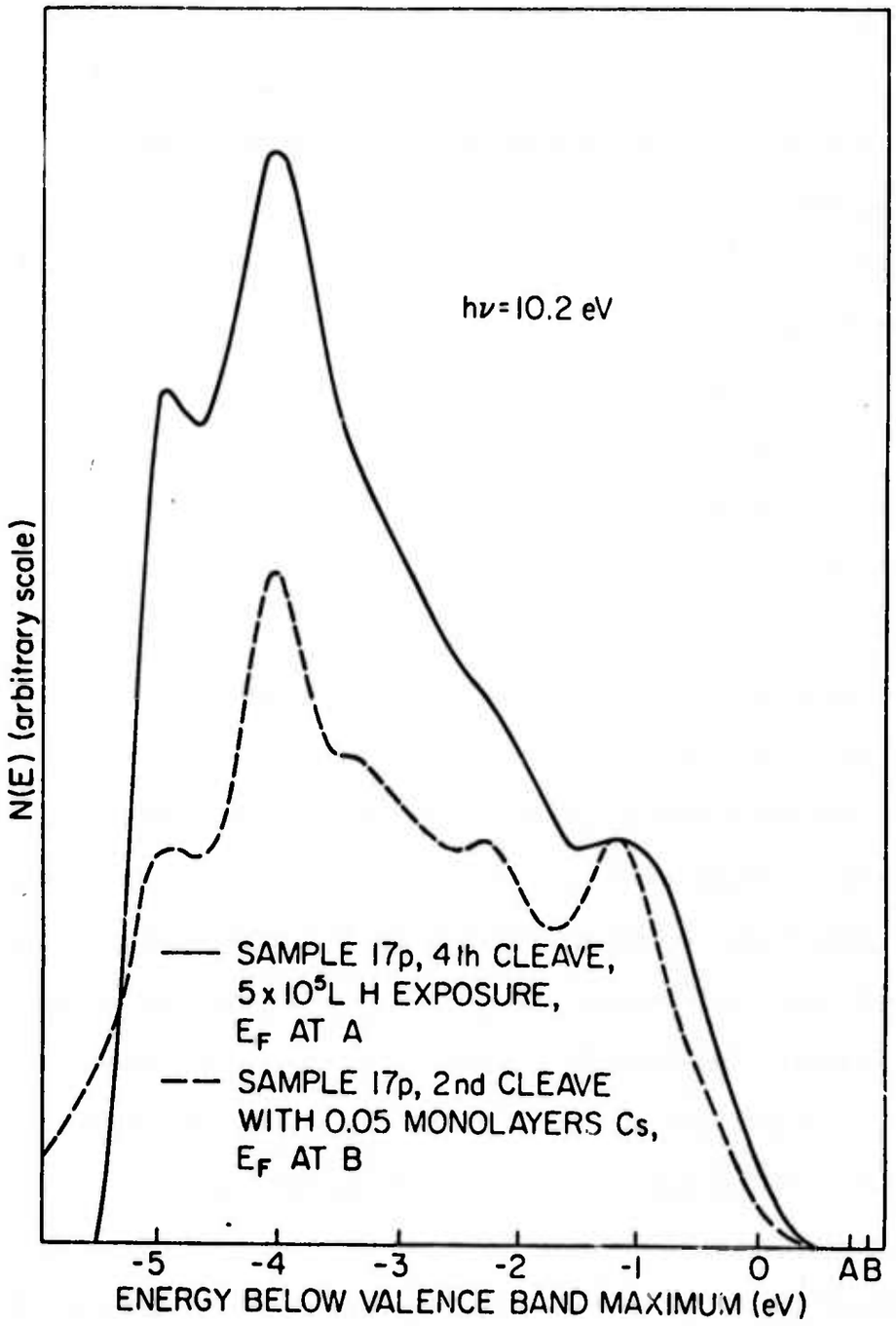

FIG. 12--b) 5 X 10^5L H exposure, 0.05 monolayers Cs coverage.

sufficiently similarly to Cs on GaAs that the H can be thought of as an alkali metal adsorbed on the GaAs.

No changes in the EDCs with time were seen which would suggest desorption of the H at room temperature, as was seen for CO on GaAs. However, at low exposures it was possible to heat clean the H covered GaAs, with partial success. After the 6×10^{4} L exposure the sample was heated to 235° C as measured by a thermocouple at the base of the sample. The sample face was probably somewhat cooler than this. This heating caused the shape of the EDC to return to the shape it had before the H exposures and the threshold for photoemission returned to the value for clean GaAs.

After the heat cleaning to 235° C, the sample was exposed to H_2 with and without the hot filament, and to the hot filament without the H_2. These exposures are described more completely below. During this group of treatments, the lowest peak in the EDCs raised somewhat with respect to the front peak, and the electron affinity dropped by about 0.1 eV, most of the changes taking place during the small H_2 exposure with the hot filament on. After this group of treatments, an attempt was made to heat clean the sample, but even heating to 370° C was not sufficient to restore the GaAs to its As-cleaved condition. At a photon energy of 10.2 eV, the EDC after heating to 370° C compared to the EDC for the GaAs immediately after cleavage had a Fermi level 0.1 eV higher, an electron affinity 0.05 eV lower, and a low energy peak somewhat higher than the front peak. These differences in the EDC probably indicate that the GaAs surface had become slightly contaminated. The H_2 exposures of 4×10^{4} L, 5×10^{5} L, 4×10^{7} L, and the exposure made by heating the sample in H_2 were made after the heating to 370° C. However, the changes seen in the EDCs with these larger H_2 exposures are much greater

than the difference between the EDCs for the freshly cleaved GaAs and the EDCs after the 370° C heating, so the effects of contamination are probably not important in the H_2 exposure results.

As mentioned in the section on experimental techniques above, molecular hydrogen was dissociated at a tungsten filament heated to approximately 1000° C in line of sight with the crystal face. To determine that the effects seen were really due to atomic hydrogen, the following combinations of exposures were made: exposures of 400L and 2×10^4L of H_2 with the filament turned off; an exposure of 2×10^4L of H_2 with the filament turned on and the sample moved out of line of sight of the filament; and an exposure in which the filament was turned on in line of sight of the sample face for 35 minutes (a time comparable to that used for the usual atomic hydrogen exposures), but no hydrogen was leaked into the system. All of the above combinations only had a very slight effect on the EDCs. A subsequent exposure of 9×10^3L with the hot filament on in line of sight of the sample face produced a much larger effect than any of the above combinations. Thus, the effects seen with hydrogen and the hot filament were not due to outgassing from the filament, evaporation from the filament, or molecular hydrogen adsorbing on the GaAs. Pretzer and Hagstrum[31] also found that molecular hydrogen does not adsorb on GaAs.

For H_2 exposures above 4×10^4L, a peak begins to build up at the low energy edge of the EDC. To show that this peak is not a resonance level from the hydrogen, EDCs for three photon energies for the 4×10^7L hydrogen exposure are plotted in Fig. 13 versus final state energy (i.e., the energy of the electrons above the valence band maximum.) The fact that the low energy peak lies at the same final state energy in the EDCs of different

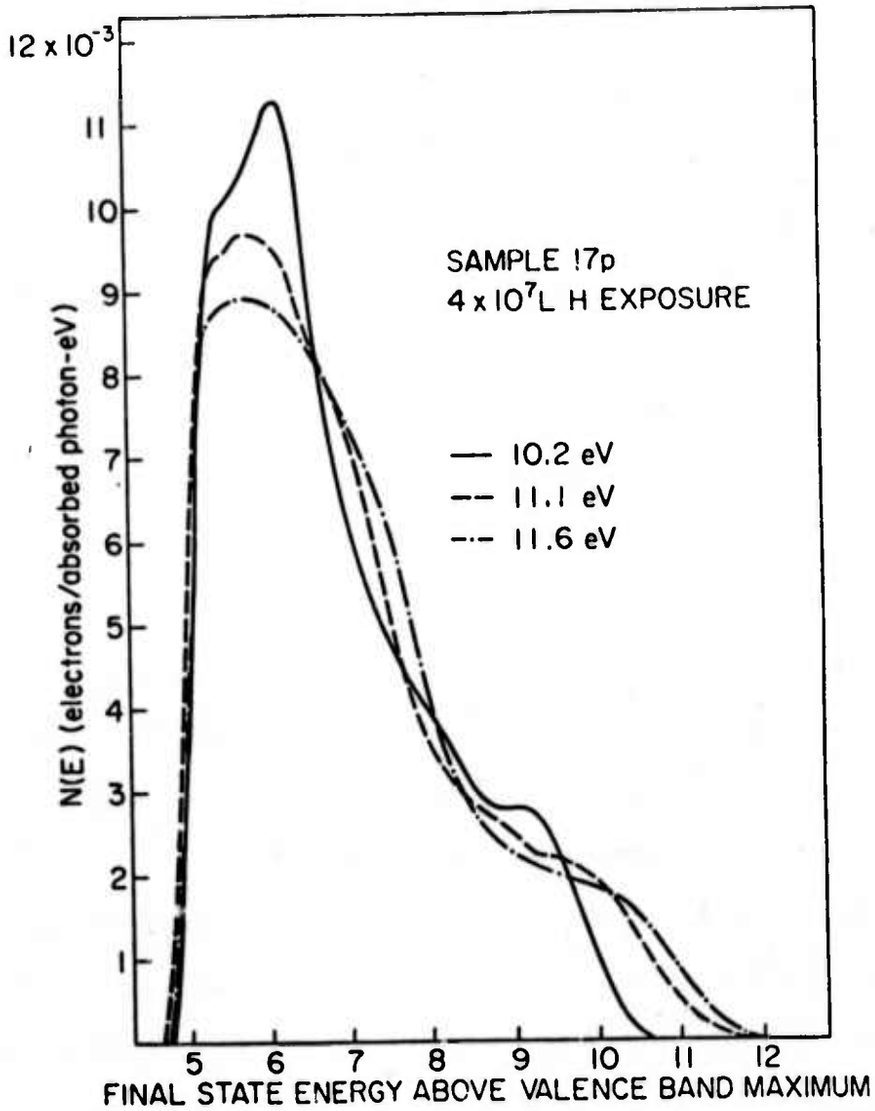

FIG. 13--EDCs for the photon energies 10.2 eV, 11.1 eV and 11.6 eV for the 4 X 10^7L atomic hydrogen exposure, plotted versus the electron final state energy above the valence band maximum. The fact that the low energy peak which develops with H exposure falls at the same energy for different photon energies in this plot indicates that the peak is caused by electrons which were inelastically scattered in passing through the layer of hydrogen adsorbed on the GaAs surface.

photon energy strongly suggests that the peak was caused by the inelastic scattering of electrons leaving the GaAs, and not by a resonance level, or extrinsic surface state, due to the adsorbed hydrogen.

After the 4×10^7 L H_2 exposure with the hot filament was made and studied, an additional exposure to 3×10^7 L of H_2 was made with the hot filament off, but with the sample heated to 415° C. The H_2 pressure was 5×10^{-3} Torr, and the sample was heated and cooled in the H_2 atmosphere. The sample was heated by a tungsten filament which was not in line of sight of the sample face. The resulting EDC is shown in Figs. 11(b) and 14 as the curve marked "heated in H_2". As the figures show, the results are different from both the lower and highest atomic hydrogen exposures. The threshold for photoemission increased by about 0.4 eV, the yield decreased, the low energy peak decreased in magnitude, and bulk structure began to reappear, but the position of the Fermi level did not change. The results suggest a different state of the hydrogen from that adsorbed at room temperature, possibly a chemical combination with the GaAs or diffusion into it.

After the sample was heated in H_2, an attempt was made to heat clean the sample by heating it in vacuum to 700° C, as measured by a thermocouple mounted near the heater end of the sample (the sample face was probably not that hot). The temperature was held at that value for several minutes. The resulting EDC, shown in Fig. 14, appeared to have a much lower H coverage than previous to the heat cleaning, but the sample still was not clean. The EDC is somewhat different from the lower exposures of H covered GaAs in that the threshold is lower and the position of the Fermi level is higher.

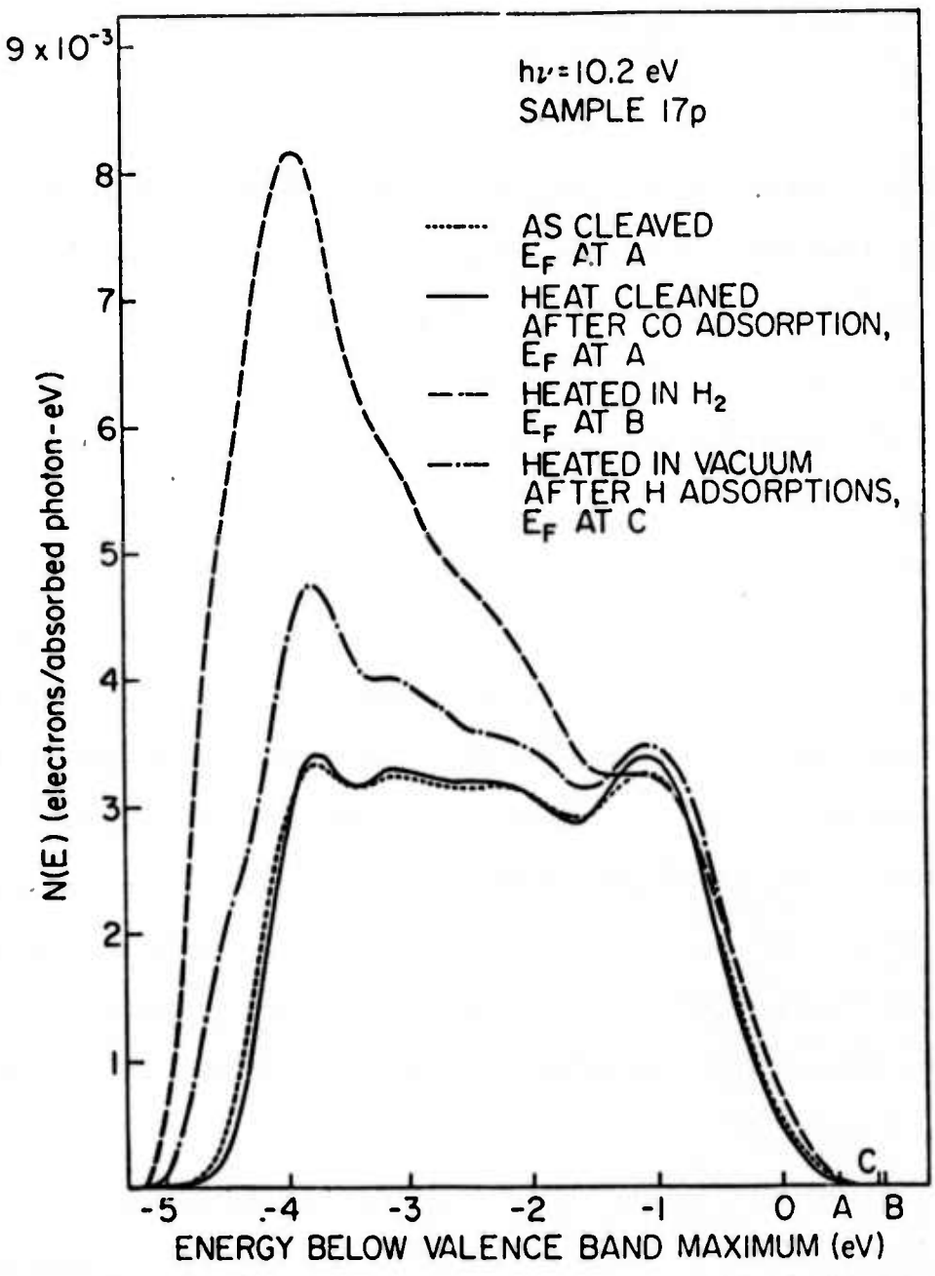

FIG. 14--A comparison of the EDCs from the GaAs as cleaved, after heat cleaning following the CO exposures, after heating in H_2, and after heating in vacuum following the hydrogen exposure. The photon energy is 10.2 eV for all the EDCs.

VI. CONCLUDING REMARKS

By comparing the data for the three gases we have adsorbed on GaAs (110), we can make a few general comments. We find that oxygen and atomic hydrogen are tightly bound to GaAs, and in both cases the adsorption of these gases causes the surface position of the Fermi level to move higher in energy on p-type GaAs. In a previous study[3,4] we found a similar tight binding and upward movement of the surface Fermi level position for Cs adsorption on p-type GaAs. On the other hand, we find that CO is only weakly bound to GaAs, desorbs at room temperature, and causes little or no Fermi level movement on p-type GaAs. Our previous study[3,4] showed that Na also desorbs from p-type GaAs at room temperature and does not change the surface position of the Fermi level. Our results from the adsorption of O_2, H, CO, Cs and Na, therefore, indicate that in the case of p-type GaAs, where the Fermi level is not pinned at the surface by surface states on the clean material, tightly bound adsorbates induce new Fermi level pinning, whereas weakly bound adsorbates do not. For n-type GaAs we only have data for O_2 and Cs adsorption. The results indicate that adsorption of Cs and O_2 does not change the strong Fermi level pinning present on the clean n-type GaAs surface at least for the exposures used in this experiment.

From this study and a previous study,[3,4] we find that CO, H, Cs and Na all lower the threshold for photoemission when adsorbed on GaAs. The lowering of the threshold for photoemission is believed to be caused by the formation of a surface dipole layer. The fact that both weakly bound CO and Na, and tightly bound H and Cs can cause a threshold lowering indicates that bonding is not required to form the dipole layer. In the case of CO and Na, at least, the dipole layer must result from polarization of the adsorbate (or the GaAs surface layer) rather than from actual charge transfer

or bonding. O_2 adsorption did not significantly change the threshold, which shows that an adsorbate can be tightly bound without producing a dipole layer.

REFERENCES

1. C. R. Helms, Ph.D. dissertation, Stanford University, 1973, unpublished.
2. H. Ibach and J. E. Rowe, Surf. Sci. 43, 481 (1974).
3. G. B. Fisher, W. E. Spicer, P. C. McKernan, V. F. Pereskok and S. J. Wanner, Appl. Optics 12, 799 (1973).
4. H. R. Phillip and H. Ehrenreich, Phys. Rev. 129, 1550 (1963).
5. R. C. Eden, Ph.D. dissertation, Stanford University, 1967, unpublished.
6. R. C. Eden, Rev. Sci. Instrum. 41, 252 (1970).
7. D. E. Eastman and J. J. Donelon, Rev. Sci. Instrum. 41, 1648 (1970).
8. L. F. Wagner and W. E. Spicer, Surf. Sci. 46, 301 (1974).
9. I. Lindau and W. E. Spicer, J. Electron Spect. 3, 409 (1974).
10. R. Dorn, H. Lüth and G. J. Russell, Phys. Rev. B10, 5049 (1974).
11. H. Lüth and G. J. Russell, Surf. Sci. 45, 329 (1974).
12. L. F. Wagner and W. E. Spicer, Phys. Rev. B9, 1512 (1974).
13. W. E. Spicer and R. C. Eden, in Proceedings of the Ninth International Conference on the Properties of Semiconductors Vol. 1, (Nauka, Leningrad, 1968), p. 65.
14. A. J. Rosenberg, J. Phys. Chem. Solids 14, 175 (1960).
15. Henry T. Minden, J. Electrochem. Soc., 109, 733 (1962).
16. P. E. Gregory, W. E. Spicer, S. Ciraci and W. A. Harrison, Appl. Phys. Lett. 25, 511 (1974); P. E. Gregory and W. E. Spicer, Bull. Am. Phys. Soc. 19, 213 (1974); S. Ciraci, W. A. Harrison, P. E. Gregory, W. E. Spicer, and L. F. Wagner, Bull. Am. Phys. Soc. 19, 214 (1974).

17. H. Ibach, K. Horn, R. Dorn and H. Lüth, Surf. Sci. 38, 433 (1973).

18. D. E. Eastman and J. L. Freeauf, Phys. Rev. Lett. 33, 1601 (1974).

19. P. E. Gregory and W. E. Spicer, to be published.

20. R. Ludeke and L. Esaki, Phys. Rev. Lett 33, 653 (1974).

21. J. L. Freeouf and D. E. Eastman, to be published in CRC Critical Reviews in Solid State Sciences.

22. W. E. Spicer and P. E. Gregory, to be published in CRC Critical Reviews in Solid State Sciences.

23. R. Ludeke and A. Koma, to be published in CRC Critical Reviews in Solid State Sciences.

24. T. E. Madey and J. T. Yates, Jr., J. Vac. Sci. Tech. 8, 525 (1974).

25. W. Ranke and K. Jacobi, Surf. Sci. 47, 525 (1975).

26. J. R. Arthur, J. Appl. Phys. 18, 4023 (1967).

27. B. Goldstein and D. Szostak, Appl. Phys. Lett. 26, 111 (1975).

28. W. A. Harrison, to be published.

29. D. E. Eastman and W. D. Grobman, Phys. Rev. Lett. 28, 1378 (1972).

30. M. Henzler, Surf. Sci. 36, 109 (1973).

31. D. D. Pretzer and H. D. Hagstrum, Surf. Sci. 4, 265 (1966).

32. B. A. Joyce and J. H. Neave, Surf. Sci. 34, 401 (1973).

33. W. J. M. van Velzen and A. E. Morgan, Surf. Sci. 39, 255 (1973).

34. P. E. Gregory and W. E. Spicer, Phys. Rev. B, to be published.

CHAPTER 3

PHOTOEMISSION STUDIES OF THE GaAs-Cs INTERFACE

I. INTRODUCTION

Although metal-semiconductor contacts have been studied extensively, no generally accepted model for the formation of Schottky barriers has emerged. Historically, the most commonly used model asserts that the Fermi level is pinned at the metal-semiconductor interface by surface states on the semiconductor.[1,2] However, Heine[3] has suggested that the semiconductor surface states cannot really exist in contact with a metal. He has proposed a model in which the Fermi level pinning is caused by electron wave functions from the metal tailing into the semiconductor band gap. He, Inkson,[4] Phillips,[5] and others have suggested various interactions between the semiconductor and metal. The Fermi level pinning is the result of these interactions rather than being primarily due to the effect of the intrinsic surface states of the clean semiconductor.

The usual studies made of metal-semiconductor contacts consist of measurements made on a diode consisting of a semiconductor and a thick metal film evaporated onto it. These measurements yield values of the Schottky barrier height,[2] but are not able to determine details of the energy structure at the interface, and they are not able to measure the surface state distribution on the clean semiconductor surface. Thus, the usual type of Schottky barrier study is not able to distinguish among the various proposed models for Schottky barrier formation, and is not able to make correlations between the barrier height and the distribution of surface states on the clean semiconductor.

Ultraviolet photoemission spectroscopy, however, is able to make measurements from the interface region directly by studying metal-semiconductor contacts where the metal film is at most several monolayers thick. By studying the energy spectrum of electrons emitted into vacuum from the metal semiconductor interface as a function of the thickness of the metallic layer, a large amount of information about the formation of Schottky barriers can be obtained. Furthermore, it is possible to study the energy distribution of surface states on the clean semiconductor surface using this technique. Thus, it is possible to make correlations between the barrier height and the density of surface states on the clean semiconductor surface.

The work presented here on Cs-GaAs contacts shows that the Fermi level pinning position changes as a function of the metal thickness in a complicated way. Also, as the Cs coverage increases, the valence band edge of the GaAs broadens and tails into the energy gap. Although the pinning position of the Fermi level seems to be correlated with the surface state distribution measured by photoemission on the clean GaAs surface, the details of the behavior cannot be explained solely by the presence of the surface states. An explanation of the results seems to require elements of several of the different proposed theoretical models. Although much more experimental and theoretical work will be necessary to obtain a definitive picture of the metal-semiconductor contact, we believe the present work gives considerable new insight into the problem.

II. EXPERIMENTAL DETAILS

The experiment was carried out on the (110) face of a single crystal of GaAs which had been cleaved in ultra-high vacuum by squeezing the crystal

between a tungsten carbide blade and an annealed OFHC copper anvil. Four different GaAs single crystals were studied and are described in Table 1. The most detailed work was done on sample 17p. The samples were 1 cm × 1 cm in cross section.

The experiment was contained in a stainless steel, ion-pumped chamber with a base pressure of about 1×10^{-10} Torr as measured on a Redhead gauge. Cs or Na was applied in small doses to the sample from vapor generated by conventional Cs or Na-chromate channels. The Cs and Na channels were not in direct line of sight of the GaAs crystal, in order to reduce contamination by impurities from the channels. During Cs or Na evaporation, the pressure rose to at most 6×10^{-9} Torr, except for the experiments on sample 14n where the pressure rose to a maximum of 2×10^{-8} Torr.

It is not possible to measure coverage of Cs or Na directly when Cs or Na channels are used as a source because the Cs or Na which is evolved is normally in the form of neutral atoms. Therefore, a qualitative measure of the progress of Cs or Na coverage was made during the evaporation of Cs or Na by monitoring the photoyield at a photon energy of 6 eV for low coverages, and monitoring the white light photoyield for larger cesium coverages. Using this technique it was possible to stop the cesiation after only small amounts of cesium were applied. Since it was not possible to measure cesium coverage directly with our experimental apparatus, we have used yield data to estimate the cesium coverage. Madey and Yates[6] have presented data relating the change in work function to measured values of cesium coverage on p-type (110) GaAs, and Clemens and Mönch[7] give similar data for Cs on n-type (110) GaAs. For each Cs exposure the Cs coverage was estimated by obtaining an estimate of yield threshold from measured yield curves (or from the width of the EDCs in

TABLE 1

SAMPLES STUDIED

Sample Name	Doping (cm^{-3})	Type
14 n	6×10^{14}	n
18 n	1.7×10^{18}	n
17 p	1.5×10^{17}	p
19 p	3×10^{19}	p

TABLE 2

CESIUM EXPOSURE DATA FOR SAMPLE 17 p

Cesiation	Approximate Threshold (eV)	Coverage (GaAs (110) Monolayers)	Change in Fermi Level Position From Clear Sample (eV)
0	5.4	0	0
#1	5.4	< .001	.3
#2	5.0	.015	.4
#3	4.3	.05	.6
#4	3.9	.07	.6
#5	3.6	.09	.6
#6	3.0	.14	.55
#7		~ .3	.4

a few cases). The yield threshold was converted to a work function by correcting for the position of the Fermi level at the surface. Work function changes were then converted into cesium coverage from the data of Madey and Yates[6] for samples 17p and 19;, and from the data of Clemens and Mönch[7] for samples 14n and 18n. Madey and Yates present their data as ions deposited/cm^2. We have converted this to coverage in monolayers by allowing for their estimated 20% neutral Cs atoms, and taking a monolayer to be 8.85×10^{14} cm^{-2}, consistent with Clemens and Mönch.[7] The values of Cs coverage thus obtained are used throughout this paper.[8]

After each exposure of Cs or Na, photoemitted electron energy distribution curves (EDCs) were measured for several photon energies, and the yield was measured for photon energies from threshold to 11.6 eV. The yield was measured relative to a Cs_3Sb photodiode which has a calibration traceable to the U. S. Bureau of Standards.[9] The yield was corrected for the reflectivity of GaAs from the data of Phillip and Ehrenreich[10] as tabulated by Eden.[11] Unless otherwise stated, EDCs presented in this paper are normalized so that the area under the EDC is proportional to the yield at the photon energy at which the EDC was measured.

EDCs were measured using the standard A.C. modulated retarding potential technique with a hemispherical energy analyzer.[12] The light source was a McPherson 225 vacuum monochromator with a hydrogen discharge lamp having a hot filament. Light entered the sample chamber through a LiF window having a high energy cutoff of 11.8 eV.

A copper emitter could be substituted for the GaAs crystal. EDCs measured from the copper emitter were used to calibrate the system so that the position of the Fermi level on the GaAs EDCs could be determined.[13]

Copper EDCs were measured frequently, and especially after each Cs or Na exposure, to correct for any changes in the collector work function caused by contamination or Cs or Na adsorption.

Knowledge of escape depth and band bending are necessary to interpret UPS data. The escape depth of electrons emitted from the GaAs at the photon energies involved in the measurement of EDCs ($7.7\ \text{eV} \lesssim h\nu \lesssim 11.8\ \text{eV}$) has not been determined, but available data for other materials[14] suggests that it is 20 Å or less. For sample 17p the band bending length, calculated using the depletion approximation, is over 600 Å for 0.5 eV band bending. Thus for sample 17p, the position of structure in the EDCs with respect to the Fermi level is representative of the position of the bands at the GaAs surface. On the other hand, for sample 19p the band bending length is comparable to the probable escape depth. It will be shown later in this paper that for sample 19p the short band bending length may cause the measured difference between the Fermi level and the valence band maximum to be somewhat less than the actual value at the surface.

III. RESULTS

Cesium was applied to all four GaAs samples shown in Table 1, and sodium was applied to a second cleave of sample 17p. The most detailed study of Cs on GaAs was made on sample 17p. Small amounts of Cs were applied to the surface of the first cleave of sample 17p in seven separate doses. EDCs for sample 17p at a photon energy of 10.2 eV are shown in Fig. 1, photoemitted yield curves are shown in Fig. 2, and a summary of the data for sample 17p is given in Table 2. In Fig. 1 an EDC for clean GaAs is shown at the bottom; EDCs for successively larger Cs coverages are shown vertically. The EDCs are placed so that the first peaks are

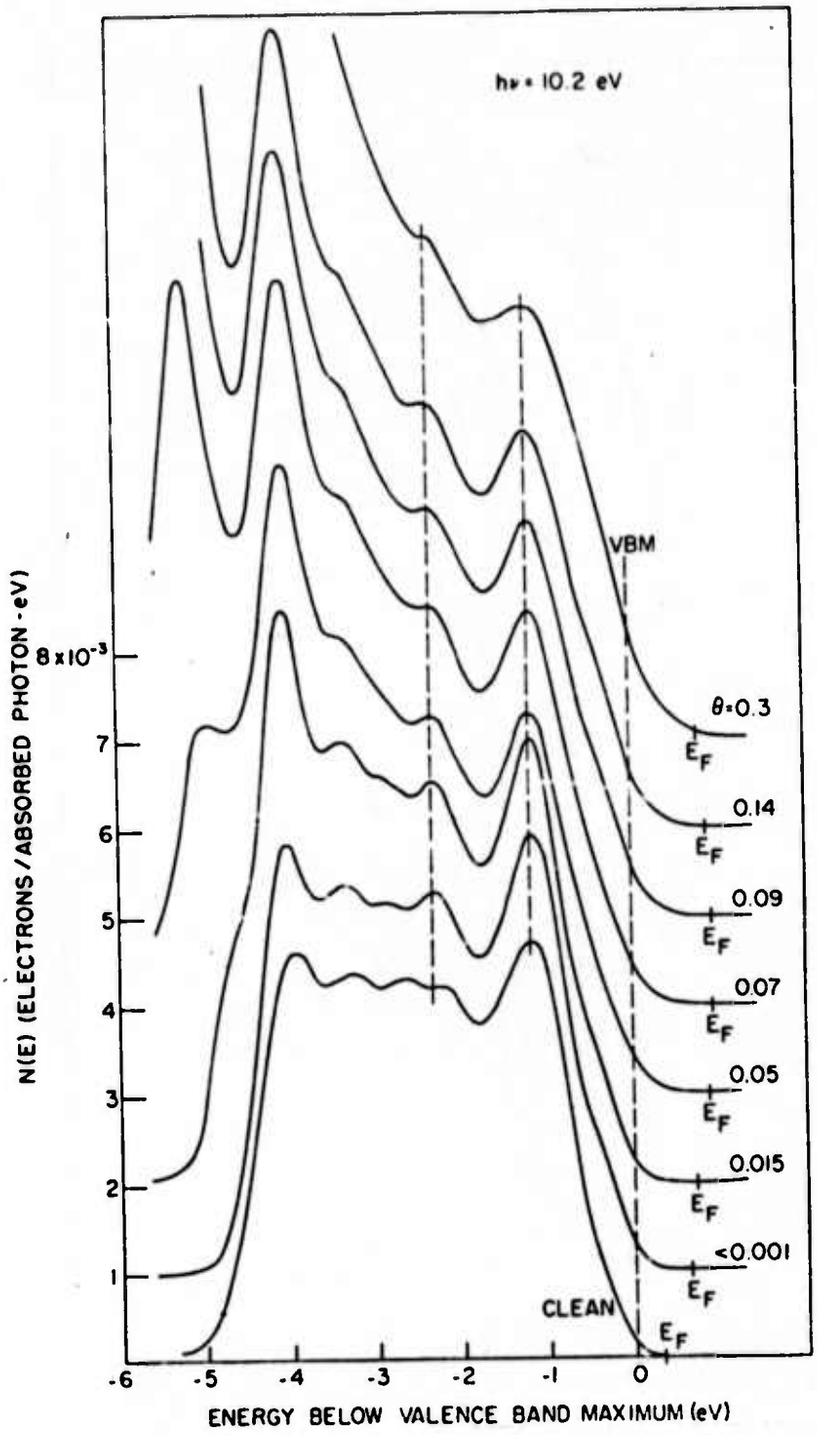

FIG. 1--EDCs for sample 17p at a photon energy of 10.2 eV as a function of cesium coverage, θ.

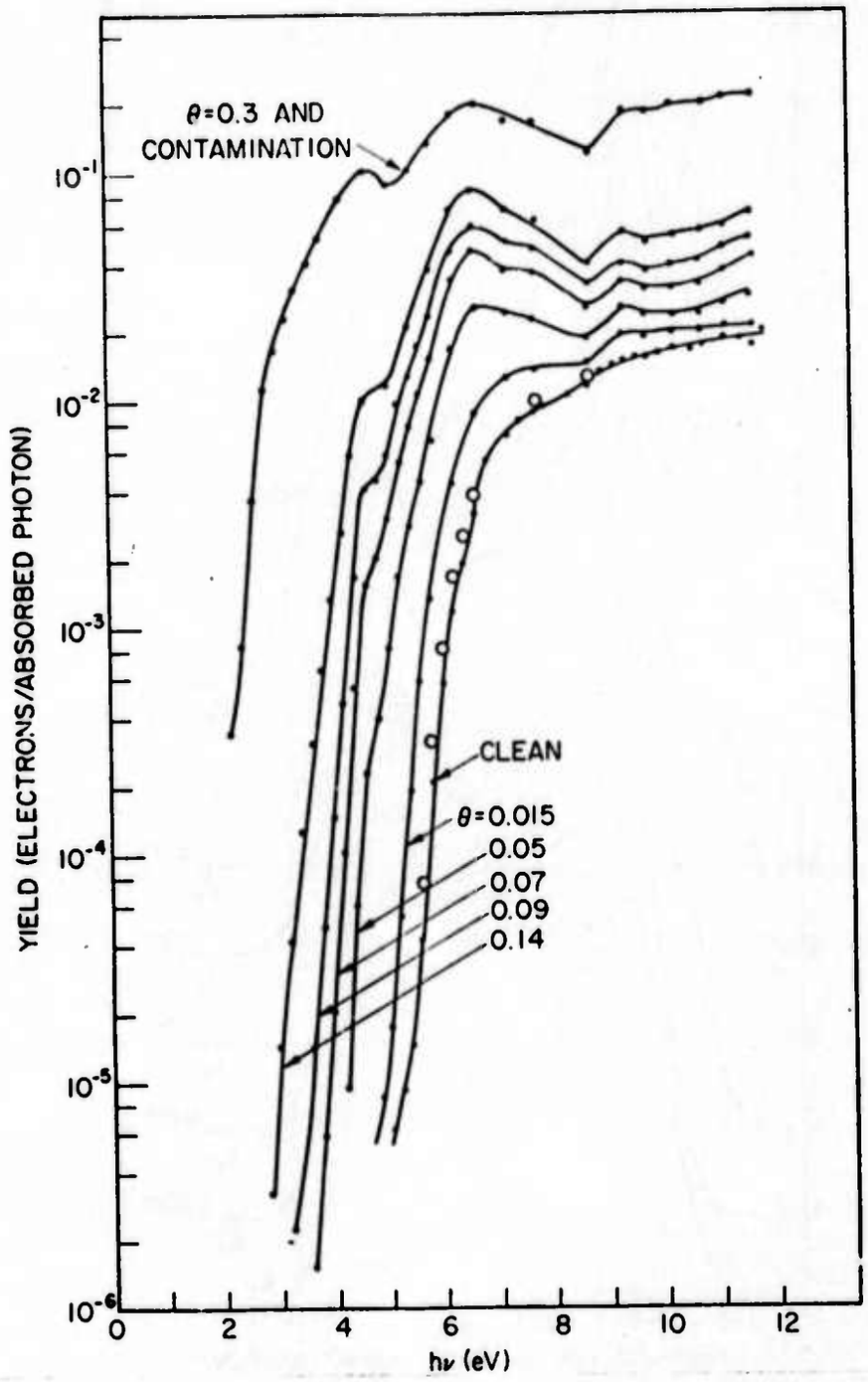

FIG. 2--Spectral yield curves for sample 17p as a function of cesium coverage, θ. The open circles are data points for the cesium coverage of < .001 monolayer.

aligned. The Fermi level position determined from the copper reference is indicated for each EDC. The great increase in yield and the threshold lowering caused by the Cs coverage force us to show only the high energy portion of the EDCs for the higher Cs coverages.

Note that throughout this paper we have defined a monolayer in terms of the GaAs (110) surface; that is, one monolayer of Cs by this definition would correspond to one Cs atom for each surface Ga and As atom. By this definition a saturation coverage of Cs occurs at a coverage less than one monolayer. This definition may be somewhat artificial, but since the exact Cs saturation coverage is not known, the use of the GaAs surface as a reference is necessary in order to have a fixed reference point.

There are two features of Fig. 1 which are important for a study of Schottky barriers; the movement of the Fermi level with Cs coverage, and movement of states into the forbidden gap. The upward movement of the Fermi level with respect to the valence band maximum is evident in Fig. 1, and indicates downward bending of the valence band. A very small Cs exposure causes the bands to bend down by 0.3 eV. Additional Cs causes more band bending, to a maximum of about 0.6 eV; still more Cs causes the band bending to decrease somewhat.

The movement of states into the forbidden gap is more clearly seen in Fig. 3, where the first peak in each EDC has been normalized to the same height. Independent of the normalization, a straight line extrapolation of the upper edge shows that the upper edge of the EDC moves to higher energies, with respect to the peaks of the EDCs, as the Cs coverage is increased.

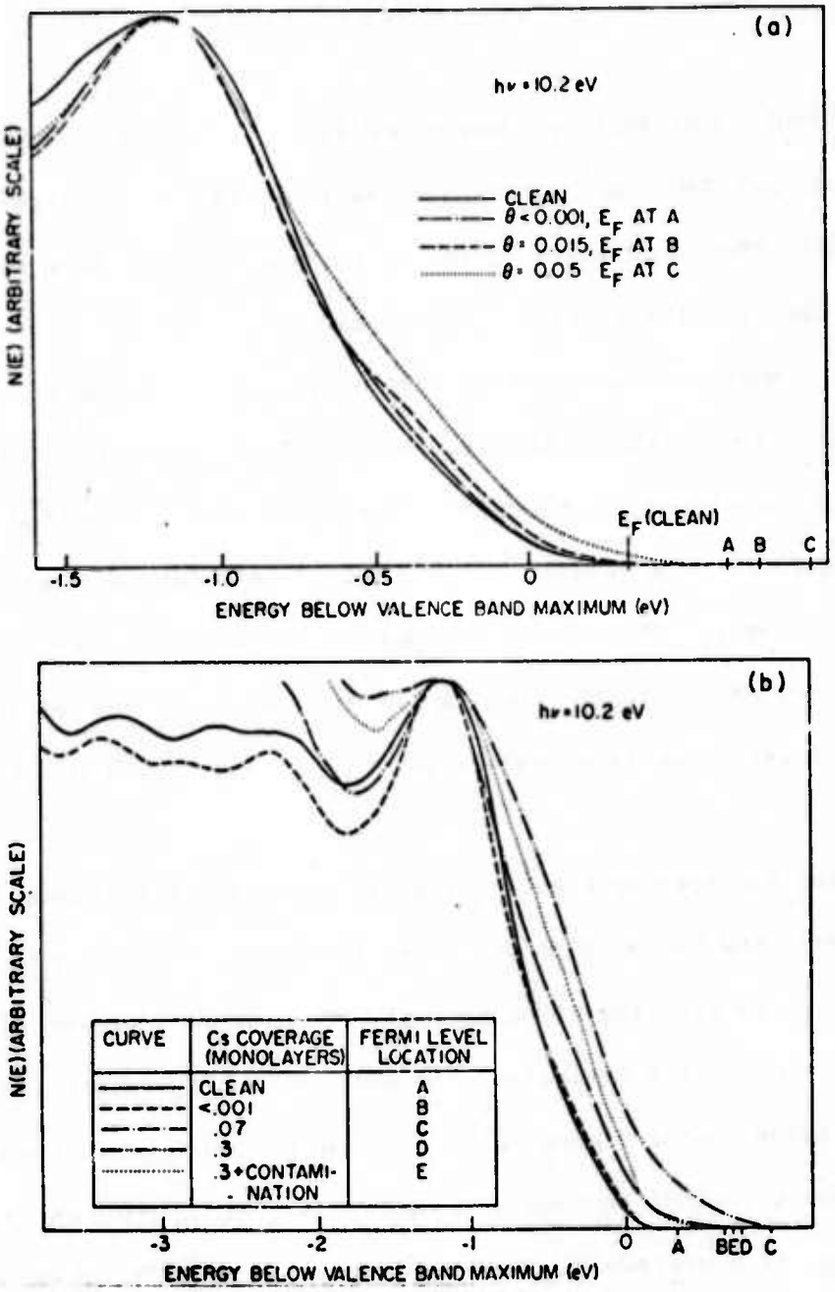

FIG. 3--The high energy portion of EDCs at a photon energy of 10.2 eV showing the upward movement of states into the energy gap as Cs coverage is increased. Part a shows the lowest Cs coverages on an expanded scale, while part b shows the effect up to the highest coverages. Letters A, B, etc. give the Fermi level location as given in the key for each part of the figure.

Figure 3a shows that even at the lowest coverages there is a small buildup of emission near the base of the peak, even though the upper part of the peak has become slightly narrowed by the Cs exposure. By a coverage of 0.05 monolayers, the broadening of the first peak has become quite noticeable. Figure 3b shows the larger Cs coverages. By a Cs coverage of 0.3 monolayers the broadening is quite substantial. Also note that for coverages beyond 0.05 monolayers a high energy tail begins to develop, and by 0.3 monolayers the tail is quite large and extends up to the Fermi level.

The curve marked 0.3 monolayers + contamination in Fig. 3b shows the result of exposing the surface having 0.3 monolayers of Cs coverage to contamination produced by the outgassing of a hot filament which had not previously been heated in the course of the experiment. The broadening and the high energy tail were greatly reduced by the contamination, and the Fermi level position was lowered. Similar effects were achieved by exposure to oxygen.

Sample 19p was given a total of three cesium exposures. EDCs for a photon energy of 10.2 eV are shown in Fig. 4 for sample 19p. The band bending behavior of sample 19p is similar to that of sample 17p, as is the movement of states into the forbidden gap. One difference in behavior is the appearance of a shoulder (A in Fig. 4) and a peak (B) on the cesiated sample 19p. Structures A and B are not seen in the clean GaAs EDCs and are not clearly present in the EDCs for cesiated sample 17p, although the shoulder A is in a similar position to the high energy tail on sample 17p for the larger Cs coverages. The reason for this discrepancy is not clear.

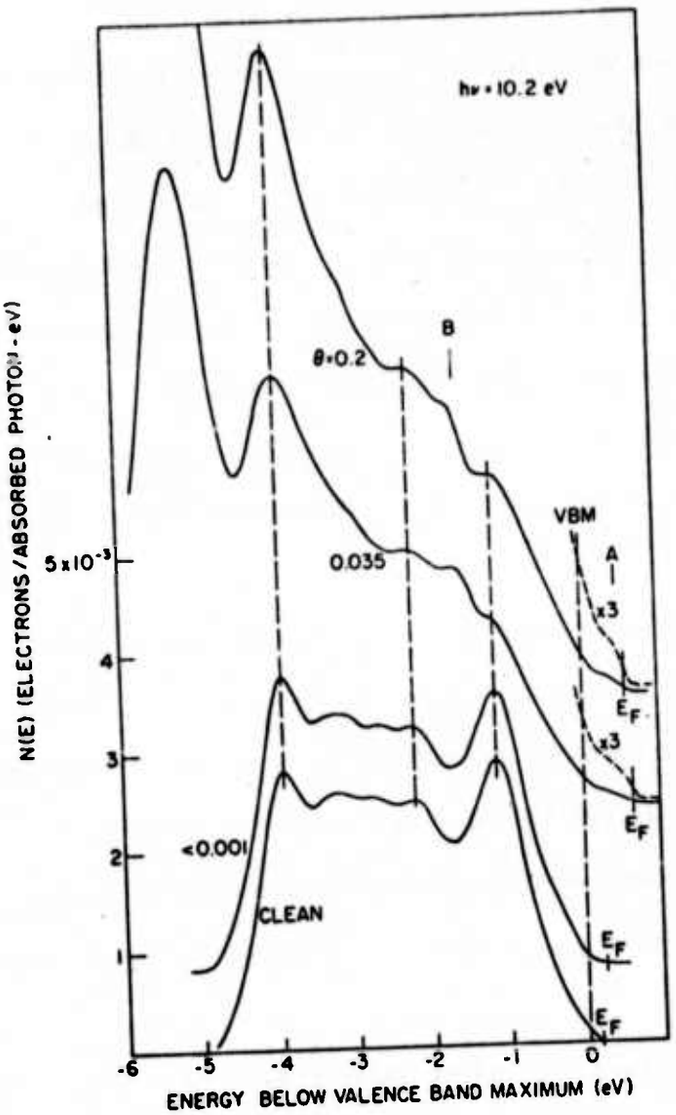

FIG. 4--EDCs for sample 19p at a photon energy of 10.2 eV as a function of cesium coverage, θ. A and B refer to structure not seen in EDCs from Cs covered sample 17p.

The extra structure present in the 19p EDCs was visible in EDCs taken at different photon energies and was visible in the two heaviest cesiations, although the structure is less sharply defined in the heaviest cesiation. As can be seen by comparison of Figs. 1 and 3, for the heaviest Cs coverage on sample 17p, there is extra emission at approximately the same energy as peaks A and B in sample 19p, although no distinct peaks evolve. As is shown in Fig. 3, when sample 17p was contaminated after the last cesiation (caused by outgassing of a hot filament), this extra emission was greatly reduced. These facts lead us to believe that the extra structure in the EDCs from sample 19p was not caused by contamination. The origin of the extra structure, however, is not clear.

The band bending behavior of the two n-type samples with Cs was different from that of the two p-type samples. On clean p-type GaAs, the bands are flat to within experimental error, while on clean n-type GaAs the Fermi level is pinned at about mid-gap, resulting in about 0.5 eV band bending for sample 14n and about 0.7 eV for sample 18n.[15] Application of Cs to the p-type samples caused large changes in the Fermi level pinning position, while it left the pinning on the n-type samples relatively unchanged.

Figure 5 shows EDCs for sample 18n clean and with Cs for $h\nu$ = 10.2 eV. It can be seen that the Fermi level position changes a small amount, less than 0.1 eV, as Cs is applied. Prior to deposition of the Cs, sample 18n had been exposed to 10^3 Langmuirs of oxygen. The O_2 produced no changes in the EDCs, and the sticking coefficient for O_2 on (110) GaAs is about 10^{-5}.[16] Thus we believe that the behavior of sample 18n is approximately the same as it would have been if it had not been exposed to the oxygen.

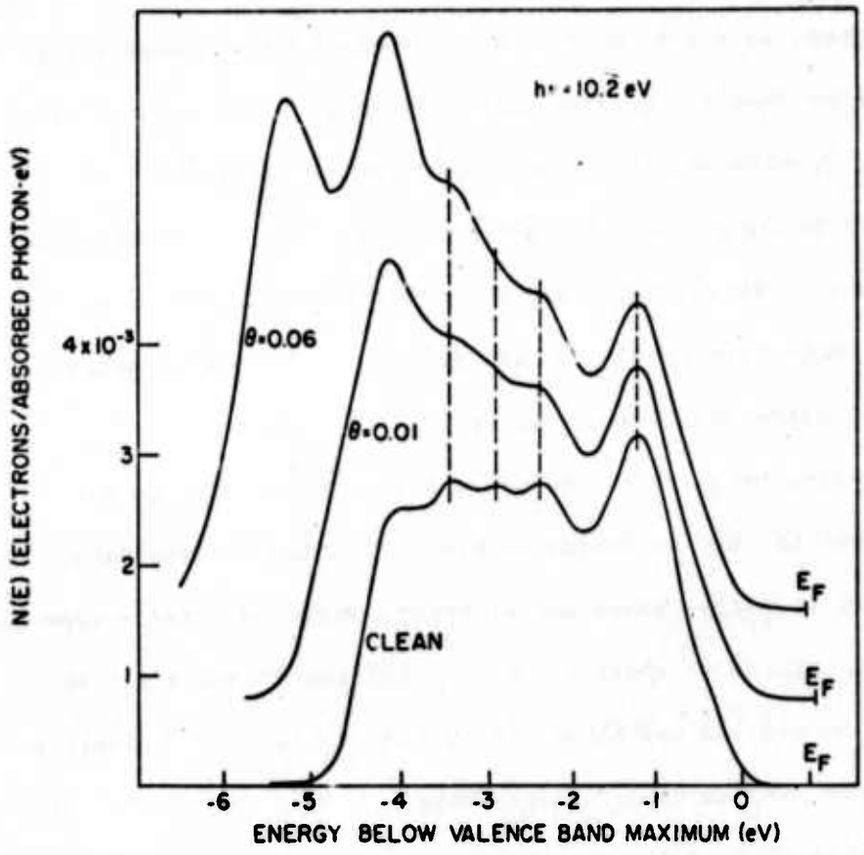

FIG. 5--EDCs for sample 18n at a photon energy of 10.2 eV as a function of cesium coverage, θ.

The movement of states into the forbidden gap and broadening of the first peak with Cs coverage were also seen for the two n-type samples and are shown in Fig. 6, where sample 14n is shown at the top and 18n at the bottom. The amount of broadening seen on the n-type samples is about the same as that seen on the p-type samples at comparable Cs coverages. Note that for sample 14n, with Cs on the surface, there is a high energy tail extending nearly to the Fermi level.

Figure 7 summarizes our data for the pinning position of the Fermi level by Cs at the surface for the four GaAs samples studied here. Two different cleaves of sample 17p are shown. The one having only three data points was first exposed to sodium, and as will be discussed later, the Cs exposure was made after the Na was removed. Note in Fig. 7 that the two p-type samples show large changes in their Fermi level pinning position,[17] and for both samples the band bending is greater at intermediate coverages than it is for the larger coverages. The limited data for the two n-type samples indicates that the pinning position on the cesium covered surface is slightly higher than on the clean surface.

The line of Fig. 7 marked VBM is the position of the valence band maximum for the clean surface. The dotted line rising up from the VBM line is the extrapolated upper edge of the EDC, with Cs coverage. The extrapolated upper edge was determined by making a straight line extrapolation that cuts off the high energy tail. Thus at the higher coverages there is a considerable amount of emission above this edge, extending up to the Fermi level for the highest Cs coverages.

The application of sodium to sample 17p produced the rather unexpected result that althogh Na will stick temporarily to GaAs, under vacuum it

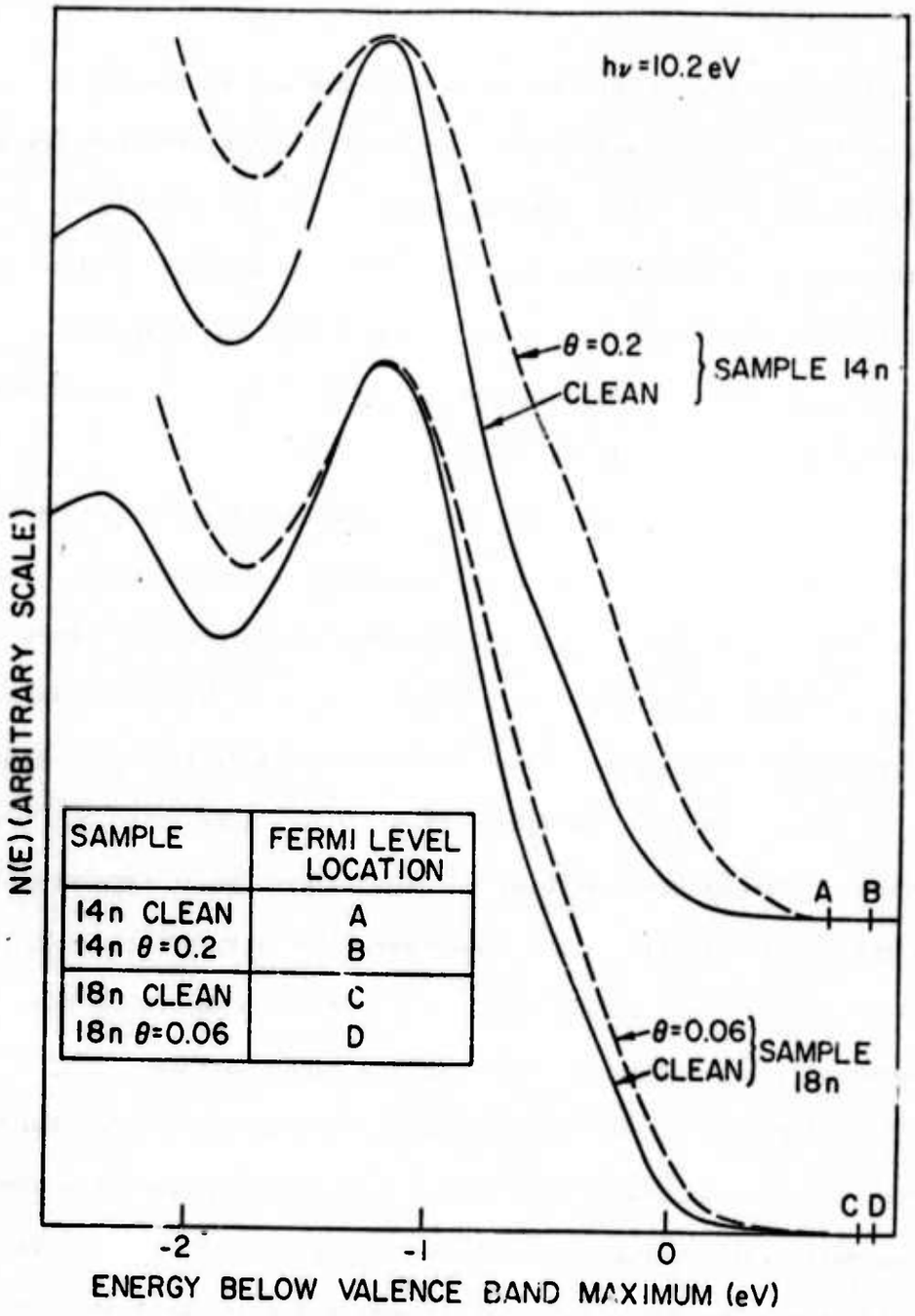

SAMPLE	FERMI LEVEL LOCATION
14n CLEAN	A
14n θ=0.2	B
18n CLEAN	C
18n θ=0.06	D

FIG. 6--The high energy portion of EDCs at a photon energy of 10.2 eV for samples 14n (upper) and 18n (lower) showing the upward movement of states into the energy gap as Cs coverage is increased.

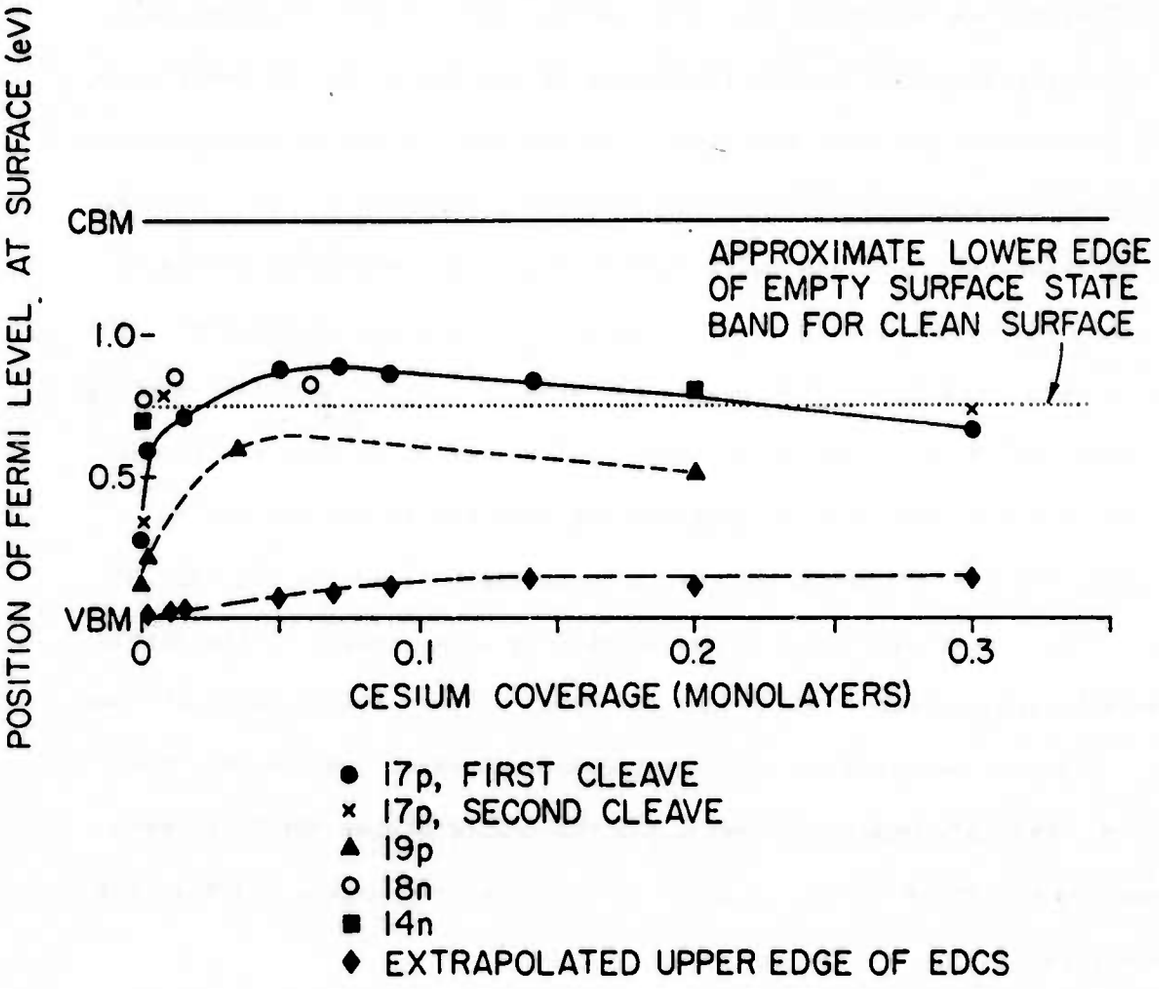

FIG. 7--Position of the Fermi level at the surface relative to the valence band maximum (VBM) and conduction band minimum (CBM) as a function of cesium coverage for the samples studied here. The positions of the VBM and CBM are shown for clean GaAs. The movement of states upward into the energy gap is indicated by the extrapolated upper edge of the EDCs.

evaporates over a period of hours. Figure 8 shows EDCs at a photon energy of 10.2 eV for Na on sample 17p. The bottom curve is for the clean GaAs. The top curve was taken within 15 minutes of the end of the Na deposition. The curves in between show the changes in the EDCs as the Na re-evaporates. After about 3 days the Na had almost completely evaporated. Mild heating to approximately 100° C was sufficient to remove the remaining traces of Na. This very weak binding of Na to GaAs is in contrast to the very tight binding of Cs on GaAs. Flash desorption studies[18] have shown that heating to almost 700° C is necessary to remove all traces of Cs from the surface.

To show that the lack of band bending with the Na was not due to any peculiarities of the cleave, or to contamination, cesium was applied to the same cleave after the Na was removed by mild heating of the sample. Subsequent application of Cs caused the bands to bend downwards in approximately the same manner as on the first cleave to which only Cs had been applied. The band bending behavior for the second cleave which had been exposed to Na before the Cs is shown in Fig. 7 as the points labeled "17p second cleave".

Figure 8 also shows another large difference in the behavior of Na on GaAs compared to that of Cs on GaAs: the Fermi level pinning position is changed by only a slight amount at the heaviest Na coverages, and in fact the Fermi level pinning position is slightly lowered, rather than raised, by the Na on the surface. The Na does lower the threshold for photoemission and raise the yield, however.

In an effort to get more Na to stick to the GaAs, Na was evaporated with the GaAs held at liquid nitrogen temperature. Immediately after evaporation, EDCs showed only a structureless scattering peak. After several

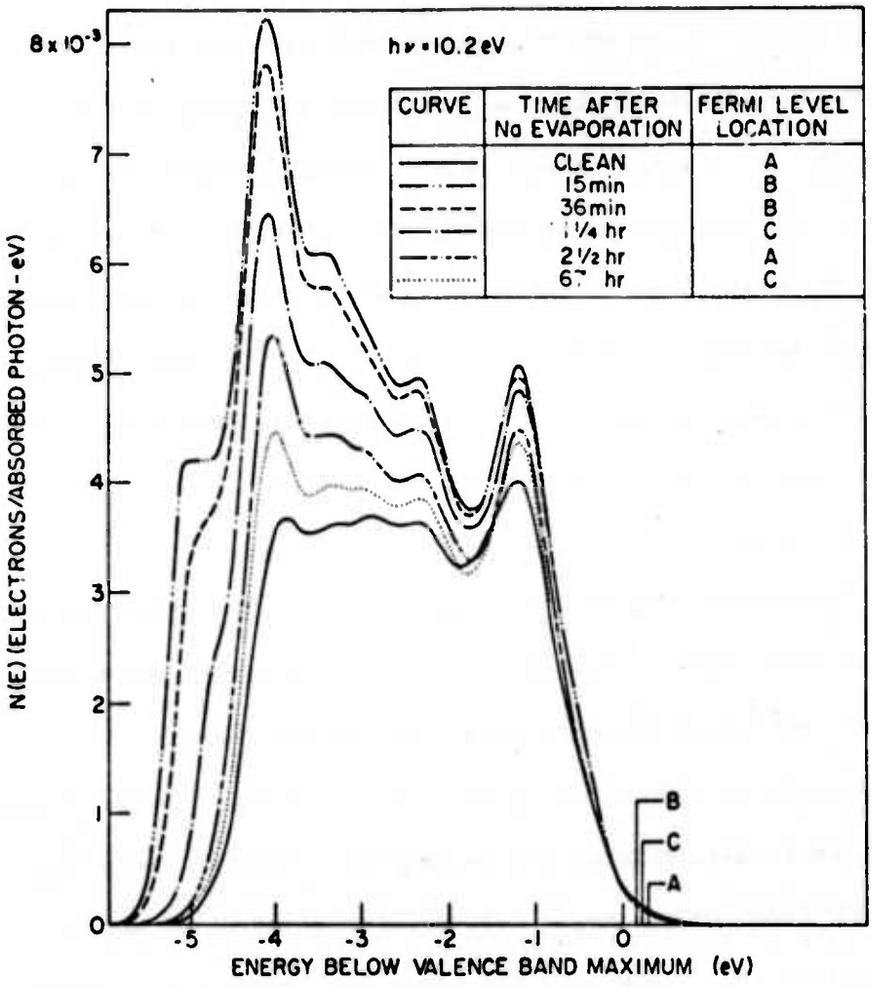

FIG. 8--EDCs for sample 17p showing the effect of sodium on the GaAs surface. The highest curve shows an EDC taken 15 minutes after the Na evaporation. The intermediate EDCs show changes with time as the Na leaves the surface, approaching the shape of the bottom EDC for the clean GaAs before Na was applied to the surface. The EDCs were taken at room temperature and at a photon energy of 10.2 eV.

hours and warming to 130° K, an EDC with characteristic GaAs peaks was obtained. It showed a threshold about 0.5 eV lower than that of the highest curve in Fig. 8, a larger yield, and no change in Fermi level pinning position. Further changes in the sample temperature caused only as much as ± 0.1 eV shift in the Fermi level pinning position, but since it was not possible to separate effects due only to the cooling of the sample from effects caused by changes in the Na coverage caused by evaporation, the measurements on the cooled sample were not pursued further. Warming removed all of the Na.

There was a negligible movement of states into the forbidden gap for Na covered GaAs at room temperature, but a small measureable upward movement of states for the liquid nitrogen cooled Na covered GaAs.

As far as we know, no data relating Na coverage on GaAs to the change in the work function is available in the literature. However, measurements of coverage vs work function for Na on sputter cleaned Ge (111) and Si (111) have been published.[19] Although the materials, surface and cleaning technique are different from that of this paper, and the Na did not evaporate from the Ge or Si, the values of work function change from Reference 19 can be used to give a crude estimate of our Na coverage on GaAs. At room temperature, the greatest change in work function we saw for Na on GaAs was about 0.5 eV. From the data of Reference 19, this would correspond to a coverage of 0.05 - 0.1 monolayers. For the coverage with the sample at liquid nitrogen temperature, there was a work function drop of about 1 eV. Assuming that the larger shift is due to increased coverage and is not caused by the lower temperature, the data of Reference 19 would correspond to a coverage of 0.2 to 0.25 monolayers.

IV. DISCUSSION

Figure 9 shows a model for the density of surface states on the clean (110) GaAs surface, derived from photoemission measurements[15,20] and theoretical studies.[15,21] The bottom half of the bandgap is free of surface states; any filled surface states lie below the valence band maximum. Empty acceptor-type surface states lie in the upper half of the bandgap. The approximate edge of the empty surface state band is indicated in Fig. 7.

When the surface state model shown in Fig. 9 is compared with the Fermi level pinning positions for metal-GaAs Schottky barriers from previous studies,[2] an interesting problem becomes evident. Although experimental measurements of Schottky barrier heights are usually explained in terms of pinning of the Fermi level by surface states, the pinning positions reported for most metals on GaAs[2] fall in the lower half of the band gap, about 0.1 to 0.3 eV below the position we find for the lower edge of the empty surface state band on the clean GaAs. Freeouf and Eastman[22] have found that the Schottky barrier pinning position is well correlated with the position of the empty surface state band for a number of III-V materials, but the Schottky barrier pinning position for Au on these materials, determined from previous studies,[2] falls below the lower edge of the empty surface state band. It is possible that the empty surface state distribution seen by Freeouf and Eastman has been distorted by matrix element effects or by excitonic effects.[23] Such a distortion may sharpen and lower the measured distribution (our Fermi level pinning measurements determine the lower edge of the distribution, as discussed below.) Such effects are not likely to change the observed correlation

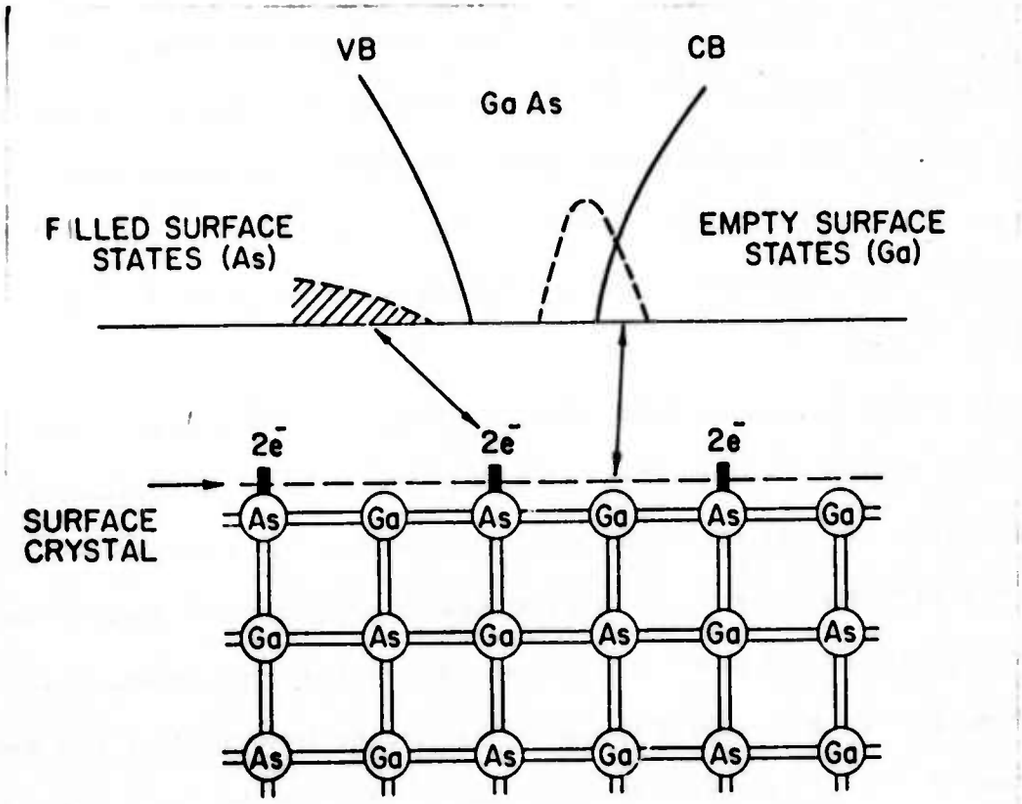

FIG. 9--Model for the clean GaAs (110) surface derived from photoemission studies and theoretical work.[15,20] The upper part shows the energy location of the surface states: empty surface states fill the upper half of the energy gap, while filled surface states (which have not been detected) lie below the valence band maximum. The lower part of the figure shows the spatial location of the surface states: the empty surface states are primarily associated with surface Ga atoms, while the filled surface states are primarily associated with surface As atoms.

between the position of the empty surface state band and the Schottky barrier pinning position.

It may be asked if the lower pinning position for Schottky barriers on GaAs could be caused by a tail of empty surface states extending below the empty surface state edge shown in Fig. 7. Our data from the clean GaAs samples allows us to set an upper limit on the number of states in any such tail. Using the measured band bending of about 0.5 eV in the case of sample 14n, a calculation using the depletion approximation shows that the surface charge required to produce this band bending is about 6×10^{10} electrons/cm^2. This is the total number of filled surface states for sample 14n. Averaging the Fermi level positions from our available EDCs at 10.2 eV for clean samples 14n and 18n shows that the Fermi level on sample 18n is about 0.02 eV higher on sample 18n than on 14n. This very small change in pinning position with a large change in doping shows that the Fermi level for sample 14n is at the edge of a large density of surface states. Since the thermal broadening of the Fermi function at room temperature gives a significant probability of occupation up to 0.1 eV above the Fermi level, the electrons on the surface of sample 14n must be mostly located above the Fermi level in the high density of empty surface states, rather than in a tail extending below the empty surface state band. Any such tail must contain much less than 6×10^{10} states/cm^2, and it is doubtful if such a low density of states could be the cause of Fermi level pinning in Schottky barriers.

As will be discussed below, we believe our data indicates that the empty surface state band represents a first approximation to the Fermi level pinning position for Schottky barriers, but the presence of the metal

on the surface causes the electronic structure of the surface to be modified in such a way as to cause the actual pinning position to differ from the position of the empty surface state band on the clean GaAs.

Figure 7 shows the pinning position of the Fermi level at the surface as a function of cesium coverage for the four GaAs samples studied. The data for Fig. 7 was measured from EDCs made at a photon energy of 10.2 eV. This photon energy was used because it is believed that at 10.2 eV the upper edge of the EDC for clean GaAs represents the valence band maximum. Since direct transitions dominate the EDCs of GaAs,[11,24] the upper edge of the EDC does not necessarily represent emission from the valence band maximum. However, two features of the EDCs at 10.2 eV lead one to believe that the upper edge of the EDCs at 10.2 eV does represent emission from the valence band maximum: 1) by plotting the position of the upper edge of the EDC relative to the position of the Fermi level for clean GaAs, it is found that the upper edge is at the highest energy in the photon energy range of 10 to 11 eV, and 2) there is a small shoulder on the upper edge of the EDCs in a small range of photon energies around 10.2 eV which has the characteristics of a transition at Γ in the Brillouin zone, the location of the valence band maximum in k space.[25]

The Fermi level points in Fig. 7 were measured using the first peak in the EDCs as a reference point because the peak is sharp and easily located.[26] As can be seen in Figs. 1, 4 and 5, alignment of the first peak of the EDCs for various Cs coverages brings the other peaks into close alignment. The line marked VBM, for valence band maximum, in Fig. 7 is taken from the extrapolated upper edge of the EDC for clean GaAs. The upper edge of the EDC for clean GaAs, measured from the first peak, comes to within 0.05 eV

of the same energy for the four samples studied. States move into the forbidden gap and the first peak broadened with cesium exposure in a similar manner on all four samples (see Figs. 3 and 6 for the broadening of sample 17p). The extrapolated upper edge of the EDC moves to higher energies as the Cs coverage is increased. This movement of the upper edge is also shown in Fig. 7. By extrapolating the upper edge of the EDC, the high energy tail was cut off, so for the larger Cs coverages there is appreciable emission from above the extrapolated upper edge. This effect will be discussed more completely below.

From Fig. 7 it can be seen that the movement of the Fermi level at the surface is similar for samples 19p and 17p, but that the Fermi level remains about 0.2 eV closer to the valence band maximum for sample 19p than it does for sample 17p. A likely explanation for the lower Fermi level pinning position for sample 19p is that the heavy doping of sample 19p produces very sharp band bending. For both p-type samples the bands bend down, but for sample 19p the band bending length is comparable to the electron escape depth. Thus for sample 19p the highest energy electrons escaping from deepest in the GaAs originate far enough below the surface that the valence band is closer to the Fermi level than it is at the surface. The depletion approximation is probably not very accurate for a sample doped as heavily as 19p, but it allows us to make a rough calculation to see if the above explanation is reasonable. The depletion approximation gives a total band bending length of 50 Å for sample 19p, and 630 Å for sample 17p, assuming a band bending of 0.5 eV at the surface. Calculating the band bending 10 Å below the surface, we find a difference between the position of the valence band maximum at the surface and 10 Å below

the surface of 0.2 eV for sample 19p and 0.02 eV for sample 17p. The 10 Å depth is reasonable in view of the expected electron escape depth, and the calculated 0.2 eV difference in band bending at that depth is about what is seen in Fig. 7. This simple calculation gives us confidence that the difference shown in Fig. 7 is at least partly due to the difference in band bending lengths.

It is important to learn what role the empty surface states that reside in the upper half of the band gap on clean GaAs play in the formation of Schottky barriers. The data shown in Fig. 7 suggest that the empty surface states may play an important part in the determination of the Fermi level pinning position, but that it is not simply a matter of filling these states with electrons from the metal.

One might be tempted to assume that the Fermi level pinning is due to simple filling of the empty surface states and/or bulk acceptor states with electrons from the metal. However, it is easy to show that this can not be reconciled with the existing data. For example, if this were the case the Fermi level should not drop with increasing coverage as it does (see Fig. 7) for coverages above about 0.05 monolayers.

Thus, it is important to realize that there may be interactions between the surface states and the metal which also play a role in determining the pinning position.

These might, for example include: some degree of mixing of surface state and metal wave functions,[3] dielectric effects[4,5,27] or some combination of these effects. Other work suggests this also, for example the slight dependence of the pinning position on electro-negativity of the metal.[2]

Once all of this has been said, it is important to note that the final pinning position is within tenths of an eV of the bottom of the empty surface states. Thus, a strong correlation exists between the pinning position and the bottom of the empty surface states and deviations of the pinning position from this energy due to metal-surface state interactions are only on the scale of tenths of an electron volt.

Riach and Peria[19] studied Cs on p-type Ge and obtained a curve showing the position of the Fermi level at the surface that is similar to our Fig. 7, in that the Fermi level rises sharply for small coverages of Cs and then falls with larger exposures. The drop with larger exposures is much steeper and drops farther than on GaAs, however. Their explanation for their data is similar to our explanation for the Cs-GaAs data: the behavior at low coverages can be explained as the Cs acting as a donor level, but for larger coverages it is necessary to assume that the surface state distribution is changed by the presence of the Cs on the surface.

Uebbing and Bell[28] have studied Cs-GaAs Schottky barriers with about 900 Å of Cs 'frozen' onto a GaAs surface at liquid nitrogen temperature. The GaAs was cleaved and the Cs was evaporated under ultra-high vacuum. They found a barrier height of 0.63 eV, a result which is in agreement with the Fermi level pinning position we find here for the larger Cs coverages. When plotted versus electronegativity, the Cs-GaAs Schottky barrier height fits the trend of the data of Mead[2] for Schottky barrier heights from other metals on GaAs. This fact shows that Cs-GaAs Schottky barriers are similar to Schottky barriers formed with other metals. Thus, any explanation of the Cs-GaAs Schottky barrier height should apply to Schottky barriers on GaAs formed with other metals.

Scheer and Van Laar[17] have also reported the pinning of the Fermi level on GaAs caused by Cs. They based their conclusions on an interpretation of yield data. The pinning position they report (0.44 eV above the valence band maximum) is about 0.2 eV below the position reported here. However, it is likely that in their experiment the Cs also caused the upward movement of states into the energy gap as seen in our study. In that case their measurement should be compared to the distance between the Fermi level and the extrapolated upper edge of the EDCs as shown in Fig. 7. Making that comparison, the value of Fermi level pinning position found by Scheer and Van Laar[17] is in good agreement with the position at highest coverage reported here.

It is interesting to note that from the electronegativity of Na, extrapolating the trend of the data of Mead,[2] we would expect a Na-GaAs Schottky barrier to have a pinning point 0.6 eV above the valence band maximum. Our data, however, shows no pinning caused by Na on GaAs. We do not know of any Schottky barrier studies made on a thick Na film on GaAs, but it would be quite surprising if Na on GaAs did not form a Schottky barrier. It is possible that if a thicker layer of Na could be applied to the GaAs that pinning of the Fermi level would occur.

It should be noted that the ionization potential of Na (5.15 eV) is considerably larger than that of Cs (3.9 eV), so that the Na is less likely to form a positive ion at the GaAs surface. If Cs forms an ionic bond with the surface and Na does not, the fact that Cs causes band bending and sticks tightly while Na does not would be explained. It appears that there may be an activation energy for transfer of an electron from the Na to GaAs.

The broadening of the first peak and high energy tailing caused by Cs coverage, shown in Figs. 3 and 6, is probably evidence of an interaction between the Cs and the GaAs. Before discussing the possible inter-

actions, we will first discuss several possible experimental artifacts which might be cited as a cause for the broadening, and will show that the artifacts cannot explain the observed broadening. Possible artifacts are: 1) reduction of the resolution of the energy analyzer caused by uneven deposition of Cs on the collector surface, 2) contamination of the cesiated surface, and 3) uneven deposition of Cs on the GaAs surface.

The resolution of the energy analyzer can be checked by measuring the broadening of the Fermi edge of the copper sample used to determine the position of the GaAs Fermi level. Measurement of the width of the Fermi edge of the Cu EDCs taken at a photon energy of 7.7 eV showed that for sample 17p, for all seven Cs coverages, the width for 10% to 90% of the edge height was 0.2 to 0.27 eV, with the sharpest Fermi edge for the 0.001 monolayer coverage, and the broadest Fermi edge for the 0.09 and 0.3 monolayer coverages. Thus any changes in analyzer resolution are much too small to account for the observed broadening of the first peak.

Contamination as a source of broadening can be ruled out. Although there may have been a small amount of contamination of the Cs film during the course of the experiment, there were no changes with time in the EDCs that could be attributed to contamination. The seventh cesiation of sample 17p was heavily contaminated, however, by the outgassing of a filament which had not been heated previously during the course of the cesiations. The result is shown in Fig. 3b as the curve for 0.3 monolayers + contamination. As can be seen in the figure, the broadening is greatly reduced by the contamination. Thus contamination reduced the broadening instead of causing it. Exposure of the contaminated 0.3 monolayer cesiation to 24 Langmuirs of oxygen caused an additional small decrease in the broadening.

Uneven coverage of Cs on the GaAs would have two effects; a variation in work function over the surface, and a variation in band bending over the surface. A variation in work function would cause a broadening of the low energy edge of the EDC, but not the high energy edge. Figure 7 shows that the band bending changes by only a small amount over a wide span of Cs coverages, so that band bending variations over the surface could not be sufficiently large to cause the observed behavior. Furthermore, one would expect that with additional Cs coverage, non-uniformities in coverage would tend to disappear. In fact the broadening increases with coverage.

Having shown that experimental artifacts are not the cause of the broadening, it remains to decide what is the cause. The broadening was also seen by Eden[11] for Cs on GaAs on a heavily doped p-type sample comparable to sample 19p. Eden explained the broadening as being caused by emission from within the band bending region. If electrons were excited from a range of depths within the band bending region which corresponded to a large variation in the amount of band bending, peaks in the EDCs would be broadened. However, sample 17p shows the same sort of broadening as sample 19p, and for sample 17p the band bending length, calculated from the depletion approximation, is much greater than the electron escape depth. For the bands to bend sharply enough to cause the effect seen here, there would have to be some source of band bending besides the unscreened acceptors in the depletion region.

One such source of band bending is the interaction described by Inkson.[4] He has developed a model of Schottky barriers in which the image potential associated with the metal layer causes the valence band of the semiconductor to rise, and the conduction band to drop, causing the semiconductor energy gap to shrink to zero at the interface. Although the movement of the band edge seen here is not as extreme as suggested by

Inkson, it may be due to the mechanism suggested by him. The Fermi level pinning appears to be largely caused by the empty surface state band, and the conventional depletion region band bending seems to be present. If we add to this picture an upward band bending of the valence band, similar to that proposed by Inkson,[4] we can explain the observed data. The combined picture for the valence band bending would be a downward band bending extending from about 600 Å into the GaAs for sample 17p and about 50 Å for sample 19p, followed by a short upward band bending starting ~ 5 Å from the Cs-GaAs interface. The upward band bending would bring the tail of the valence band edge up to the Fermi level. In this picture the peaks in the EDCs would come from electrons excited from behind the 5 Å up-bent region. Electrons excited from the sharply up-bent region would contribute to the broadening and tailing of the first peak, the sharpness of the bending smearing out any structure from the last 5 Å.

While the above reasoning shows that grafting Inkson's model onto a more conventional Schottky barrier model can explain the observed data, it is clear that more theoretical work is necessary to see if such a combination of models can in fact be made, and what effect the empty surface state band would have on Inkson's model.

Another possible explanation for the broadening of the first peak is emission from electrons in states caused by the presence of the Cs on the surface. This emission could have two origins: emission from metallic Cs or emission from electron wave functions tailing into the GaAs band gap from the Cs in resonance states, such as those suggested by Heine.[3] However, the possibility of emission from metallic Cs seems unlikely to us. The broadening and tailing seen does not look at all like the sum of a GaAs EDC and a bulk Cs EDC.[29,30]

Emission from Cs resonance states seems like a possible explanation for the broadening; however, there are some possible objections to this

explanation. The lack of any structure in the broadened and tailing region is one such objection. Intuitively one would feel more comfortable attributing structure in the EDC to a Cs-induced level, rather than a broadening of structure already present. Perhaps a more important objection is the fact that Heine's model was developed to account for pinning in the absence of true surface states, on the assumption that the intrinsic surface states would join onto Bloch waves in the metal and would thus be removed.[3] However, our data indicates that the empty surface state band remains in the presence of the Cs, although it may be modified somewhat by the Cs. Furthermore, Freeouf and Eastman have reported that the empty surface state band remains when several monolayers of Pd are evaporated onto the GaAs surface.[22] Apparently the empty surface states are so well localized on the surface Ga atoms that they do not strongly interact with the metal.

Whatever the detailed explanation for it, the broadening and tailing of the first peak seems to indicate some type of interaction of the Cs with the GaAs beyond simply filling the existing surface states. Comparison of Figs. 3 and 7 shows that the downward movement of the Fermi level pinning position occurs at about the same Cs coverage as appreciable broadening of the first peak, that is, at about 0.07 monolayers. Thus, both the broadening and the downward movement of the Fermi level pinning position probably are the result of the same mechanism.

V. CONCLUSIONS

The use of photoemission has allowed us to study the interface between a metal and a semiconductor for metal coverages below a monolayer. For even very low Cs coverages the Fermi level pinning and band bending characteristic of a Schottky barrier are evident. However, as the Cs

coverage is increased the Fermi level pinning position changes in a complicated way which cannot be explained in terms of the surface state distribution present on the clean surface.

At the lowest coverages of Cs, the Fermi level pinning behavior can be explained by assuming that the Cs gives up an electron to the GaAs, and the net positive surface charge caused by the Cs^+ ion causes downward band bending which is limited by the empty surface state band. At higher coverages, however, two effects are seen which cannot be explained in terms of the surface state distribution on the clean surface: the Fermi level pinning position moves downward somewhat, and the leading peak of the EDC becomes broadened. A narrowing of the band gap caused by image forces, as proposed by Inkson,[4] seems to explain our data qualitatively if it is assumed that the narrowing occurs over a very short distance (approximately 5 Å), and if the narrowing is superimposed on conventional band bending picture in which surface states are present. Theoretical work on a model incorporating the above features would be very useful.

Other proposed interactions[3,5,27] between the Cs and GaAs may also explain the observed behavior if they can be reconciled with the presence of surface states which apparently persist in the presence of metal on the surface.

The data presented in this paper gives strong evidence that pinning by intrinsic surface states is not sufficient in itself to explain the formation of Schottky barriers, and indicates that some of the features of more sophisticated models[3,4,5,27] may be present. However, much more experimental and theoretical work will be necessary to determine the complete picture.

APPENDIX

We can examine the Fermi level movement up to the point when it starts to move back down, for sample 17p on the basis of a simple model of the empty surface state band. We will base our model on a combination of our work and that of Freeouf and Eastman.[22] For the empty surface state distribution we will take a triangular distribution starting 0.7 eV above the valence band maximum, peaked at 0.9 eV above VBM, and falling to zero again at 1.4 eV above VBM. The total number of states we will take as one per surface atom (two states per surface Ga atom), or 9×10^{14} cm^{-2}. Our purpose here is to give the reader some indication of what may be happening. The details of the model should not be taken seriously.

For the first cesiation with coverage estimated below 0.001 monolayers, the surface states play no part. The observed 0.3 eV band bending change requires a surface charge of about 7×10^{-11} carriers/cm^2, or 8×10^{-4} monolayers. If the cesium is completely ionized, this calculated value is in good agreement with the estimated coverage.

For the third cesiation, with estimated coverage of 0.05 monolayers, the Fermi level has penetrated about 0.2 eV into the empty surface state band. Approximating the Fermi function by a step function, this would give a surface charge of about 2.6×10^{13} electrons/cm^2, and incidentally would put the Fermi level right at the peak of the distribution. This compares to a cesium coverage of (0.05 monolayers)$(8.85 \times 10^{14} cm^{-2})$ = 4.43×10^{13} Cs atoms/cm^2. Again it appears that, assuming this model, most of the Cs is ionized.

If we assume that the work function drop is caused by a dipole caused by the Cs donating electrons to the GaAs and remaining on the surface as an ion, we can use the measured drop in threshold to get an estimate of the Cs ion density of the surface.

The formula for the potential drop in going through an infinite (in two dimensions) dipole sheet is $V = a\rho/\epsilon$, where a is the spacing and ρ the surface charge density. If we take $a = 5$ Å and $\epsilon = 8.84 \times 10^{-12}$ farad/meter (the value of the dielectric constant for free space), we can generate the following table:

TABLE A-1

Cesiation	Threshold Drop	Estimated Coverage (monolayers)	ρ (ions/cm^2)	ρ (monolayers)	Percent of Ionization of Surface Cs Atoms
#1	0	< .001	--	--	--
#2	.4	.015	4.42×10^{12}	.005	33%
#3	1.1	.05	1.22×10^{13}	.0137	27.5%
#4	1.5	.07	1.66×10^{13}	.0187	26.8%
#5	1.8	.09	1.99×10^{13}	.0225	25%
#6	2.4	.14	2.65×10^{13}	.03	21%
#7	4	.3	4.42×10^{13}	.05	16%

Considering the many approximations and simplifications involved, the two values calculated for the surface charg density for Cs #3, 1.22 and 2.6×10^{13} cm^{-2}, are very close.

Beyond the third cesiation the Fermi level pinning drops. Either the empty surface state band has become modified, or it is emptying out. As can be seen from Table A-1, the surface charge for the dipole to reduce the work function must continue to increase, however. Thus one cannot explain the data in terms of simple filling of existing states.

REFERENCES

1. John Bardeen, Phys Rev. 71, 717 (1947).
2. C. A. Mead and W. G. Spitzer, Phys. Rev. 134, A713 (1964); C. A. Mead, Solid State Elect. 9, 1023 (1966).
3. Volker Heine, Phys. Rev. 138, A1689 (1965).
4. J. C. Inkson, J. Phys. C: Solid State Phys. 5, 2599 (1972); J. Phys. C: Solid State Phys. 6, 1350 (1973).
5. J. C. Phillips J. Vac. Sci. Technol. 11, 947 (1974).
6. T. E. Madey and J. T. Yates, Jr., J. Vac. Sci. Tech. 8, 39 (1971).
7. H. Clemens and W. Monch, to be published
8. The data of Reference 6 shows a sharper drop of work function with Cs coverage than the data of reference 7, increasing to a 25% difference at 0.3 monolayers. We are treating this difference as a real difference between n and p type GaAs, although it could be partly due to a difference in experimental technique between the two groups.
9. G. B. Fisher, W. E. Spicer, P. C. McKernan, V. F. Pereskok and S. J. Wanner, Appl. Optics 12, 799 (1973).
10. H. R. Phillip and H. Ehrenreich, Phys. Rev. 129, 1550 (1963).
11. R. C. Eden, Ph.D. dissertation, Stanford University, 1967, unpublished.
12. R. C. Eden, Rev. Sci. Instrum. 41, 252 (1970).
13. L. F. Wagner and W. E. Spicer, Phys. Rev. Lett 28, 1381 (1972).
14. I. Lindau and W. E. Spicer, J. Electron Spect. 3, 409 (1974).
15. P. E. Gregory, W. E. Spicer, S. Ciraci and W. A. Harrison, Appl. Phys. Lett. 25, 511 (1974).
16. R. Dorn, H. Lüth and G. J. Russell, Phys. Rev. B. 10, 5049 (1974).

17. J. J. Scheer and J. Van Laar, Solid State Comm. 5, 303 (1967).

18. B. Goldstein and D. Szostak, Appl. Phys. Lett. 26, 111 (1975).

19. G. E. Riach and W. T. Peria, Surf. Sci. 40, 479 (1973).

20. D. E. Eastman and J. L. Freeouf, Phys. Rev. Lett. 33, 1601 (1974).

21. J. D. Joannopoulos and M. L. Cohen, Phys. Rev. B 10, 5075 (1974).

22. J. L. Freeouf and D. E. Eastman, to be published.

23. G. J. Lapeyre and J. Anderson, Bull. Am. Phys. Soc., Series II, 20, 359 (1975).

24. W. E. Spicer and R. C. Eden, in Proceedings of the Ninth International Conference on the Properties of Semiconductors Vol. 1, (Nauka, Leningrad, 1968), p. 65.

25. J. L. Shay, W. E. Spicer and F. Herman, Phys. Rev. Lett. 18, 649 (1967).

26. In Fig. 7 the position of the Fermi level for zero Cs coverage for both samples 19p and 17p is perhaps 0.1 eV too high, based on the calculated bulk position of the Fermi level. For both samples 19p and 17p on cleaves that were studied, but which were not used in the cesiation studies, the surface position of the Fermi level was found to be in agreement with the bulk position. This variation in the position of the Fermi level at the clean surface seems to be correlated with the quality of the cleave. In any case, relative changes in the position of the Fermi level as shown in Fig. 7 can be measured with confidence to an accuracy of 0.05 eV.

27. A. J. Bennett and C. B. Duke, Phys. Rev. 160, 541 (1967); Phys. Rev. 162, 578 (1967).

28. J. J. Uebbing and R. L. Bell, Appl. Phys. Lett. 11, 357 (1967).

29. N. V. Smith and G. B. Fisher, Phys. Rev. B3, 3662 (1971).

30. P. E. Gregory, P. Chye, H. Sunami and W. E. Spicer, to be published.

CHAPTER 4

ULTRAVIOLET PHOTOEMISSION STUDY OF CESIUM OXIDE FILMS ON GaAs

I. INTRODUCTION

Negative electron affinity (NEA) photocathodes have been studied extensively in recent years in an attempt to extend efficient infrared response to wavelengths longer than 1 micron.[1] By applying Cs-oxide surface layers to III-V alloys with bandgaps less than 1.2 eV, it is possible to construct photocathodes with long wavelength thresholds somewhat beyond one micron, but the maximum yield that can be obtained decreases strongly as the long wavelength threshold is increased. Two different models have been developed to explain the NEA photocathode properties: the dipole model[2,3] and the heterojunction model.[4,5,6] These two models postulate quite different properties for the cesium oxide activating layer. However, both models can be adjusted to fit the experimental spectral yield data for NEA photocathodes with a wide range of bandgaps. Therefore, experimental data in addition to yield measurements is needed to decide which, if either, model is correct. A knowledge of the correct model should be useful in deciding how improvements can be made in NEA photocathodes. In this paper we present ultraviolet photoemission measurements of Cs oxide layers on GaAs and compare the measurements to those previously reported for a bulk Cs-oxide film.[7] By comparing electron energy distribution curves (EDCs) from the Cs oxide layer on GaAs to EDCs from bulk Cs oxide, some direct information on the properties of the Cs oxide layer required for NEA activation of GaAs can be obtained. Measurements similar to those reported here on a variety of narrower bandgap III-V alloys should provide sufficient data to choose between the dipole and heterojunction models.

The dipole and the heterojunction models for NEA photocathodes differ in the properites assumed for the Cs-O activating layer. The dipole model assumes that the Cs oxide layer is of monolayer thickness for all III-V

alloys, independent of bandgap.[3] In one version of the dipole model, Fisher, Enstrom, Escher and Williams[2] suggest a double dipole layer consisting of a monolayer of Cs plus a monolayer of Cs_2O. The difference in work function between the III-V material, the Cs layer and the Cs_2O layer gives rise to a potential barrier at the surface. By approximating the barrier as a rectangular semitransparent barrier 8 Å thick by 0.28 eV above the vacuum level, they were able to fit their measured escape probability data for $Ga_xIn_{1-x}As$ NEA photocathodes having bandgaps from 0.7 to 1.4 eV and dopings of 3×10^{19} cm^{-3} to 2×10^{18} cm^{-3}. In their calculations they took into account the width of the internal energy distribution of excited electrons and energy changes in the band bending region. Their model assumed a constant work function independent of bandgap.

The heterojunction model[4,5,6,8] assumes that the Cs oxide layer is Cs_2O, an n-type semiconductor with a 2 eV bandgap. According to this model, a heterojunction is formed between the III-V material and the Cs_2O, with a heterojunction barrier at the III-V - Cs_2O interface. For III-V materials with a bandgap below about 1.2 eV, the heterojunction barrier becomes the dominant factor in determining the long wavelength response. The Cs_2O is assumed to have appreciable band bending, with a band bending length of about 50 Å. This band bending lowers the work function at the Cs_2O vacuum surface, with thicker Cs_2O layers having a lower work function for increasing thicknesses up to 50 Å. The electron transmission through the Cs_2O layer decreases with increasing thickness, so for a given bandgap III-V material there is a tradeoff between workfunction and electron transmission, resulting in an optimum Cs_2O layer thickness. The optimum thickness increases with decreasing bandgap.

Combined Kelvin probe and photoyield measurements of GaSb[4] have shown that the work function decreases with an increasing number of Cs-O_2 treatments, in agreement with the band bending part of the heterojunction model. The yield threshold did not decrease below 1.2 eV, in agreement with the statement that an interfacial barrier is the limiting factor in the long wavelength response on sufficiently narrow bandgap III-V materials. Tunneling through the barrier or excitation over it can extend the long wavelength response somewhat.[9] The heterojunction model has been used to explain the changes in yield spectra as a function of Cs oxide treatments on n- and p-type $InAs_xP_{1-x}$.[9]

As the above discussion indicates, the major difference between the dipole and heterojunction models is the thickness of the Cs oxide activating layer. The dipole model assumes a constant thickness, independent of bandgap, while the heterojunction model assumes a Cs oxide whose thickness increases with decreasing bandgap. The Cs oxide of the dipole model is assumed to be of monolayer thickness, so thin that the Cs oxide cannot be considered to have bulk Cs oxide properties. In contrast, the heterojunction model assumes that the Cs oxide layer is thick enough to have a band structure and band bending, although it is recognized that the Cs oxide is thin enough that the spacing between ionized donors is comparable to the Cs oxide thickness, so the band bending must be regarded as an approximation to the true behavior.[4] There is agreement that on GaAs the thickness approaches one or two molecular layers; there is disagreement as to whether the thickness is greater on the smaller bandgap materials.

A measurement of the Cs oxide layer thickness as a function of the III-V bandgap would provide a definitive test of the two models. Unfortunately the Cs oxide layers used in NEA photocathodes are so thin that direct

measurement of the layer thickness is quite difficult. In one case direct chemical analysis of the Cs content of a GaAs NEA photocathode gave a Cs content equivalent to a monolayer of Cs plus a monolayer of Cs_2O.[10] In most cases, however, estimates of the Cs oxide layer thickness are made by measuring the total Cs and O_2 flux directed at the III-V sample during activation and assuming a sticking coefficient. The sticking coefficient may well change during the course of activation,[11] so such measurements of thickness must be considered to be only estimates of thickness. Such estimates in the past have given a Cs oxide thickness of about 8 Å, independent of bandgap,[2] 4 to 10 monolayers on GaAs,[12] and approximately 7 Å on GaAs, 14 Å on InP, and 29 Å on a $GaAs_xSb_{1-x}$ alloy.[4] Goldstein has used Auger spectroscopy and LEED to develop a model for the Cs oxide activating layer on GaAs. In his model, the Cs-oxide layer is amorphous, about 10 Å thick, and there is no definite ratio between the amount of Cs and amount of oxygen in the layer.[11]

Ultraviolet photoemission spectroscopy (UPS) can supplement the above types of measurements by providing information about the electronic properties of the Cs oxide activating layer and information about the relative thickness of different layers. The ability of UPS to provide this information is based on the surface sensitivity of UPS. The surface sensitivity is determined by the escape depth of unscattered electrons from the material being studied. The escape depth from GaAs has not been determined, but escape depth values from other materials[13] suggest that for GaAs the escape depth is 10 to 25 Å for electrons excited to 10 eV above the Fermi level. The escape depth increases below 10 eV, so photoemission using visible and infrared light is much less surface sensitive than photoemission using ultraviolet light. It should be emphasized that the escape depth

for unscattered hot electrons is determined principally by electron-electron scattering and is a property of the bulk material, not of the surface treatment.

II. EXPERIMENTAL PROCEDURE

A. Bulk Cesium Oxide

We have previously reported photoemission data from the oxidation of a thick cesium film.[7] We will use EDCs from that experiment in the analysis of our data from cesium oxide on GaAs. The bulk cesium oxide experiment was performed by evaporating a thick Cs film from a Cs ampoule onto a liquid nitrogen cooled copper substrate under ultra-high vacuum. The film was oxidized at liquid nitrogen temperature by exposing it to high purity oxygen admitted to the vacuum chamber through a leak valve. EDCs were measured for oxygen exposures in the range of 1L to 4×10^4 L.[14] The oxygen exposures produced large changes in the EDCs, indicative of the formation of different cesium oxides. Here we will be concerned with the higher oxygen exposures only.

B. Cesium oxide on GaAs

The experiment was performed on a 1.5×10^{17} cm^{-3} p-type, Zn doped, GaAs single crystal. This doping is 1 to 2 orders of magnitude lower than that used to make optimum NEA photocathodes. The sample was cleaved in ultra-high vacuum, exposing a (110) face. Cesium vapor was supplied from a conventional cesium chromate channel, and high purity oxygen was admitted through a leak valve. The pressure was monitored by a Redhead cold-cathode ultra-high vacuum gauge. In order to avoid possible contamination of the sample, hot filament vacuum gauges were not used.

EDCs were measured with an A.C. retarding potential analyzer.[15] The surface Fermi level of the sample was determined by measuring EDCs from a copper emitter formed by in situ evaporation. This allowed the Fermi level to be located on the sample EDCs.

The high energy cutoff of the LiF window on the vacuum chamber limited the photon energy range to $h\nu \leq 11.8$ eV. Monochromatic light for $2.2 \text{ eV} \leq h\nu \leq 11.8$ eV was supplied by a McPherson model 225 monochromator with a hydrogen discharge lamp; light intensity was monitored with a Cs_3Sb phototube having known sensitivity.[16] For yield measurements below 2.2 eV, a Bausch and Lomb monochromator with a tungsten light source was used, and light intensity was monitored with an S-1 phototube. The yield values in this paper are given in electrons per absorbed photon - that is, the yield has been corrected for the reflectivity of Phillip and Eherenreich[17] as tabulated by Eden.[18] The GaAs reflectivity has been used even for the heavily cesium oxide covered GaAs. Although the GaAs reflectivity may not be completely appropriate in that case, it is probably the best approximation available since even "thick" Cs oxide layers are probably thin (order 20 Å) compared to thicknesses necessary to dominate the optical properties (order 100 Å). Unless otherwise specified, the EDCs in this paper have been normalized so that the area under an EDC is proportioned to the yield at the photon energy for which the EDC was measured.

The cesium oxide surface layer on the GaAs was formed at room temperature by a sequence of Cs and O_2 exposures. The surface treatments are summarized in Table 1. For convenience in discussion, we have labeled the treatment steps with Roman numerals. These labels will be used to identify curves in the figures below. EDCs and yield spectra were measured after

TABLE 1

SUMMARY OF SURFACE TREATMENTS
Each treatment was applied in addition to the previous treatments.

Treatment Number	Description	Approximate O_2 Exposure During Treatment	Relative Change in White Light Sensitivity During Treatment
I	Cs only, applied to clean GaAs	None	--
II	O_2 exposure	20L	--
III	Cs exposure	None	7.6
IV	7 (Cs + O_2) exposures	~ 1L	3.2
V	4 (Cs + O_2) exposures	16L	.94
VI	5 (Cs + O_2) exposures	110L	.89
VII	2 (Cs + O_2) exposures	11L	.057

each treatment labeled in Table 1. Treatments were applied in the order listed in Table 1, from top to bottom. During the surface treatments the white light yield was monitored; the change in white light yield is shown in Table 1 as the ratio of the white light yield following the treatment to the white light yield preceeding the treatment. Treatments I and III were Cs exposures with no O_2, while treatment II was an O_2 exposure only.

A "yo-yo" technique was used for the Cs + O_2 treatments. O_2 exposures were made at the same time the Cs channel was evolving Cs. The procedure was to apply Cs until the white light yield reached a peak value, then to make a brief O_2 exposure to reduce the white light yield, after which the Cs exposure was continued until the white light yield again reached a peak. The sequence was repeated several times in each treatment. The number of Cs and O_2 sequences in each treatment is indicated in Table 1. Each Cs + O_2 treatment was followed by a Cs exposure that increased the white light yield to a peak value. (Treatment II was an O_2 exposure only, and was not followed by a Cs exposure until treatment III.)

The oxygen exposures caused a rapid drop in the white light yield. The drop in white light yield ranged from a factor of 3 after one of the O_2 exposures of treatment IV to a drop of 10^4 after one of the O_2 exposures of treatment VI. After the O_2 exposure the Cs caused the white light yield to increase again. The peak value of white light yield increased during treatment IV, but decreased during treatments V, VI and VII, indicating excess thickness in those cases.

The values of oxygen exposure given in Table 1 are the approximate total value of O_2 exposure made during each treatment. The value given for treatment IV is an estimate. The O_2 exposures for that treatment were short bursts for which it was not possible to make accurate exposure measurements.

III. RESULTS AND DISCUSSION

Yield spectra measured after each surface treatment are shown in Fig. 1, a log plot in Fig. 1(a) and a linear plot for treatments I, III and IV in Fig. 1(b). As the figure shows, treatments I, III, and IV all produced a high peak yield, but treatment IV produced a slightly lower threshold energy than treatments I and III, (thus the maximum in white light sensitivity). Treatment II lowered the yield for all photon energies and increased the threshold of response by about 1 eV. Treatment V lowered the yield, but did not raise the threshold, while treatments VI and VII both lowered the yield and raised the threshold. As the EDCs will show, treatments VI and VII produced a thick cesium oxide layer on the GaAs surface. The maximum yield produced after treatments I, III and IV is somewhat less than can be obtained from the best NEA photocathodes because the doping used here is 1 to 2 orders of magnitude lower than is usually used for NEA photocathodes.

Figures 2-4 show EDCs measured after each treatment step. The EDCs were measured for $h\nu$ = 10.2 eV.

The low tail extending from -5 eV to zero in the EDCs for treatments I-IV is recognizable as emission from the bulk GaAs. Figure 5 shows the high energy tail region of the EDCs from Figs. 2 and 3 enlarged, along with an EDC from the clean GaAs for comparison. Figure 5(a) shows the complete EDC for clean GaAs and the corresponding part of the EDCs for treatments I-V; Fig. 5(b) shows the high energy peak from Fig. 5(a). As Fig. 5(a) shows, peaks from the clean GaAs EDC are still present after treatment I. These peaks can be identified with features in the band structure for bulk GaAs;[18,19] the peaks are produced by electrons that did not lose energy in a scattering event before being emitted from the GaAs.

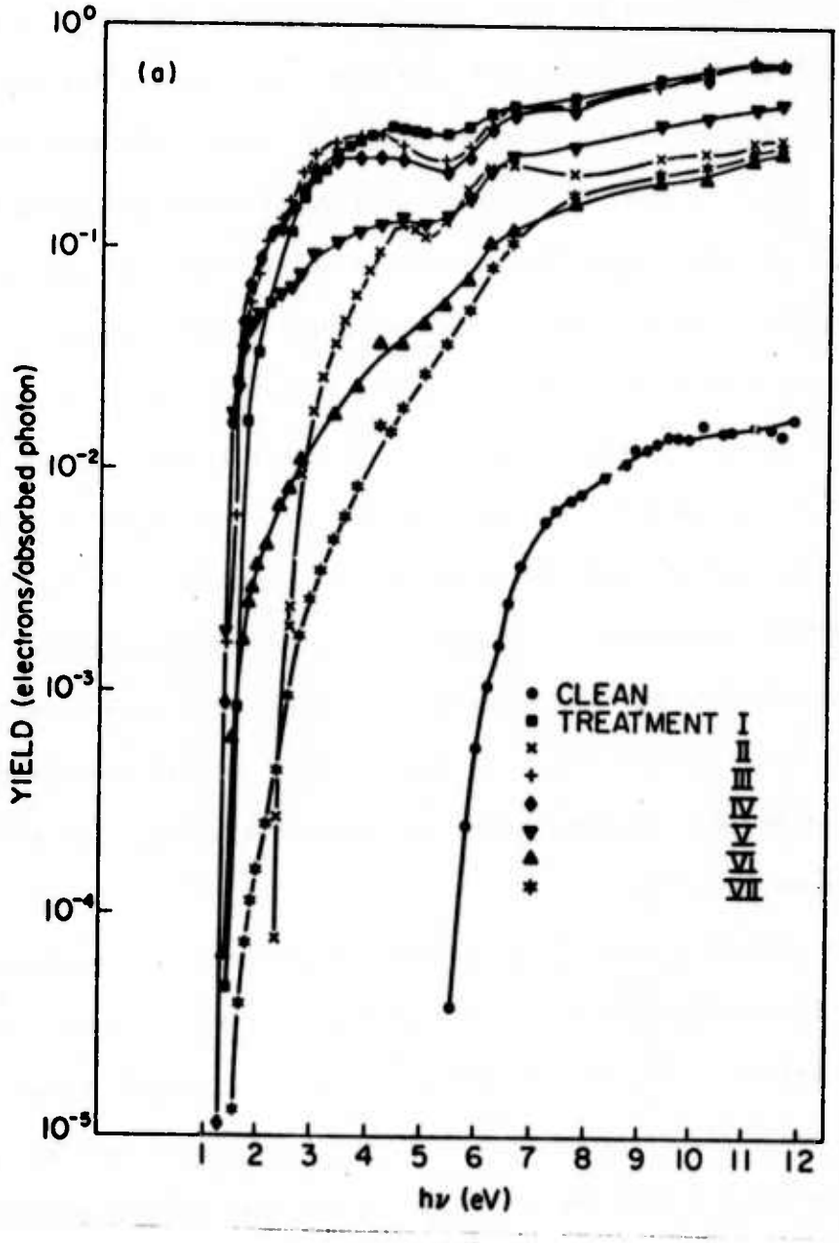

(a)

FIG. 1--a)Semilog plot of the yield spectra for clean GaAs, and for the seven surface treatments. The symbols are plotted at the points for which the yield was measured.

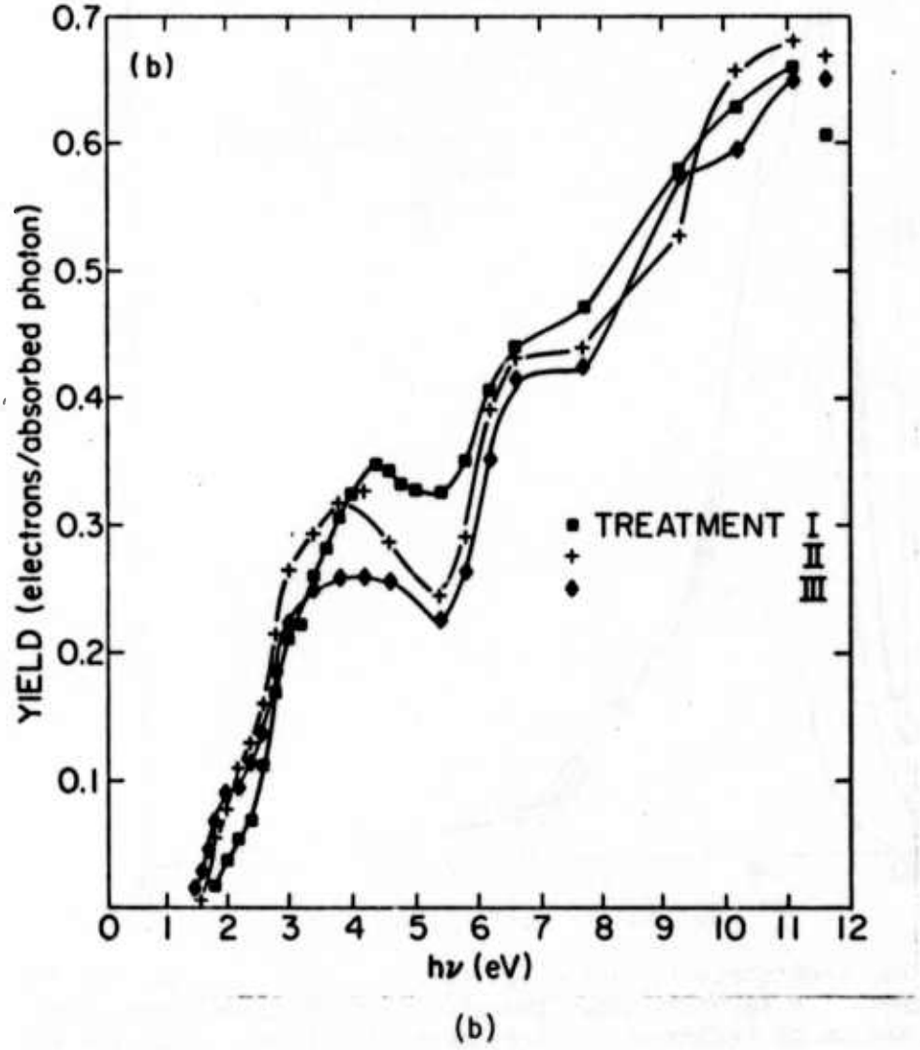

(b)

FIG. 1--b) Linear plot of the yield spectra for the three treatments from part a having the highest peak yield.

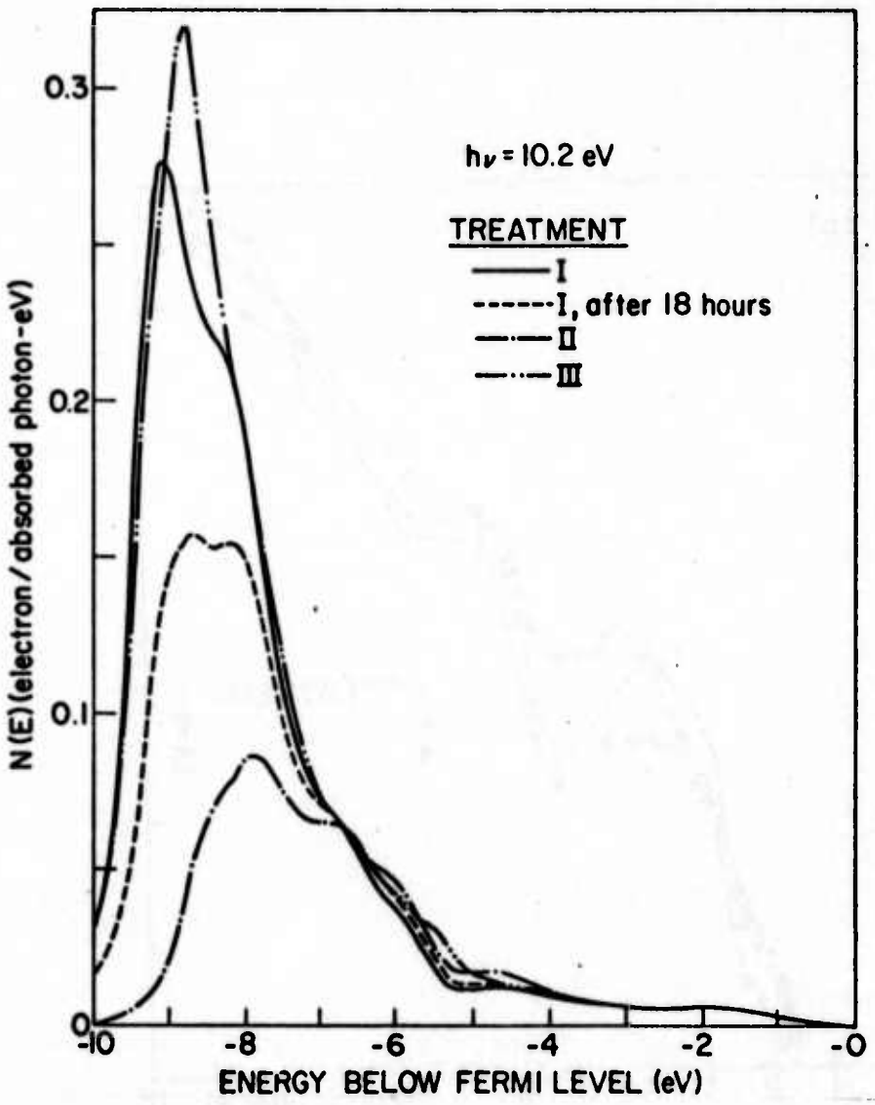

FIG. 2--EDCs for treatments I, II and III for hν = 10.2 eV. The EDC for treatment I + 18 hours shows the effect of 18 hours under ultra high vacuum on tratement I. Treatment II was made after the EDC for treatment I + 18 hours was measured.

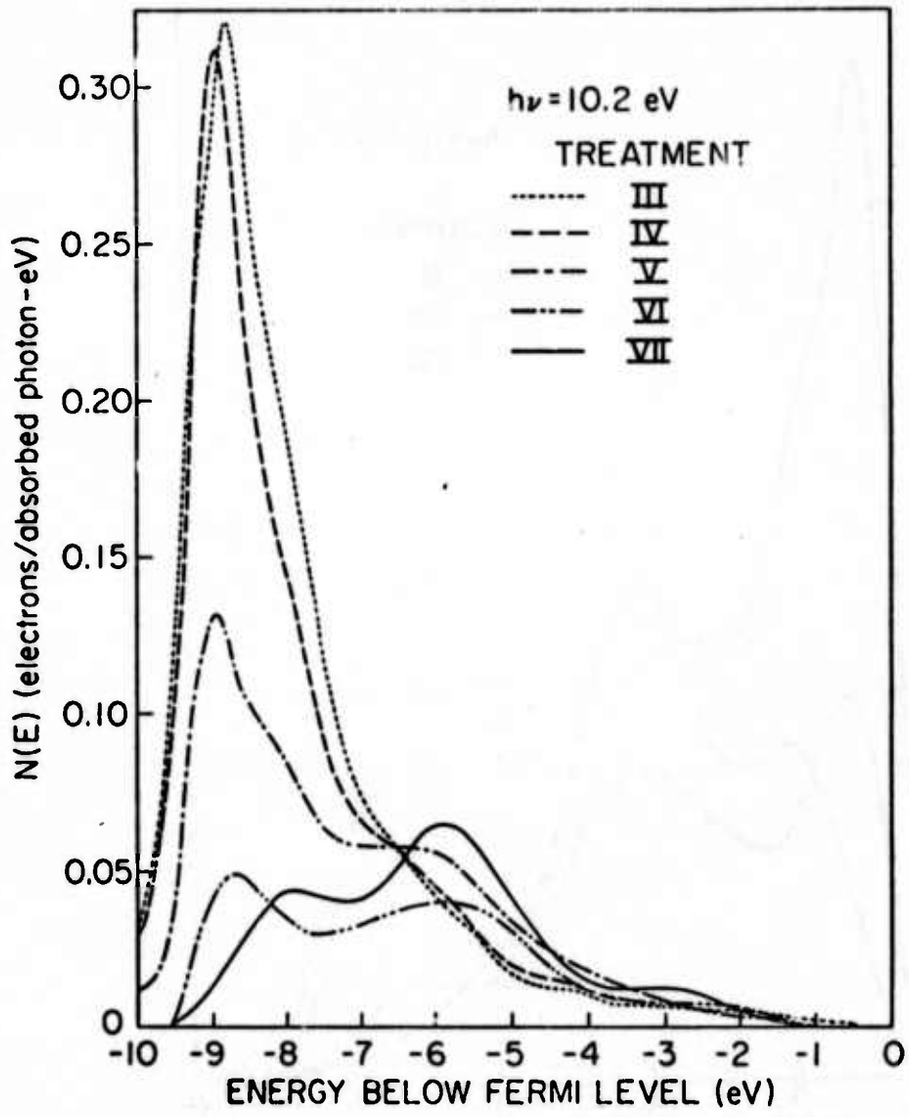

FIG. 3--EDCs for treatments III through VII for hν = 10.2 eV. Note that the EDCs for treatments V through VII are quite different than the EDCs for treatments III and IV. The EDC for treatment VII closely resembles an EDC for a bulk Cs oxide.

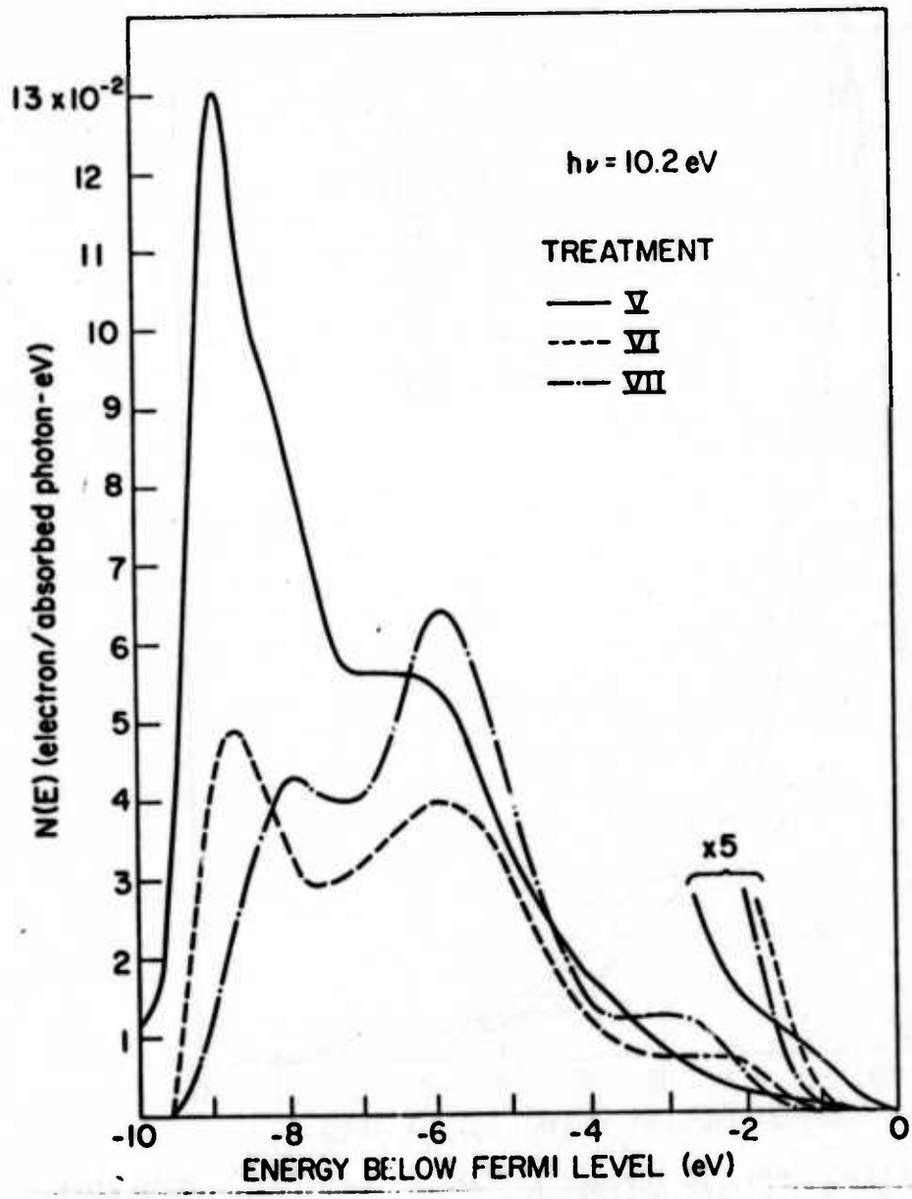

FIG. 4--EDCs for treatments V, VI and VII plotted on a different scale than the EDCs of Fig. 3. The expanded scales show that there is no detectable emission above -1 eV for treatments VI and VII.

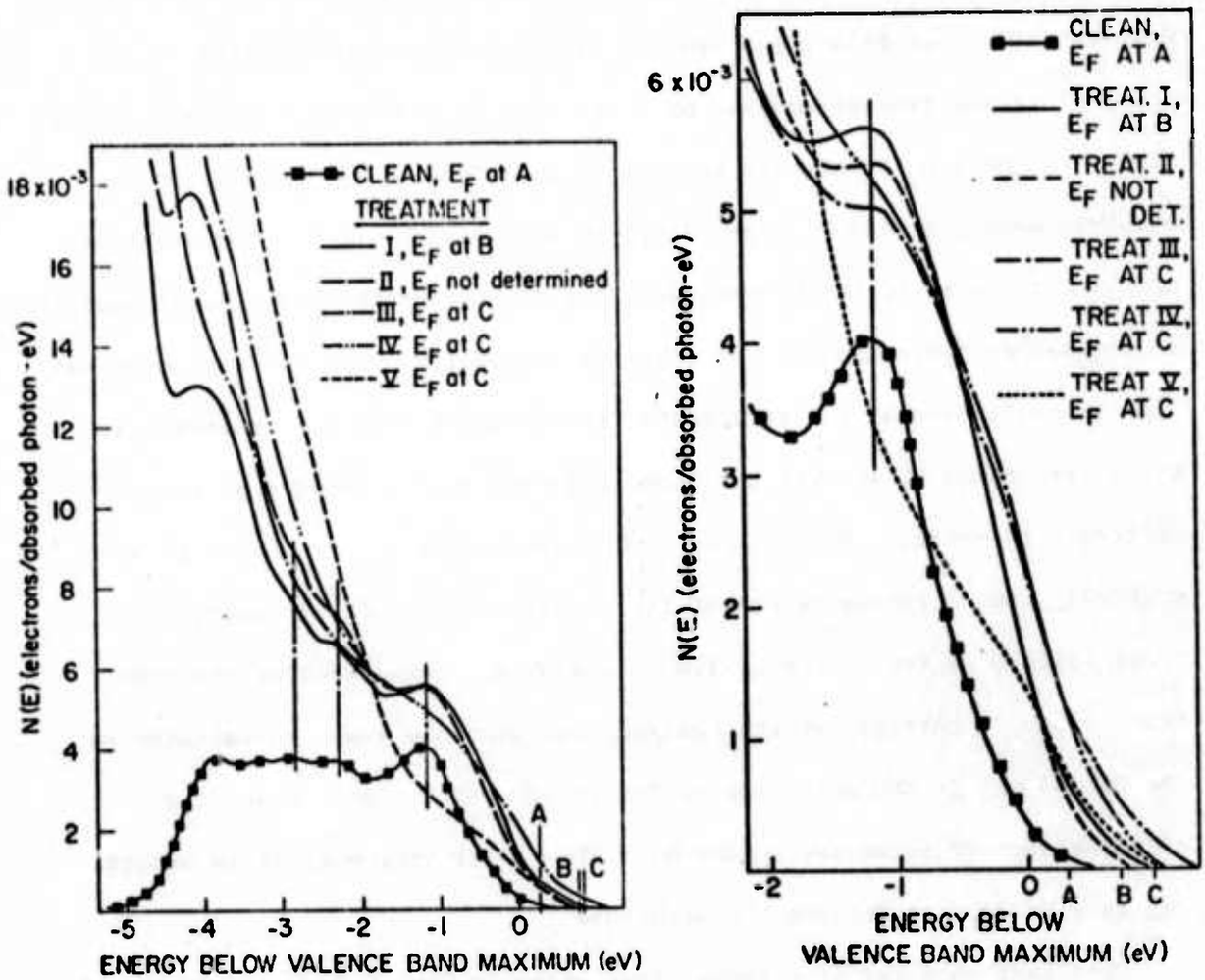

(a) (b)

FIG. 5--a) EDCs for clean GaAs and for the high energy tail of the EDCs for treatments I through V, from Figs. 2 and 3. Note that structure from the clean GaAs is still clearly present in the EDCs for treatments I through IV. The symbols on the EDCs are for curve identification and do not represent data points. b) The high energy peak of the EDCs from part a on an expanded scale. Note that the high energy peak is not significantly reduced for treatments I through III, but the peak became a shoulder after treatment IV, and was greatly reduced by treatment V.

For treatments II, III and IV, Fig. 5 shows that the high energy peak, associated with the GaAs, is not significantly reduced by the treatments. However, the other GaAs peaks are not present. The disappearance of the other peaks was probably caused by a decrease in the energy analyzer resolution. The Cs + O_2 treatments apparently contaminated the surface of the electron energy analyzer, degrading the energy resolution. The sharpness of the Fermi edge of the Cu emitter (used to monitor the Fermi level position) provides some indication of the analyzer resolution. The Cu Fermi edge was significantly broader for treatments III through V than for treatment I. After treatments VI and VII the Fermi edge was so broadened that it was difficult to detect. Part of the broadening of the Cu Fermi edge is undoubtedly due to contamination of the Cu emitter itself. However, the inner surface of the energy analyzer is also Cu, evaporated at the same time as the Cu emitter, so the analyzer was probably also contaminated by the Cs and O_2, to the detriment of the energy resolution. Thus, the disappearance of structure in the GaAs EDCs after treatment II is probably due to a failure to resolve the structure.

The fact that the high energy peak shown in Fig. 5 is not significantly reduced in treatments II through IV from its magnitude following treatment I indicates that the Cs-oxide layer remains thin compared to the escape depth for 10 eV electrons for the first four treatments. The dramatic drop in the high energy peak following treatment V indicates that the thickness of the Cs oxide layer is comparable to the 10 eV electron escape depth for that treatment. As will be discussed below, the EDC measured after treatment V contains both structure from the GaAs and from a Cs-oxide layer.

The low energy peak in the EDCs of Figs. 2 and 3 is caused by electrons which were scattered, and by secondary electrons created in that scattering process,before being emitted. A comparison of the area under the low energy peak with the area under the high energy tail in the EDCs of Figs. 2 and 3 shows that the majority of the yield comes from scattered or secondary electrons. For example, for treatment III, over 90% of the area of the EDC is under the scattering peak, for $h\nu$ = 10.2 eV. However, as Fig. 5 shows, there is no significant reduction in unscattered electron emission for treatments I through IV.

Figure 2 shows that 18 hours after treatment I was made the threshold for photoemission had increased by 0.3 eV (seen by the movement of the lower edge of the EDC to higher energy), consequently reducing the height of the low energy peak. This increase in threshold was probably caused by either cesium desorption or by contamination by residual gases in the 3×10^{-10} Torr vacuum. Exposure of the surface to 20L of O_2 (treatment II) caused a further increase in threshold and reduction in height of the low energy peak. Treatment III restored the EDC to a shape very similar to that of treatment I and treatment IV produced an EDC very similar to that of treatments I and III.

Figure 5 shows that the EDCs from treatments III and IV are not identical, however. The high energy peak can still be resolved after treatment III, but it is only a weak shoulder after treatment IV. The Fermi level broadening of the Cu emitter is not significantly different for treatments III and IV, so the weakening of the high energy structure is not a resolution effect.

Treatment V caused a great reduction of the high energy structure at -1.3 eV, as Fig. 5 shows. After treatments VI and VII the high energy GaAs peak is completely gone, as can be seen in the expanded scale portion of the high energy portions of the EDCs in Fig. 4. The EDCs of Figs. 3-5 show that treatment IV represents a transition in which structure in the EDC characteristic of the GaAs is reduced, while new structure grows at -2 and -6 eV. The threshold for photoemission was increased by treatments V, VI and VII, causing a large drop in the low energy peak.

The EDC from treatment VII strongly resembles EDCs from a thick film of Cs which had been oxidized at liquid nitrogen temperature.[7] To a lesser extent, the EDC from treatment VI also resembles the EDCs from bulk cesium oxide. Figure 6 compares the EDC from treatment VII to the bulk cesium oxide EDC most like it. We have chosen the bulk cesium oxide EDC for which the peak spacing most closely matches the peak spacing of the treatment VII EDC. Figure 7 compares the EDC from treatment VI with the cesium oxide EDC which most closely resembles it.

The oxidation of the thick Cs film at liquid nitrogen temperatures[7] produced dramatic changes in the shape of the EDCs and a large increase in the yield for O_2 exposures up to 500L. These changes were interpreted as being caused by the formation of different Cs oxides. Emission from the Fermi level could still be detected in the EDCs up to the 500L O_2 exposure, indicating either that metallic Cs was present at the surface or that the Cs oxide itself was metallic. The EDCs for O_2 exposures less than 500L do not resemble the Cs-oxide on GaAs seen here.

For O_2 exposures above 500L, the change in shape of the bulk Cs oxide EDCs was not large, as a comparison of Figs. 6 and 7 will show. There

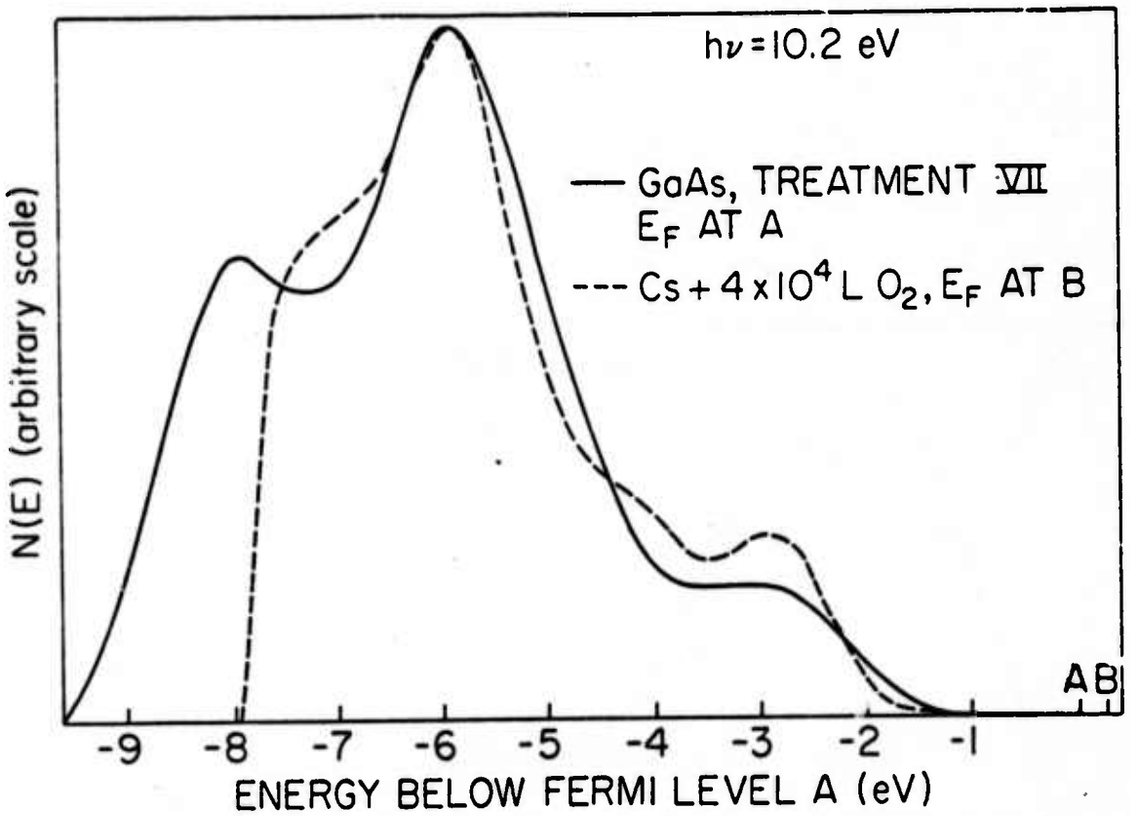

FIG. 6--An EDC for GaAs with the Cs-oxide layer from treatment VII compared to an EDC for thick Cs film exposed to 4 X 10^4L of O_2, for hν = 10.2 eV. The bulk Cs-oxide EDC is taken from Reference 7.

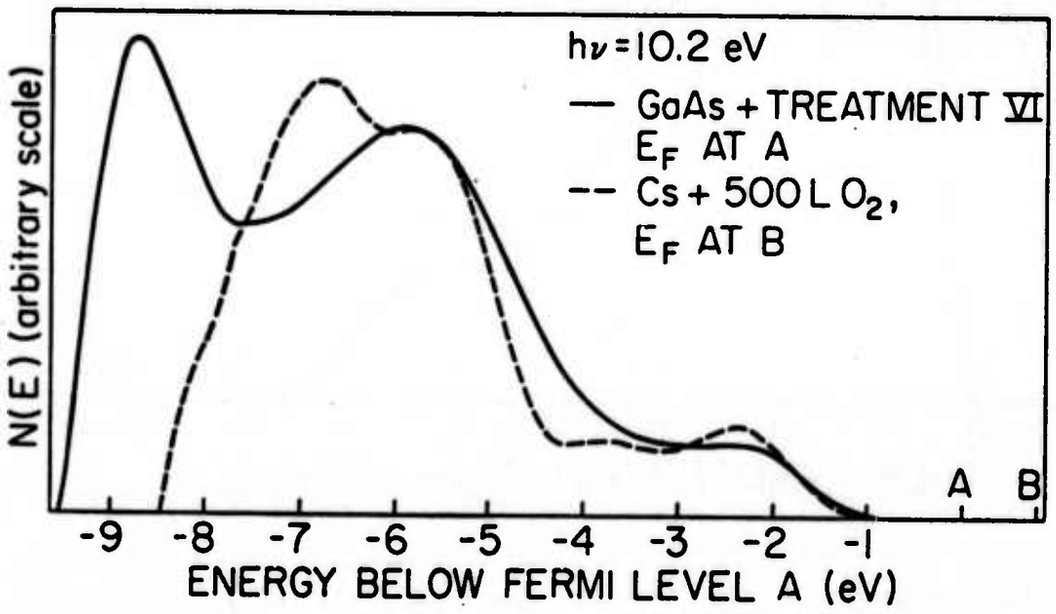

FIG. 7--An EDC for GaAs with the Cs-oxide layer from treatment VI compared to an EDC for a thick Cs film exposed to 500L of O_2, for $h\nu$ = 10.2 eV. The bulk Cs-oxide EDC is taken from Reference 7.

is a small change in peak spacing, which is the basis of our identification of the 500L oxide with treatment VI and the 4×10^4L oxide with treatment VII. The major difference between the 500L and 4×10^4L oxide EDCs is that the threshold for photoemission increased by about 1 eV with the larger oxygen exposure. The 4×10^4L O_2 was the largest exposure studied in the bulk Cs oxide experiment. The shape of the EDCs appeared to be stabilizing at that point, representing a more stable form of Cs oxide. The thick Cs oxide on the GaAs resembles this stable, or saturated, bulk Cs oxide.

Figure 8 shows EDCs for the same treatment and the same cesium oxide as Fig. 6, but for the photon energy 7.7 eV rather than 10.2 eV. The agreement between the EDCs at 7.7 eV is less apparent than at 10.2 eV because there is less structure in the EDCs at 7.7 eV. However, note that the same Fermi level spacing between the bulk cesium oxide EDCs and the EDCs from treatment VII produces a good agreement in the positions of the peaks in both Figs. 6 and 8. (The Fermi level positions shown in Figs. 6 and 8 for the bulk cesium oxide and for treatment VII are within the experimental error of being at the same position. As discussed above, the Cs + O_2 treatments caused a broadening of the Fermi edge of the Cu emitter, making the determination of the Fermi level location subject to an error of 0.3 to 0.4 eV for treatments VI and VII. It was also not possible to make an accurate determination of the Fermi level position for the bulk cesium oxide EDCs for O_2 exposures above 500L.[7])

There are two differences between the EDCs from treatment VII and from the 4×10^4L O_2 bulk cesium oxide. The threshold for photoemission is about 1 eV lower for treatment VII than for the bulk cesium oxide, as is apparent from Figs. 6 and 8, and the yield is higher for treatment VII.

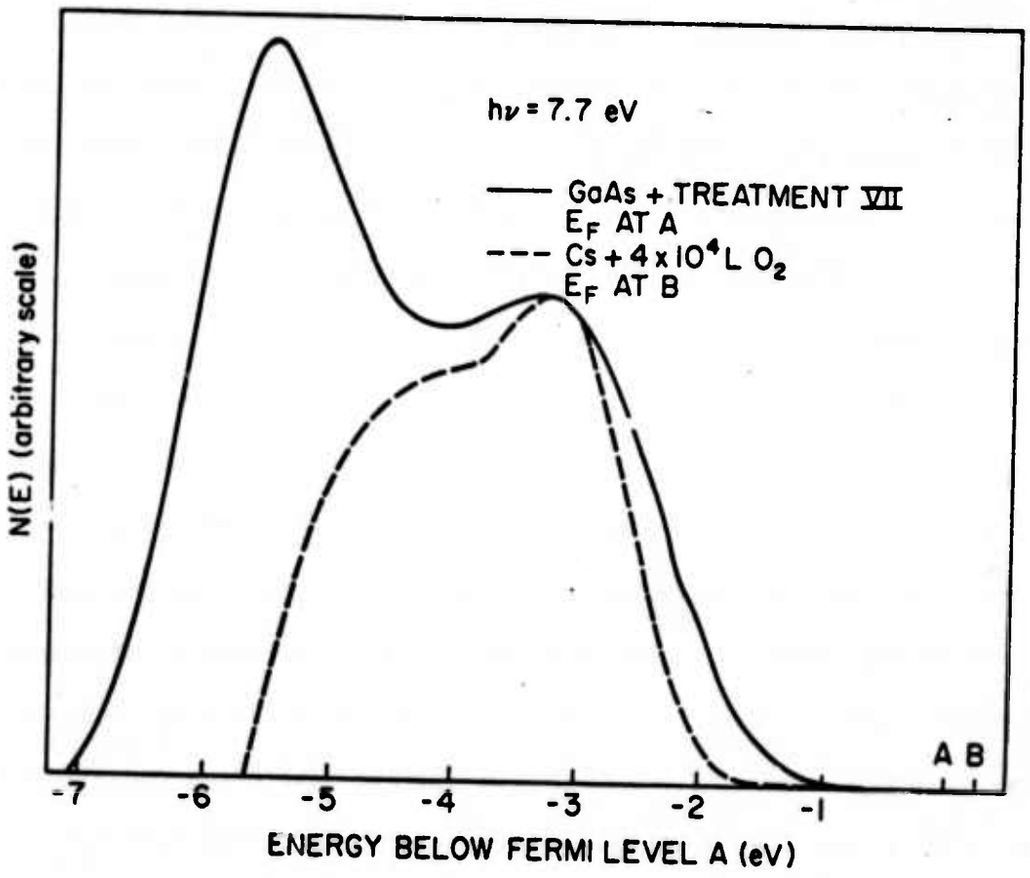

FIG. 8--EDCs for the same treatment on GaAs and the same bulk Cs-oxide as in Fig. 6, but for hν = 7.7 eV. The relative Fermi level positions are the same as in Fig. 6.

The difference in yield is not shown in Figs. 6 and 8, which have been normalized to equal height at the major peaks.

The difference in threshold for photoemission may be due to the difference in temperature at which the EDCs for the bulk cesium oxide and for treatment VII were measured. When the bulk cesium oxide film was allowed to warm from liquid nitrogen temperature to room temperature the resulting EDCs had a lower threshold, nearly equal to that of treatment VII, and a low energy peak much larger than that of treatment VII. (It is possible that the bulk cesium oxide peak was contaminated somewhat during the nine hours that elapsed while it was warming.)

Other data consistent with the interpretation of the threshold difference as a temperature effect is contained in the work of Davey.[20] He reported that for Cs oxide on silver, and on oxidized silver, the thermionic work function increased by 0.3 eV when the sample was cooled from room temperature to -40° C.

Another possible explanation for the difference in threshold is that the threshold might have been increased if more Cs + O_2 exposures had been made after treatment VII. The threshold is slightly higher for treatment VII than for treatment VI, and there is less low energy emission for treatment VII. Possibly more Cs + O_2 exposures would have increased the threshold further. Unfortunately, the cesium channel was exhausted after treatment VII, so that no further Cs exposures were possible.

The difference in yield between the bulk cesium oxide and treatment VII is fairly large. If the bulk cesium oxide EDCs were drawn to the same scale as the EDCs for treatment VII, the bulk cesium oxide curve in Fig. 6 would be lower by a factor of 4.3, and in Fig. 8 by a factor of 1.6. The cause of this difference in yield has not been determined.

The EDCs of Figs. 6 and 8 are remarkably similar considering the different ways in which the cesium oxides were formed; the treatment VII oxide was formed at room temperature on GaAs by a series of Cs and O_2 exposures, while the bulk oxide was formed at liquid nitrogen temperature by exposing a thick cesium film on a copper substrate to oxygen. The bulk cesium oxide was formed by oxidation only - no cesium was added after the initial cesium evaporation. The similarity of the EDCs for treatment VII and for the 4×10^4 L O_2 exposure cesium oxide is convincing evidence that a cesium oxide was formed on the GaAs by the Cs + O_2 treatments. Baer[21] observed EDCs similar to those for our treatment VII after [12] Cs + O_2 treatments on GaAs, with somewhat less low energy emission. However, at that time no bulk Cs oxide EDCs were available for comparison.

Figure 6 shows that it is possible to form a cesium oxide layer with bulk cesium oxide properties on GaAs at room temperature by applying Cs + O_2 treatments, but the thick Cs oxide layer produces lower yield and a higher threshold than the optimum Cs + O_2 treatment, as is shown in Fig. 1. The data provides some qualitative information about the cesium oxide layer thickness, but quantitative information cannot be obtained at present. The cesium oxide layer is thick enough to block emission of the high energy electrons from the GaAs. This can be seen in Fig. 5(b), which shows that for treatment V the leading GaAs peak is greatly reduced. Figure 4 shows that for treatments VI and VII there is no resolvable emission from the GaAs at the high energy edge of the EDC. However, it is possible that the low energy peak in the EDCs for treatments V through VII is scattered and secondary electrons from the GaAs. Thus, it appears that the cesium oxide layer for treatments VI and VII is thick enough to block high energy electrons from the GaAs and to strongly diminish the number of low energy electrons

from the GaAs. Unfortunately the scattering length for electrons in cesium oxide has not been determined, so the disappearance of the GaAs structure from the EDCs does not allow us to determine the cesium oxide layer thickness. If we estimate the electron escape depth in Cs oxide for 10 eV electrons to be 10 Å, then the Cs oxide film would be less than 10 Å thick for treatments I through IV, about 10 Å thick for treatment V, and approximately 20 Å thick for treatments VI and VII. The 10 Å escape depth is not unreasonable compared to the escape depth in other materials.[13]

Baer estimated that his cesium oxide film, which produced EDCs similar to those from our treatment VII, was about 24 Å thick.[21] That thickness does not seem unreasonable for the cesium oxide layer of treatment VII. On the other hand, Uebbing and James estimate 7.2 Å of Cs_2O for each one Langmuir of oxygen used in the Cs + O_2 treatments, assuming that all the oxygen sticks.[4] As Table 1 shows, assuming 7.2 Å for each 1L of O_2 would give unreasonably thick layers in our case. Our oxygen exposures were larger than those of Uebbing and James, and the sticking coefficient for oxygen probably decreased rapidly during the oxygen exposure.

Figure 1 shows that the yield decreased for treatments V, VI and VII; it was these treatments during which the thick cesium oxide layer was formed. On the other hand, treatments I, III and IV all produced surfaces which gave high yield, and there is no evidence of emission from the cesium oxide layer in EDCs from these treatments. Figure 5 shows that emission from the GaAs at the high energy edge of the EDCs is not strongly diminished by treatments I, III, and IV. Thus, it appears that for optimum yield from GaAs the cesium oxide layer is thin enough that it is transparent to electrons up to the highest energy electrons produced in this experiment.

There seems to be general agreement in the literature that the cesium oxide layer required to activate GaAs is very thin.[2,4] Our findings here are in qualitative agreement with that model for the GaAs activating layer.

For narrower bandgap III-V materials the predictions of the two models for the cesium oxide layer diverge. The heterojunction model[4,5] predicts thicker cesium oxide layers on the narrower bandgap materials, whereas the dipole model predicts a cesium oxide monolayer only, independent of the bandgap.[2] Experiments similar to those reported here should be able to provide a qualitative comparison of the thickness of the activating layer required for the different bandgap III-V materials. It may be useful to extend the measurements to higher photon energies to increase the surface sensitivity of the photoemission measurements.

IV. CONCLUSIONS

The EDCs presented in this paper contain two features relevant to understanding the Cs oxide surface layer: structure from the Cs oxide layer itself, and structure from high energy electrons from the GaAs. Structure from the Cs oxide layer should be apparent in the EDCs for a Cs oxide layer of thickness comparable to the electron escape depth in the GaAs if the Cs oxide layer has electronic properties characteristic of bulk Cs oxide. Even a Cs-O thickness of about 8 Å is within a factor of 3 of the expected electron escape depth in the GaAs for 10 eV electrons. On the other hand, if the Cs oxide layer does not have bulk electronic properties, no structure characteristic of the Cs oxide layer would be expected in the EDCs. Previous measurements of the EDCs from bulk Cs oxides[7] are used here to identify structure characteristic of bulk Cs oxides.

The presence or absence of GaAs structure in the EDCs provides information on the thickness of the Cs oxide layer. Although the hot electron scattering length in Cs oxide layers has not been measured, it is probably not greatly different from that in other materials. A thick layer of Cs oxide would appreciably attenuate the electrons from the GaAs passing through the layer, with a greater attenuation for the higher energy electrons than for the lower energy electrons. Thus, by going to higher hV one might be able to see the Cs oxide much better.

We have measured EDCs from GaAs with varying thicknesses of Cs oxide surface treatments. No emission characteristic of the Cs oxide is seen in the EDCs for surface treatments that produce the highest yield and lowest threshold. However, for Cs oxide layers thicker than those which produce optimum yield, the EDCs are characteristic of the Cs oxide and there is no structure from high energy electrons from the GaAs. These results are consistent with the estimates that the Cs oxide layer is approximately a monolayer thick for optimum yield on GaAs,[2,4,11] and the results indicate that the activating layer does not have bulk Cs oxide electronic properties. Measurements similar to those presented here on III-V materials with bandgaps narrower than GaAs should make it possible to decide if the heterojunction model or the dipole model best describes the Cs oxide activating layer.

We appreciate the assistance of Dr. I. A. Babalola in performing this experiment.

REFERENCES

1. For a general review, see R. L. Bell, Negative Electron Affinity Devices, Clarendon, Oxford (1973); W. E. Spicer and R. L. Bell, Pub. Astron. Soc. Pacific 84, 110 (1972); and references 3 and 6 below.
2. D. G. Fisher, R. E. Enstrom, J. S. Escher, and B. F. Williams, J. Appl. Phys. 43, 3815 (1972).
3. B. F. Williams and J. J. Tietjen, Proc. IEEE 59, 1489 (1971).
4. J. J. Uebbing and L. W. James, J. Appl. Phys. 41, 4505 (1970).
5. H. Sonnenberg, Appl. Phys. Lett. 14, 289 (1969).
6. R. L. Bell and W. E. Spicer, Proc. IEEE 58, 1788 (1970).
7. P. E. Gregory, P. Chye, H. Sunami and W. E. Spicer, J. Appl. Phys., to be published.
8. A. F. Milton and A. D. Baer, J. Appl. Phys. 42,5095 (1971).
9. L. W. James, G. A. Antypas, J. J. Uebbing, T. O. Yep and R. L. Bell, J. Appl. Phys. 42, 580 (1971).
10. A. H. Sommer, H. H. Whitaker and B. F. Williams, Appl. Phys. Lett. 17, 273 (1970).
11. B. Goldstein, Surf. Sci. 47, 143 (1975).
12. A. A. Turnbull and G. B. Evans, Brit. J. Appl. Phys. (J. Phys. D) ser. 2 1, 155 (1968).
13. I. Lindau and W. E. Spicer, J. Electron. Spect. 3, 409 (1974).
14. L = Langmuir = 10^{-6} Torr-second.
15. R. C. Eden, Rev. Sci. Instrum 41, 252 (1970).
16. G. B. Fisher, W. E. Spicer, P. C. McKernan, V. F. Pereskok and S. J. Wanner, Appl. Optics 12, 799 (1973).

17. H. R. Phillip and H. Ehrenreich, Phys. Rev. 129, 1550 (1963).

18. R. C. Eden, Ph.D. dissertation, Stanford University 1967, unpublished.

19. W. E. Spicer and R. C. Eden, in Proceedings of the Ninth International Conference on the Properties of Semiconductors, Vol. 1 (Nauka, Leningrad, 1968) p. 65.

20. J. E. Davey, J. Appl. Phys. 28, 1031 (1957).

21. A. D. Baer, Ph.D. dissertation, Stanford University, 1971 (unpublished) pp. 111-126.

CHAPTER 5

SURFACE STATES AND SCHOTTKY BARRIER PINNING ON InP AND GaAs

In 1947, Bardeen[1] explained semiconductor Schottky barriers in terms of Fermi level pinning due to intrinsic surface states. This concept has been widely accepted and used with considerable success.[2] However, in the last decade, theoretical questions have been raised concerning the survival of intrinsic surface states when a metal overlayer is added to the surface[3] and new mechanisms have been advanced to explain the Fermi level pinning at the semiconductor-metal interface.[3,4,5]

Conventional Schottky barrier studies alone do not allow one to experimentally determine the origin of the pinning states and their relation to the empty states on the clean surfaces since one only locates the pinning states after the metal has been added. On the other hand, recent ultraviolet photoemission spectroscopic (UPS) techniques provide means for examining the surface before and after a metal is applied.[6,7] Using these techniques the energy distribution of surface states on clean GaAs and InP has been determined and important correlations have been obtained between the location of the intrinsic empty surface states and the Schottky barrier heights. However, careful measurements do not support a pinning due to simple filling of existing surface states by electrons from the metal.

In this work, we report careful studies made while a metal, cesium, is added to the surface in small fractions of a monolayer. By this means changes in the electronic structure at the interface (including the Fermi level position) can be followed as the cesium coverage is increased. A major question in the addition of submonolayer quantities of a metal to a semiconductor is whether a uniform atomic coverage is achieved or whether the metal tends to clump into islands which may be several atomic layers thick. Clumping is not such a problem with Cs. Because of the strong

dipole induced by Cs on a III-V semiconductor, the Cs 'wets' the semiconductor extremely well and the repulsion between induced dipoles serves to keep the surface atoms well separated.[8,9,10,11] Further, the second layer is not stable but will evaporate.[11]

The induced dipoles produce a reduction in the work function which is determined by the fraction of Cs coverage. The change in work function with coverage has been measured for both n and p-type GaAs,[9,10] providing us with a method of determining the Cs coverage. Since such measurements are not available for InP, we use there the figures from GaAs, recognizing that this may introduce a certain amount of error. Thick films of Cs have been formed on p^{++} GaAs at low temperature and the Schottky barrier heights measured[12] were found to fall on the same curve of barrier height versus electronegativity as the wide range of other metals for which Schottky barriers have been studied.[2] This allows us to make contact between the results from these studies and those of other metals on GaAs. Since UPS here samples approximately 20 Å into the sample (i.e., the bulk),[13] changes in the electronic structure at the interface can be referenced to strong structure in the energy distribution curves (EDCs) which is due to direct optical transitions characteristic of the bulk of the semiconductor.

Four crystals of GaAs doped 6×10^{14} n (14n), 1.7×10^{18} n (18n), 1.5×10^{17} p (17p), and 3×10^{19} p (19p) and one crystal of InP doped 6×10^{17} n-type were studied. Base pressure was approximately 10^{-10} Torr. Clean surfaces were prepared by standard cleaving techniques and Cs was added by standard vapor deposition techniques at room temperature. EDCs were measured by standard techniques,[14] and the Fermi level position was determined by measuring EDCs from a Cu reference. For clarity in the data presented here, a monolayer of Cs is taken to correspond to a Cs atom over

each Ga or As surface atom (i.e., 8.85×10^{14} atoms/cm^2). With this definition of monolayer, the minimum work function corresponds to a coverage of approximately 0.3 monolayer.[9,10]

UPS measurements on the clean semiconductor surface have shown that for GaAs there are no filled surface states in the lower half of the band gap, but a band of empty surface states lies in the upper half of the band gap, with a lower edge at 0.75 ±0.05 eV above the valence band maximum.[6,16] The situation is similar for InP, where the lower edge of the empty surface state band is 0.25 eV below the conduction band minimum.[17]

Figure 1 shows EDCs for GaAs sample 17p with increasing Cs coverage. To emphasize emission near the valence band maximum, Fig. 2 shows the high energy edge of some of the EDCs from Fig. 1, normalized to equal height at the first peak. (Note from Fig. 1 that normalization to yield also makes the first peaks nearly the same height.) An insert in Fig. 2 gives the Fermi level pinning position versus Cs coverage for all the GaAs samples studied. Figure 3 summarizes the Fermi level pinning data for the InP sample.

Two important results are contained in Figs. 2 and 3; the change in pinning position of E_f and the rise in energy of the leading edge of the EDC with Cs coverage. For both GaAs and InP, the pinning position of E_f for large Cs coverage is $\sim$ 0.1 eV below the edge of the empty surface state band. However, the movement of the pinning position as the Cs coverage is increased cannot be explained simply by filling the surface states present on the clean surface. Note in particular the drop in pinning position at larger coverages. This movement of the pinning position of E_f is an indication of strong interactions between the semiconductor and the Cs.

The rise in energy of the leading edge of the EDC with increasing Cs coverage, which was seen for both n and p-type GaAs and for InP, is another indication of strong interactions between the Cs and the semiconductor.

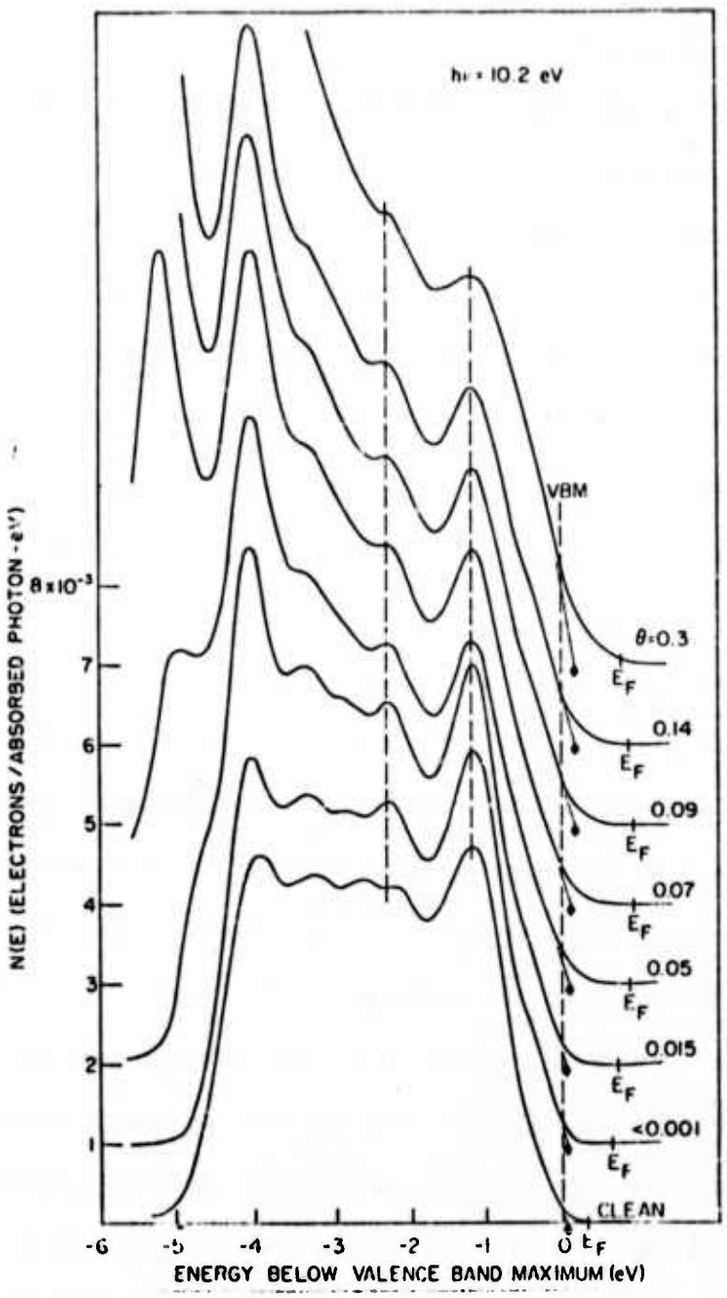

FIG. 1--EDCs for GaAs sample 17p as a function of Cs coverage, θ. The diamond-shaped marks indicate the extrapolated upper edges, also shown in the inset of Fig. 2. The EDCs are normalized to yield.

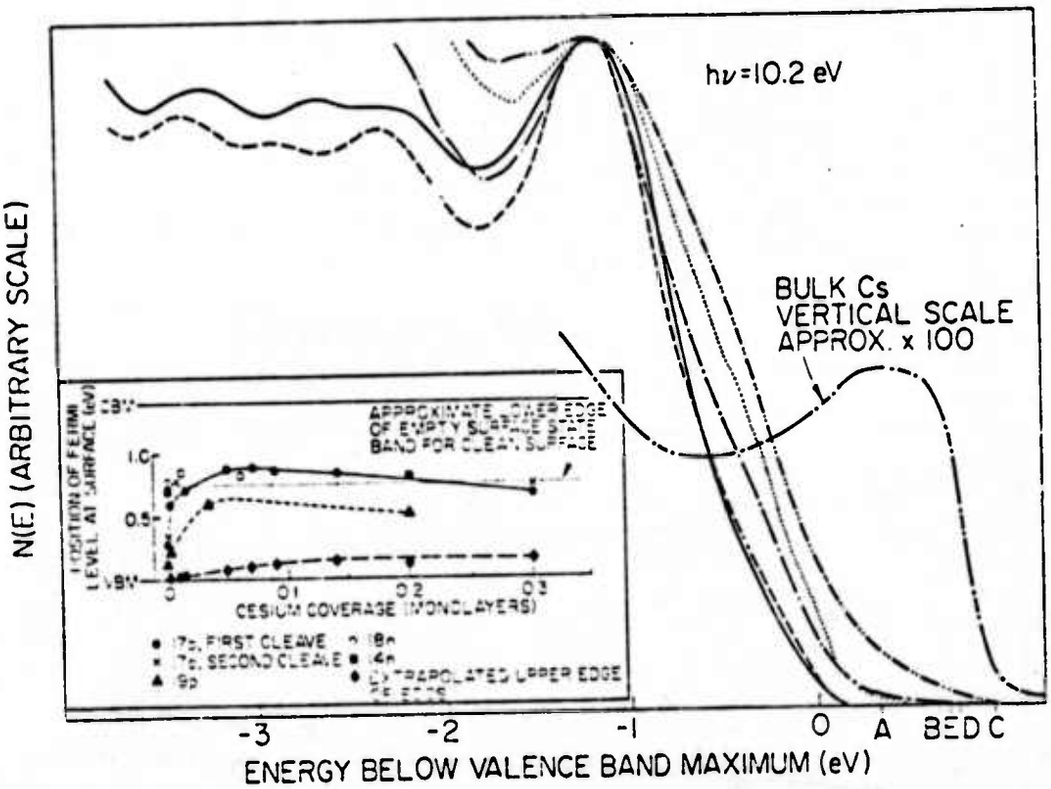

FIG. 2--Upper edge of EDCs from Fig. 1 replotted, normalized to equal height for the first peak, showing upward movement of leading edge with increasing Cs coverage. Solid line, clean GaAs, E_f at A; dashed line $\theta < 0.001$ monolayers, E_f at B; dash-dot, $\theta = 0.07$, E_f at C; dash-double dot, $\theta = 0.3$, E_f at D; dotted, $\theta = 0.3$ + contamination, E_f at E. Inset: Fermi level pinning position vs. θ for 4 GaAs samples.

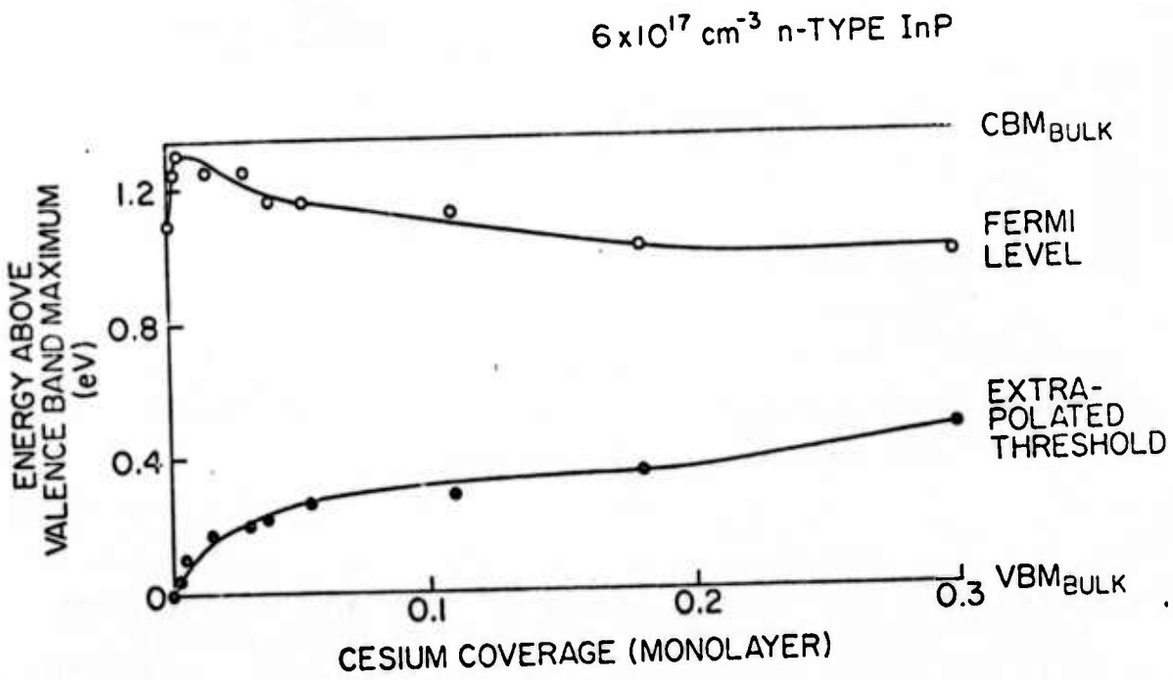

FIG. 3--Fermi level pinning position and extrapolated upper edge of EDC for n-type InP versus Cs coverage.

Clearly, new states are appearing in the energy gap. The most straightforward explanation is that the valence band maximum at the surface is rising in energy as Cs is added to the surface, suggestive of the bandgap narrowing at the surface as proposed by Inkson.[4] An EDC for bulk Cs[17] is shown in Fig. 2 to emphasize that this new emission does not arise from a simple addition of photoemission from metallic Cs to that from GaAs.

The vertical scale of Fig. 2 is arbitrary. However, on an absolute scale the peak heights for the GaAs are within 20% of the same height (see Fig. 1). The bulk Cs emission is smaller by a factor of ~ 100. Thus, if the extra emission is coming from Cs, the Cs is not in a state representative of bulk Cs, but is strongly affected by the GaAs substrate.

Mead et al.[2] found that the Fermi level was pinned 1/3 of the band gap above the valence band maximum for most Au-III-V semiconductor Schottky barriers. GaAs fitted this pattern, but InP deviated quite far from it. We find the edge of the intrinsic empty surface state band to be about 0.3 eV above the Fermi level pinning position reported by Mead for Au on both GaAs and InP. Thus the same correlation is found between empty surface state position and Fermi level pinning position for a material which obeys the 1/3 rule and one which does not. This is strong evidence that the correlation is not accidental.

We have referenced the Fermi level position and extrapolated thresholds of Figs. 2 and 3 to a peak in the EDCs. It is important to note that the peaks on the GaAs EDCs are caused by transitions within the bulk band structure.[18] This fact is shown by the complex movement of the positions of the peaks in the EDCs as $h\nu$ is changed. As Fig. 1 shows, the peaks present in the clean GaAs EDCs are present also in the Cs covered GaAs EDCs. It has been shown that the movement of peaks in the EDCs with changes in $h\nu$ is essentially the same for clean and heavily Cs covered GaAs.[18]

It should be noted that if the leading edge of the EDC is used as a reference instead of a peak, the downward movement of the Fermi level pinning position would become more extreme at higher Cs coverages, a fact which is even more strongly at variance with conventional Schottky barrier theory.

In conclusion, application of a metal (Cs) to the clean (110) surface of both GaAs and InP produces an upward movement of the leading edge of the EDCs. This, as well as the detailed movement of the Fermi level with Cs coverage, indicates strong interactions between the metal and semiconductor which can be explained neither in terms of simple donation of electrons from the metal into the empty surface states nor as a simple addition of photoemission from metallic Cs to that from GaAs (see Fig. 2). Further details of the GaAs work are in press.[19] Inkson has examined the screening of the semiconductor surface by a metal[4] and concluded that the semiconductor band gap at the interface would be reduced by this interaction. The upward movement of the valence band edge seems to be, at least qualitatively, in agreement with that suggestion. However, to the first approximation it is not these interactions (although they may explain the small regular variation in pinning positions with electronegativity of the metal), but the position of the bottom of the intrinsic empty surface state band (associated with the column III metal)[6,7] which appears to play the dominant role in locating the pinning position of the Fermi level at the metal-semiconductor interface.

REFERENCES

1. J. Bardeen, Phys. Rev. 71, 717 (1947).
2. C. A. Mead and W. G. Spitzer, Phys. Rev. 134, A713 (1964); C. A. Mead, Solid State Elec. 9, 1023 (1966).
3. V. Heine, Phys. Rev. A138, 1689 (1965).
4. J. C. Inkson, J. Phys. C. 5, 2599 (1972); J. Phys. C. 6, 1350 (1973); J. Vac. Sci. Tech. 11, 943 (1974).
5. J. C. Phillips, J. Vac. Sci. Tech. 11, 947 (1974).
6. P. E. Gregory, W. E. Spicer, S. Ciraci and W. A. Harrison, Appl. Phys. Lett. 25, 511 (1974); P. E. Gregory and W. E. Spicer, to be published.
7. D. E. Eastman and J. L. Freeouf, Phys. Rev. Lett. 33, 1601 (1974).
8. J. B. Taylor and I. Langmuir, Phys. Rev. 44, 423 (1933).
9. T. E. Madey and J. T. Yates, Jr., J. Vac. Sci. Tech. 8, 39 (1971).
10. H. Clemens and W. Monch, to be published.
11. F. G. Allen and G. W. Gobeli, Phys. Rev. 144, 558 (1966).
12. J. J. Uebbing and R. L. Bell, Appl. Phys. Lett. 11, 357 (1967).
13. I. Lindau and W. E. Spicer, J. Elect. Spectros. 3, 409 (1974).
14. R. C. Eden, Rev. Sci. Instrum. 41, 252 (1970).
15. P. E. Gregory and W. E. Spicer, to be published.
16. P. W. Chye, I. A. Babalola, T. Sukegawa and W. E. Spicer, to be published.
17. N. V. Smith and G. B. Fisher, Phys. Rev. B3, 3662 (1971); P. E. Gregory, P. Chye, H. Sunami and W. E. Spicer, J. Appl. Phys. 46, 3525 (1975).
18. R. C. Eden, Ph.D. dissertation, Stanford University, 1967, unpublished; W. E. Spicer and R. C. Eden, Proc. of the Ninth International Conference on the Properties of Semiconductors, Vol. 1 (Nauka, Leningrad, 1968), p. 65
19. P. E. Gregory and W. E. Spicer, Phys. Rev. B15, in press.

CHAPTER 6

GaSb SURFACE STATES AND SCHOTTKY BARRIER PINNING

Surface state studies of clean cleaved (110) GaSb and of cesium on (110) GaSb are reported. These results which represented work of two cleaves on an n-type[1] and one cleave of a p-type GaSb crystal are in disagreement with recent results published by Eastman and Freeouf[2] (EF) and cast doubt on the strong generalizations made by them.

Figure 1 shows the high energy portions of photoelectron energy distribution curves (EDCs) for clean and cesiated n-type (carrier concentration 1.09×10^{18} cm^{-3}) and clean p-type (carrier concentration 1.64×10^{17} cm^{-3}) (110) GaSb at an incident photon energy of 10.2 eV. In Fig. 1, a Cs monolayer is defined as the coverage which gives minimum photoemission threshold.[3] Further experimental details are available elsewhere.[3,4] The EDCs are presented with the peaks due to direct transitions in the bulk superimposed. Fermi level positions determined to within ± 0.1 eV using a Cu reference emitter are marked near the high energy edges. The difference in energy of the positions of the Fermi level on the clean n- and p-type samples is 0.65 eV, which is almost the full bandgap. An additional determination of the n-type Fermi level based on yield measurements and the observed width of the EDC of the clean sample, is in agreement with Fig. 1 putting the surface Fermi level at the conduction band minimum (CBM). This corresponds to a flat band situation with the forbidden bandgap free of empty intrinsic surface states which would cause pinning. EF, on the other hand, showed empty surface states on GaSb as having a peak near the CBM with a tail extending below midgap and located the Fermi level on their n-type sample 0.4 eV below the CBM.

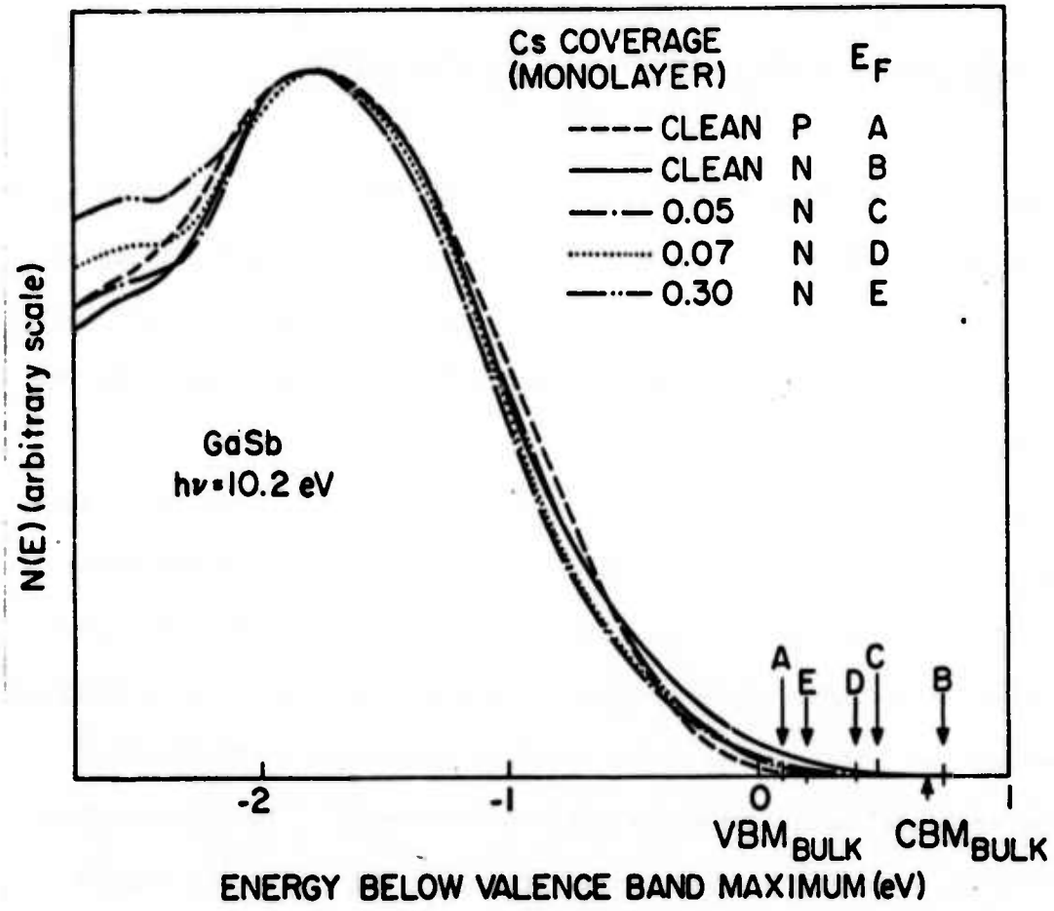

FIG. 1--The high energy portions of clean and cesiated GaSb EDCs. The Fermi level (E_F) of the n-type sample shows a large movement with cesiation and the Fermi levels of the clean p- and n-type samples differ in energy by 0.65 eV. This shows that the Fermi level of the n-type sample lies near the CBM and indicates the absence of empty intrinsic surface states which would cause pinning.

Further evidence for the intrinsic n-type Fermi level location being near the CBM is given by following the Fermi level movement with Cs addition. It is evident that with cesiation the Fermi level moved towards the valence band maximum (VBM) - taken to be 0.1 eV below the Fermi level of the clean p-type sample - and eventually moved through the bandgap by 0.55 eV and stabilized near the VBM,[5] in accordance with the Fermi level position for bulk Schottky barriers.[6] If the intrinsic Fermi level position on an n-type sample were located 0.4 eV below the CBM as reported by EF, such a large movement would be impossible. In addition, the movement upwards of the leading edge of the EDC into the original bandgap - indicative of strong Cs-semiconductor interaction in GaAs[3,7] and InP[7] was not observed in GaSb, suggesting that the metal-semiconductor interaction differs according to whether or not empty intrinsic surface states exist in the bandgap. Further evidence for a reduced interaction when empty intrinsic surface states do not lie in the bandgap is given by the fact that the Cs coverage which gives minimum photoemission threshold on GaSb is not stable (i.e., Cs is not strongly bonded to the surface); whereas, in GaAs and InP where intrinsic surface states lie in the bandgap, this coverage is stable. Thus we conclude that the Cs-GaSb Schottky barrier, where there are no empty surface states in the bandgap, is different from the Cs-GaAs and Cs-InP Schottky barriers where there are surface states in the bandgap.

The present work shows that surface state pinning may be produced at a metal-semiconductor contact even when no empty intrinsic surface states are present. Thus, it appears that the conclusion of EF, "intrinsic surface . . . states play a predominant role in determining Schottky barriers on III-V compound semiconductors" must be re-examined. If one accepts their arguments, then the Fermi level pinning for Schottky barriers on n-type GaSb should be at the CBM, not near the VBM as the literature reports[6] and as we find for Cs.

The lack of experimental details in EF paper makes a direct comparison with the present work difficult. For example, it was not clear how those authors obtained their Fermi level, nor was it clear whether they studied one or several cleaves. Lapeyre[8] has suggested that excitonic effects may be important in the Ga 3d transition used by EF to detect their empty surface states. This would result in a measured empty surface state position appreciably below that of its true energy, and could explain the difference between EF's location of the empty surface states using photoemission partial yield spectroscopy and our results. EF have considered possible excitonic or correlation effects but suggested that they are probably less than $\sim$ 0.1 to 0.2 eV; if so, they could not explain the discrepancies reported here.

The assistance of Hideo Sunami is gratefully acknowledged.

REFERENCES

1. The clean work is also in agreement with one cleave on a second n-type crystal. However, no Cs was added to that crystal.
2. D. E. Eastman and J. L. Freeouf, Phys, Rev. Lett. 34, 1624 (1975).
3. P. Gregory and W. E. Spicer, Phys. Rev. B 15 (in press, tentatively scheduled for Sept. 15, 1975 issue).
4. L. F. Wagner and W. E. Spicer, Phys. Rev. Lett. 28, 1381 (1972); L. F. Wagner and W. E. Spicer, Phys. Rev. B 9, 1512 (1974); P. E. Gregory, W. E. Spicer, S. Ciraci and W. A. Harrison, Appl. Phys. Lett. 25, 511 (1974).
5. Similar results were obtained with potassium deposition.
6. T. C. McGill, J. Vac. Sci. Technol., 11, 935 (1974).
7. W. E. Spicer, P. Gregory, P. Chye, I. A. Babalola and T. Sukegawa, to be published.
8. G. T. Lapeyre and J. Anderson, Phys. Rev. Lett. 35, 117 (1975).

CHAPTER 7
FUTURE WORK

We plan to move forward in two areas: studies of III-V materials other than GaAs, InP and GaSb, and studies of surfaces other than the (110) cleavage face. A new chamber is under construction for studying faces other than the cleavage face. Samples will be cleaned by heat cleaning and/or argon sputter cleaning. The chamber will include provision for Auger electron spectroscopy to monitor sample cleanliness, as well as the usual photoemission apparatus. This chamber should be in use within one to three months. The first sample face to be studied will be the GaAs (111) B face.

In the immediate future, work on GaSb will continue, and a sample of p-type InP will be studied. If the heat cleaning/sputter cleaning work is successful, that cleaning procedure will be used in preference to cleaving for the study of other III-V materials. Within the next year we hope to extend this work to III-V ternary or quatrinary alloys.

The photoemission work will consist of both conventional photoemission studies with photon energies below 12 eV, and high energy studies at the Stanford Synchrotron Radiation Project, with photon energies up to 300 eV. The photoemission experiments will be supplemented by studies of the empty states using low energy electron loss spectroscopy[1] and photoemission partial yield spectroscopy.[2]

REFERENCES

1. R. Ludeke and L. Esaki, Phys. Rev. Lett. 33, 653 (1974).
2. D. E. Eastman and J. L. Freeouf, Phys. Rev. Lett. 33, 1601 (1974).

FIGURES

		Page
Chapter 1.		
1.	Surface state distribution for Si and GaAs.	4
2.	Surface state model for GaAs (110).	5
3.	Surface state model for GaAs (111).	7
4.	Surface state calculations for GaAs (110).	9
5.	Suggested reconstruction for GaAs (110).	10
6.	EDCs for GaAs versus O_2 exposure.	14
7.	Model for oxygen adsorption on GaAs (110)	16
8.	Surface Fermi level position versus O_2 exposure for GaAs and Si.	17
9.	Model for O_2 adsorption on GaAs (110) for exposures causing band bending.	19
10.	EDCs for $h\nu$ = 100 eV showing As-3d and Ga-3d core shifts versus O_2 exposure.	20
11.	GaAs EDCs with different Cs coverages.	23
12.	Surface Fermi level position for InP versus Cs coverage.	25
13.	Surface Fermi level position for InP versus Cs coverage.	27
14.	Data for GaSb with several Cs coverages.	29
15.	Model of surface states for clean, (110) face of GaAs, InP, and GaSb.	31
Chapter 2.		
1a.	EDCs at $h\nu$ = 10.2 eV for sample 17p for O_2 exposures.	42
1b.	EDCs at $h\nu$ = 11.6 eV for sample 17p for O_2 exposures.	43
2.	EDCs for sample 19p for O_2 exposures.	44
3.	EDCs for sample 14n for O_2 exposures.	45
4.	EDCs for n-type Si for O_2 exposures.	47
5.	EDCs for sample 17p, heated in O_2.	52

Page

6. Surface Fermi level position versus O_2 exposure for GaAs and Si. 54
7. EDCs for three dopings of GaAs, with large O_2 exposures. 57
8. Model for GaAs (110) surface states. 60
9. Oxidation of "bad cleave". 65
10a. EDCs for CO exposure at $h\nu$ = 11.6 eV. 69
10b. EDCs as function of time after CO exposure. 69
10c. EDCs as function of time after CO exposure. 70
10d. Change in electron affinity versus time after CO exposure. 70
11a. EDCs for atomic hydrogen exposures for $h\nu$ = 10.2 eV. 76
11b. EDCs for hydrogen exposures for $h\nu$ = 11.6 eV. 77
12a. Comparison of Cs and H exposure. 79
12b. Comparison of Cs and H exposure. 80
13. EDCs versus final state energy for atomic hydrogen exposure. 83
14. Results of heat cleaning after hydrogen exposures. 85

Chapter 3

1. EDCs for sample 17p versus Cs coverage. 96
2. Yield curves versus Cs coverage. 97
3. High energy portions of EDCs for sample 17p versus Cs coverage. 99
4. EDCs for sample 19p versus Cs coverage. 101
5. EDCs for sample 18n versus Cs coverage. 103
6. High energy portion of EDCs for samples 18n and 14 n versus Cs coverage. 105
7. Surface position of Fermi level versus Cs coverage. 105
8. EDCs for Na coverage on GaAs. 108
9. Surface state model for GaAs (110). 111

Page

Chapter 4

1a. Semilog plot of yield versus surface treatment. 136

1b. Linear plot of yield versus surface treatment. 137

2. EDCs for treatments I, II, and III. 138

3. EDCs for treatments III through VII. 139

4. EDCs for treatments V, VI and VII. 140

5. High energy portion of EDCs for treatments I through V. 141

6. Comparison of EDC from treatment VII to EDC from bulk Cs-oxide. 145

7. Comparison of EDC from treatment VI to EDC from bulk Cs-oxide. 147

8. Comparison of EDC from treatment VII to EDC from bulk Cs-oxide at $h\nu$ = 7.7 eV. 148

Chapter 5

1. EDCs for GaAs versus Cs coverage 159

2. Upper edge of EDCs and Fermi level pinning versus Cs coverage on GaAs. 160

3. Fermi level pinning and extrapolated upper edge of EDC for a n-type InP versus Cs coverage. 161

Chapter 6

1. High energy portions of clean and cesiated GaSb EDCs. 166.

TABLES

Chapter 2

1. Samples studied 37

Chapter 3

1. Samples studied 93

2. Cesium exposure data for sample 17p 93

A1. Calculations for Cs coverage 124

Chapter 4

1. Summary of surface treatments 133